



**HAL**  
open science

# Functions of the transcription factor Lyl-1 in the development of the macrophage lineage

Shoutang Wang

► **To cite this version:**

Shoutang Wang. Functions of the transcription factor Lyl-1 in the development of the macrophage lineage. Embryology and Organogenesis. Université Paris Saclay (COMUE), 2017. English. NNT : 2017SACLS457 . tel-01663080

**HAL Id: tel-01663080**

**<https://theses.hal.science/tel-01663080>**

Submitted on 13 Dec 2017

**HAL** is a multi-disciplinary open access archive for the deposit and dissemination of scientific research documents, whether they are published or not. The documents may come from teaching and research institutions in France or abroad, or from public or private research centers.

L'archive ouverte pluridisciplinaire **HAL**, est destinée au dépôt et à la diffusion de documents scientifiques de niveau recherche, publiés ou non, émanant des établissements d'enseignement et de recherche français ou étrangers, des laboratoires publics ou privés.

# Fonctions du facteur de transcription Lyl-1 dans le développement du lignage macrophagique

Thèse de doctorat de l'Université Paris-Saclay,  
préparée à l'Université Paris-Sud

École doctorale n°577 :  
Structure et dynamique des systèmes vivants (SDSV)  
Spécialité: Sciences de la vie et de la santé

Thèse présentée et soutenue à Villejuif, le 27 Novembre 2017, par

**Shoutang WANG**

## Composition du Jury :

Dr. Sophie CREUZET Université Paris-Saclay	Présidente
Dr. Valérie PINET IGMM, Montpellier	Rapporteur
Dr. Julien BERTRAND Université de Genève	Rapporteur
Dr. Elisa GOMEZ-PERDIGUERO Institut Pasteur	Examinatrice
Dr. Michel MALLAT UPMC, Paris	Examinateur
Dr. Isabelle GODIN Université Paris Sud	Directrice de thèse

**UNIVERSITÉ PARIS-SUD**

**École doctorale n°577 "Structure et Dynamique des Systèmes Vivants"**

**Spécialité : Sciences de la Vie et de la Santé**

**THÈSE DE DOCTORAT**

**Soutenue le 27 Novembre 2017**

**Par Shoutang WANG**

**Fonctions du facteur de transcription Lyl-1 dans le  
développement du lignage macrophagique**

**Composition du jury:**

Directrice de thèse:	Dr. Isabelle GODIN	Université Paris Sud
Rapporteurs:	Dr. Valérie PINET	IGMM, Montpellier
	Dr. Julien BERTRAND	Université de Genève
Examineurs:	Dr. Elisa GOMEZ-PERDIGUERO	Institut Pasteur
	Dr. Michel MALLAT	UPMC, Paris
Présidente:	Dr. Sophie CREUZET	Université Paris-Saclay

## ACKNOWLEDGEMENTS

This work presented here was done at the Institut Gustave Roussy, under the supervision of Dr. Isabelle GODIN. It is my pleasure to thank the many people who helped me during the PhD study.

First of all, I would like to thank my supervisor, Dr. Isabelle GODIN, for giving me this opportunity to work in the team U1170. Thank you for all your systematic guidance, helpful suggestions, kind support and patience throughout the course of this thesis.

I would like to thank all the members of the jury, Dr. Valerie PINET, Dr. Julien BERTRAND, Dr. Elisa GOMEZ-PERDIGUERO, Dr. Michel MALLAT and Dr. Sophie CREUZET for taking time out of teaching/research/life to give critical reading of my thesis.

This thesis would not have been possible without the financial support of China Scholarship Council and Société Française d'Hématologie.

I would like to thank Dr. William VAINCHENKER, for always being prepared to help and advice; Dr. Isabelle PLO, for the general support. I am also thankful to the past and present colleagues in this lab. To Gabriel MATHERAT for the helpful discussion and continuous encouragement. To Deshan REN for the scientific assistance and friendship. I am quite happy to work in this friendly and cheerful group.

I want to acknowledge all of the students, staff and faculty members in Institut Gustave Roussy for providing a productive working atmosphere and for their scientific, administrative and moral support.

Last but not least, I would like to express the deepest gratitude to my parents for their love, care and constant support throughout the past years. Also thanks to my girl friend Tingting LEI for her understanding, accompany and endless encouragement.

# Index

<b>1 INTRODUCTION</b> .....	<b>1</b>
1.1. Ontogeny of the hematopoietic system.....	3
1.1.1 Hematopoietic stem cells .....	3
1.1.2. Hierarchical structure of mouse hematopoietic system.....	5
1.1.3. The regulation of hematopoiesis .....	6
1.1.4. Development of hematopoietic system .....	8
1.1.5. Distinct waves of embryonic hematopoiesis.....	15
1.1.6. The macrophage lineage.....	22
1.2. Development and function of microglia in mice .....	32
1.2.1 Myeloid cell types in the central nervous system.....	32
1.2.2. The development of microglia .....	34
1.2.3. Factors that regulate the development of microglia .....	37
1.2.4. Physiological roles of microglia .....	38
1.2.5 Microglial dysfunction is involved in neurodevelopmental defects.....	43
1.3. Transcription factor Lyl-1 in hematopoiesis .....	46
1.3.1 Lyl-1 function in leukemia .....	46
1.3.2 Functional roles of Lyl-1 in hematopoiesis.....	48
1.3.3 The expression pattern of Lyl-1 during hematopoietic ontogeny.....	49
<b>2 RESULTS</b> .....	<b>51</b>
2.1. Summary .....	52
2.1.1. Lyl-1 expression characterizes primitive macrophage progenitors from the first of YS-derived wave.....	52
2.1.2. Lyl-1 expressing primitive M $\Phi$ give rise to embryonic microglia.....	56
2.1.3. Lyl-1 inactivation impairs M $\Phi$ maturation at early embryonic stage.....	57
2.1.4. Lyl-1 controls embryonic microglia pool at two developmental stages.....	58
2.1.5. Lyl-1-defective microglia induce social anxiety disorders.....	60
2.1.6. Possible involvement of Lyl-1 defects in other neurologic diseases.....	61

2.2. Result 1: Lyl-1 links microglia development to neuropsychiatric disease (Article in preparation) .....	62
2.3. Result part 2: Additional data .....	112
2.3.1. <i>Lyl-1 does not influence macrophage production from AGM-HSC</i> .....	112
2.3.2. <i>Identification of the differences in genes expression between YS-derived primitive and definitive macrophage by RNA sequencing</i> .....	113
2.3.3. <i>Lyl-1 expressing primitive MΦ colonize the fetal liver</i> .....	115
2.3.4. <i>Lyl-1 deficiency leads to a reduction of the microglia pool at E12</i> .....	117
2.3.5. <i>Lyl-1 inactivation results in a reduction of inflammatory-related genes expression</i> .....	119
2.3.6. <i>Bibliographic and database information evidencing a possible involvement of Lyl-1 in human microglia in health and diseases</i> .....	120
<b>3 GENERAL DISCUSSION AND PERSPECTIVES .....</b>	<b>126</b>
3.1 Lyl-1 expression discriminates the YS-derived primitive and definitive macrophages.....	127
3.2 YS-derived primitive macrophages (Lyl-1 positive) give rise to the embryonic microglia.	129
3.3 Lyl-1 regulates the development and functions of microglia and is involved in neuro-developmental diseases. ....	131
<b>4 RÉSUMÉ DE LA THÈSE EN FRANÇAIS .....</b>	<b>134</b>
<b>5 REFERENCES .....</b>	<b>147</b>

# Figure list

<i>Figure 1: The hierarchy of hematopoietic cells.</i> .....	4
<i>Figure 2: Schematic of the heptad transcription factor complexes bound to DNA.</i> .....	8
<i>Figure 3: Schematic representation of the successive hematopoietic sites during mouse ontogeny.</i> .....	11
<i>Figure 4: Migratory and circulatory routes of hematopoietic cells in the murine embryo over developmental time.</i> .....	14
<i>Figure 5: Different hematopoietic waves during ontogeny.</i> .....	17
<i>Figure 6: Comparison between primitive and definitive erythropoiesis.</i> .....	19
<i>Figure 7: Developmental stages followed by the 3 distinct M<math>\Phi</math> waves, characterized by their phenotype, origin, differentiation potential, and lineage relationship.</i> .....	21
<i>Figure 8: Localization and functions of macrophage and monocyte subpopulations.</i> .....	23
<i>Figure 9: A Schema of the constitutive and inducible conditional gene targeting approaches.</i> .....	25
<i>Figure 10: Fate-mapping systems of macrophages and other hematopoietic cell.</i> .....	27
<i>Figure 11: Three Different Models of Fetal Macrophage Ontogeny.</i> .....	29
<i>Figure 12: The localization and genetic signature of CNS macrophages.</i> .....	33
<i>Figure 13: Microglial origin and development.</i> .....	36
<i>Figure 14: Main microglial functions during CNS development.</i> .....	42
<i>Figure 15: Schematic comparison of the two targeted alleles of Lyl1.</i> .....	48
<i>Figure 16: Lyl-1 does not influence the production of M<math>\Phi</math> from AGM-HSC.</i> .....	113
<i>Figure 17: Lyl-1<sup>+</sup> primitive M<math>\Phi</math> progenitors are present in the fetal liver at E10.</i> .....	116
<i>Figure 18: Lyl-1 deficiency leads to a reduction of the microglia pool at E12.5.</i> .....	118
<i>Figure 19: Lyl-1 inactivation results in a reduction of inflammatory-related genes expression.</i> .....	119

## Abbreviations

β-Gal:	β-Galactosidase
AGM:	Aorta-Gonad-Mesonephros
AML:	Acute Myeloblastic Leukemia
ASD:	Autism Spectrum Disorder
BDNF:	Brain-Derived Neurotrophic Factor
BFU-Es:	Burst-forming Units-erythroid
bHLH:	basic Helix-Loop-Helix
BM:	Bone Marrow
CLP:	Common Lymphoid Progenitor
CMP:	Common Myeloid Progenitor
CNS:	Central Nervous System
cpMΦ:	Choroid Plexus Macrophages
CREB1:	Cyclic AMP Receptor Element Binding Protein 1
CSF1R:	Colony Stimulating Factor 1 Receptor
DAP12:	DNAX activation protein of 12 kDa
DCs:	Dendritic Cells
E:	Embryonic Day
EMp:	Erythro-Myeloid Progenitors
ER:	Estrogen Receptor
EryP-CFCs:	Primitive Erythroid Colony-forming Cells
ETPs:	Early T Lineage Progenitors
FACS:	Fluorescence-activated Cell Sorting
FL:	Fetal Liver
Flt3:	FMS-like Tyrosine Kinase 3
GFP:	Green Fluorescent Protein
GM:	Granulo-Monocytic
GMP:	Granulocyte-Macrophage Progenitor

HSCs:	Hematopoietic Stem Cells
IGF-1:	Insulin-like Growth Factor-1
IL-1R:	Interleukin-1 Receptor
IRF8:	Interferon Regulatory Factor 8
Lmo2:	LIM domain only 2
LMPP:	Lymphoid-primed Multipotent Progenitors
LSK:	Lin <sup>-</sup> Sca-1 <sup>+</sup> c-Kit <sup>+</sup>
LT-HSC:	Long-Term Repopulating Hematopoietic Stem Cells
LTR:	Long-Term Reconstitution Assay
Lyl-1:	Lymphoblastic leukemia 1
MeCP2:	Methyl-CpG-Binding Protein 2
Mer:	Modified Estrogen Receptor
mMΦ:	Meningeal Macrophages
MΦ:	Macrophages
MPP:	Multi-potent Progenitor
MEP:	Megakaryocyte/Erythroid Progenitor
OrgD1:	Organ Cultured for 1 Day
P:	Postnatal
P-Sp:	Paraaortic Splanchnopleura
pvMΦ:	Perivascular Macrophages
Runx1:	Runt-related transcription factor 1
S:	Somite
Scf/Tal-1:	Stem Cell Leukemia/T-ALL 1
ST-HSC:	Short-Term Repopulating Hematopoietic Stem Cells
STMN1:	Stathmin
T-ALL:	T-cell Acute Lymphoblastic Leukemia
TNFs:	Tumor Necrosis Factors
YS:	Yolk Sac

# **1 INTRODUCTION**

## Objective and Organization of the thesis

Transcription factors, such as SCL/Tal-1, Lmo2, Runx1 and GATA-2, are proved to control hematopoietic cells fate decision, cellular phenotypes, and differentiation. Lyl-1 is a bHLH transcription factor that is closely related to SCL/Tal-1, which is required for hematopoietic development in the embryo. Moreover, we previously showed using the *Lyl-1<sup>LacZ</sup>* strain that Lyl-1 expression pattern during ontogeny largely overlaps with that of SCL/Tal-1, indicating that Lyl-1 may play a role during developmental hematopoiesis. My thesis mainly focuses on the Lyl-1 function in developmental hematopoiesis, which is still unknown.

Two transgenic mouse models, *Lyl-1<sup>LacZ</sup>* and *Cx3cr1<sup>GFP</sup>*, in the laboratory contributed to the studies. The key points of the studies are: (1) the effects of Lyl-1 inactivation in hematopoiesis during early embryonic development; (2) Lyl-1 expression pattern in yolk sac-derived primitive and definitive macrophage lineage; (3) the contribution of yolk sac-derived Lyl-1 positive MΦ population to microglia development; (4) the defects of macrophage/microglia development in Lyl-1 mutants; (5) the characterization of neurogenesis and behavior in adult *Lyl-1* mutants.

During the course of my thesis, I had to gather information on different fields, developmental biology, hematopoiesis and its regulation by transcription factors, macrophage and microglia development and neuro-development.

I will first give a general background about part of these fields related to my research in the introduction. I will then summarize the experiments design and the results I obtained.

Altogether, I expect that this work will contribute to a better understanding of the functions of Lyl-1 in developmental hematopoiesis and neurogenesis.

## 1.1. Ontogeny of the hematopoietic system

### 1.1.1 Hematopoietic stem cells

In adult mammals, blood cells are constantly produced from progenitors in the bone marrow (BM) to replenish short-lived mature blood cells throughout life (Cumano and Godin, 2007). This constant process initiates from a rare population of progenitors, the hematopoietic stem cells (HSCs). HSCs reside in the BM in adult mammals and can produce a series of multi-lineage progenitors, then to lineage-committed precursors. This progressive differentiation process ultimately gives rise to all types of mature blood cells, including erythrocytes, megakaryocytes, myeloid cells (monocyte/macrophage and granulocytes), dendritic cells (DCs), B and T lymphocytes and natural Killer cells (**Fig 1**) (Clements and Traver, 2013; Orkin, 2000; Weissman, 2000). Analysis of blood system regeneration *in vivo* revealed that HSCs possess two main properties, multi-potency and self-renewal, which are also the only hematopoietic cells that contain both potential (Ema et al., 2005; Hock, 2010; Morita et al., 2010; Osawa et al., 1996; Wagers et al., 2002). Multi-potency makes HSCs able to produce a differentiated progeny comprising all the different blood cell types. Self-renewal allows the maintenance of the HSC pool without cell differentiation through asymmetric cell division (Jones et al., 2015; Wilson et al., 2004). After committed differentiation, the progeny of HSCs progressively lose self-renewal capacity and becomes restricted to single lineages. BM transplantation has shown that a single HSC is capable of repopulating the entire hematopoietic system of a recipient (Dyksta et al., 2007; Kiel et al., 2005; Osawa et al., 1996; Sieburg et al., 2006; Smith et al., 1991).

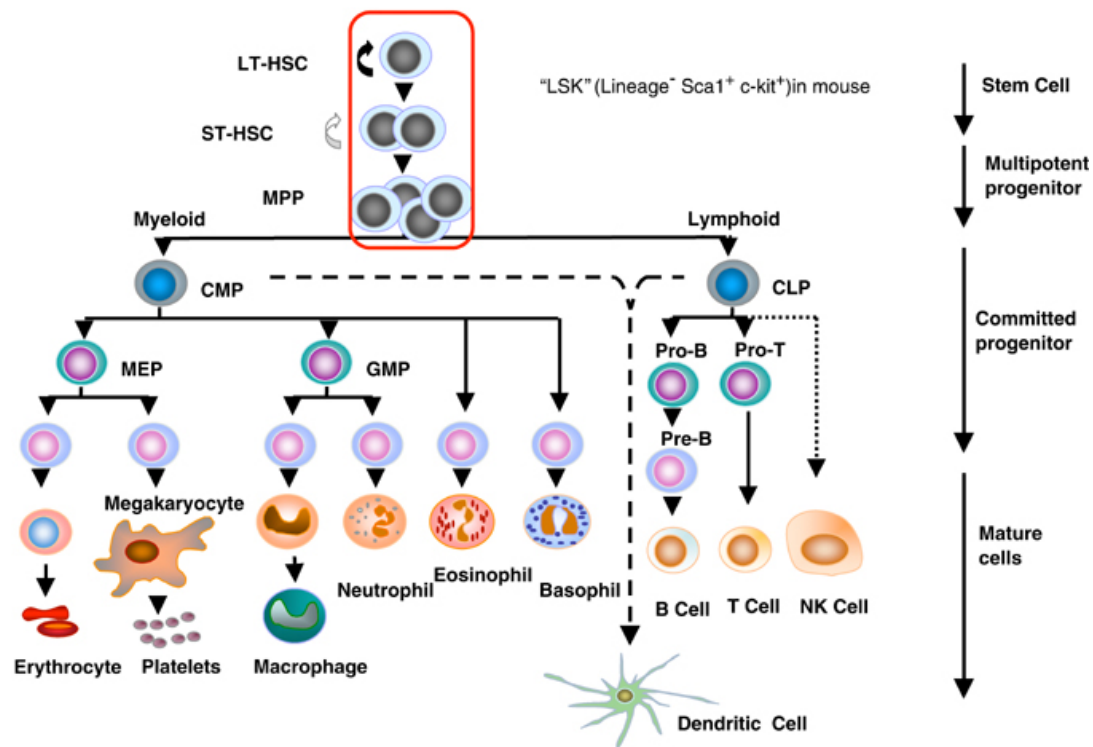


**Figure 1: The hierarchy of hematopoietic cells.**

Abbreviations: LT-HSC, long-term repopulating HSC; ST-HSC, short-term repopulating HSC; MPP, multi-potent progenitor; CMP, common myeloid progenitor; CLP, common lymphoid progenitor; MEP, megakaryocyte/erythroid progenitor; GMP, granulocyte-macrophage progenitor. The encircled pluripotent population, LT-HSC, ST-HSC and MPP are Lin<sup>-</sup>Sca-1<sup>+</sup>c-kit<sup>+</sup> as shown (Larsson et al., 2005).

### 1.1.2. Hierarchical structure of mouse hematopoietic system

Progress in investigating phenotypic and functional characterization of HSCs and other precursors has made the hematopoietic system a paradigm in stem cell biology (Orkin and Zon, 2008; Rowe et al., 2016). Experimental evidences showed that HSCs can be isolated from multi-committed progenitors and BM cells by fluorescence-activated cell sorting (FACS) based on specific phenotypic markers (**Table 1**) (Adolfsson et al., 2001; Christensen and Weissman, 2001; Kiel et al., 2005). In the mouse, HSCs have been initially extensively purified from BM by utilizing cell-surface markers,  $\text{Lin}^- \text{Sca-1}^+ \text{c-Kit}^+$  (LSK) ( $\text{Lin}^-$  corresponding to the fraction that does not express markers specific for mature cells for the various lineages, such as CD11b for macrophage, Gr1 for granulocyte, etc). But it was later shown that this fraction also contain restricted progenitors. The self-renewal has been better defined though *in vivo* functional assay named long-term reconstitution assay (LTR). This experimental approach makes use of congenic cell surface markers that differ between donor and host (e.g. CD45.1/CD45.2) to follow the progeny of multi-potential hematopoietic cells *in vivo* after transferring the HSCs into the irradiated recipient over six months. HSCs are now defined phenotypically as  $\text{Flk2}^- \text{CD34}^-$  LSK cells, also named Long-Term (LT)-HSCs (Yang et al., 2005). *In vitro* and *in vivo* assays performed to determine the differentiation potential of HSCs and of other progenitors have suggested a hierarchical structure in hematopoietic development in which self-renewal is maintained by particular subsets and multi-potency is progressively restricted (**Fig 1**) (Akashi et al., 2000; Kondo et al., 1997; Nakorn et al., 2003). It is generally accepted that LT-HSCs partially lose their self-renewal potential and transit to Short-Term (ST)-HSCs ( $\text{Flk2}^- \text{CD34}^+$ ) (Akashi, 2005; Hock and Orkin, 2005). Then ST-HSCs give rise to the multi-potent progenitors (MPPs), which no longer possess self-renewal ability yet keeping full-lineage differentiation potential. Recent evidences showed that MPPs are still heterogeneous, which is considered as a fully multi-potent but lineage-biased population (Pietras et al., 2015). Different phenotypic MPP subsets are produced in parallel by ST-HSCs at variable levels depending on hematopoietic demands. MPPs further advance to myeloid lineage by generating common myeloid

progenitors (CMPs) or lymphoid lineage by generating common lymphoid progenitors (CLPs). Collectively these committed progenitors then give rise to all the mature cells of the hematopoietic system, such as CMPs produce megakaryocyte/erythrocyte progenitors (MEPs) to follow the megakaryocyte/erythrocyte lineage or produce granulocyte-macrophage progenitors (GMPs) to follow the granulocyte/macrophage lineage. Interestingly, the major subsets of DCs can be derived either from CMP and CLP (Geissmann et al., 2010).

**Table 1: Surface marker phenotypes to separate mouse stem and progenitor cell subsets** (Galen et al., 2014)

<b>Population</b>	<b>Surface phenotype</b>
LSK	Lin <sup>-</sup> Sca-1 <sup>+</sup> c-Kit <sup>+</sup>
LT-HSC	Lin <sup>-</sup> Sca-1 <sup>+</sup> c-Kit <sup>+</sup> Flk2 <sup>-</sup> CD34 <sup>-</sup>
ST-HSC	Lin <sup>-</sup> Sca-1 <sup>+</sup> c-Kit <sup>+</sup> Flk2 <sup>-</sup> CD34 <sup>+</sup>
MPP	Lin <sup>-</sup> Sca-1 <sup>+</sup> c-Kit <sup>+</sup> Flk2 <sup>+</sup> CD34 <sup>+</sup>
Progenitor	Lin <sup>-</sup> Sca-1 <sup>-</sup> c-Kit <sup>+</sup>
CMP	Lin <sup>-</sup> Sca-1 <sup>-</sup> c-Kit <sup>+</sup> FcγII/IIIIR <sup>lo</sup> CD34 <sup>+</sup>
GMP	Lin <sup>-</sup> Sca-1 <sup>-</sup> c-Kit <sup>+</sup> FcγII/IIIIR <sup>hi</sup> CD34 <sup>+</sup>
MEP	Lin <sup>-</sup> Sca-1 <sup>-</sup> c-Kit <sup>+</sup> FcγII/IIIIR <sup>-</sup> CD34 <sup>-</sup>

### 1.1.3. The regulation of hematopoiesis

Hematopoietic progenitors features, such as cell fate decision, progenitor maintenance and differentiation, etc. are regulated by a transcription factor network that comprises, amongst others, Stem Cell Leukemia/T-ALL 1 (Scl/Tal-1), Runt-related transcription factor 1 (Runx1), LIM domain only 2 (Lmo2), which are the major regulators of hematopoietic progenitors development during ontogeny (Pina and Enver, 2007; Wilson et al., 2010). Scl/Tal-1, Lmo2 and Runx1 are believed to orchestrate the formation of the HSC pool during embryonic development. Either Scl/Tal-1 or Lmo2 (Shivdasani et al., 1995; Wilson et al., 2009) were shown to be essential for hematopoietic cell fate specification since knock out embryos exhibited early lethality due to a complete absence of blood cells. The initial step of

hematopoietic development (yolk sac hematopoiesis, see chapter 1.5) is occurring normally in *Runx1* knock out mice, but the generation of fetal HSCs is blocked in this model (Speck, 2001). However, conditional deletion of these factors in adult hematopoietic cells showed that they are not required for the maintenance of HSCs in the BM. Instead, more lineage-specific defects were seen. Conditional *Runx1* ablation inhibited CLP production, blocked B-cell and T-cell maturation, and reduced platelet formation. Similarly, conditional deletion of *Scl/Tal-1* in adult HSCs did not affect HSC engraftment, self-renewal and differentiation into myeloid and lymphoid lineages. However, differentiation into erythroid and megakaryocytic precursors was perturbed. Taken together, such comparative findings from conventional and conditional transcription factor knockout mice indicate that there is a clear difference in the requirement for different factors in the establishment versus maintenance of the HSC pool. In addition, regarding the macrophage (MΦ) lineage central to this work, the formation of the earliest myeloid transcriptional network essentially depends on Pu.1 (also called Spi1). Pu.1 deletion in mice resulted in a fatal defect in fetal liver (FL) and/or newborn hematopoiesis, including the complete absence of B cells and MΦ (Lichanska et al., 1999; Olson et al., 1995). The expression of *Pu.1* is regulated by other hematopoietic transcription factors (e.g., Runx1). Runx1 directly binds to the upstream regulatory element of the *Pu.1* gene and modulates its expression during embryonic and adult hematopoiesis (Imperato et al., 2015).

Combining transcription factor gene expression data in HSCs with genome-wide ChIP-seq analysis using the hematopoietic progenitor cell line HPC-7 revealed that *Scl/Tal-1*, *Runx1* and *Lmo2* belong to a heptad transcriptional complex, which also includes the Lymphoblastic leukemia 1 (*Lyl-1*) (Wilson et al., 2010) (**Fig 2**), suggesting that *Lyl-1* may play roles in regulation of HSCs function. Sequence analyses showed that *Lyl-1* protein closely relates to *Scl/Tal-1* that is mandatory for numerous decisions in embryonic and adult hematopoiesis (Curtis et al., 2012), as they share 82% of amino acid identity in the basic helix-loop-helix (bHLH) regions, providing the possibilities that these two proteins might bind to some common target genes and share partial biologic functions. However, sequences

outside the bHLH region of Lyl-1 and Scl/Tal-1 are largely divergent (Chan et al., 2007; San-Marina et al., 2008). Moreover, single-cell expression analysis of HSCs displayed a distinct expression pattern in HSCs between these two transcription factors (Ramos et al., 2007), and ChIP-seq analysis demonstrated that Lyl-1 has a very different pattern of transcription factor binding with Scl/Tal-1, with the majority of binding peaks over intragenic or intergenic sites rather than within 61 kb of transcription start sites, suggesting that Lyl-1 may exert specific functions during hematopoiesis (Wilson et al., 2010). The evidence pointing to Lyl-1 function during developmental hematopoiesis will be developed latter.

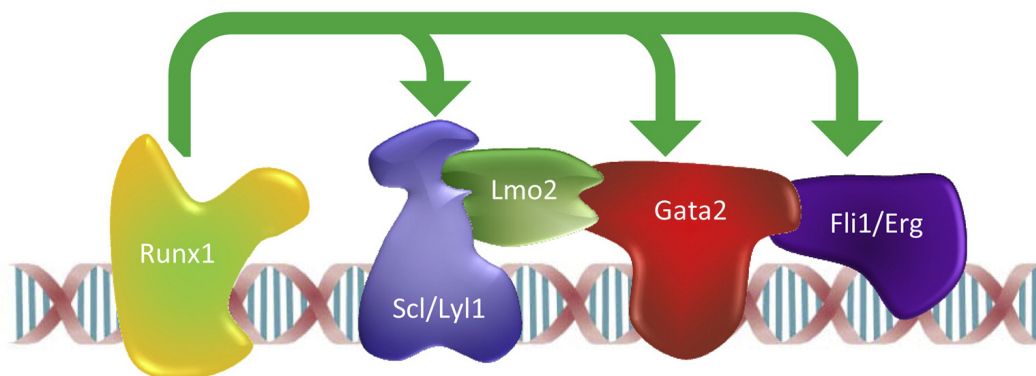


**Figure 2: Schematic of the heptad transcription factor complexes bound to DNA.**

The links between RUNX1 and SCL/LYL1/GATA2/ERG are indicated by green arrows. The order of proteins shown is for illustrative purposes rather than reflecting a particularly common arrangement of binding sites (adapted from Wilson et al, 2010).

## 1.1.4. Development of hematopoietic system

### 1.1.4.1. The main steps

Hematopoietic cells are generated during embryonic development and sequentially colonize the FL, the thymus, then the spleen, and finally the BM (**Fig 3**) (Cumano and Godin, 2007). The first hematopoietic site is the yolk sac (YS) blood islands, where the hematopoietic

activity initiates from early organogenesis (soon after gastrulation) and hematopoietic progenitors are generated *in situ* (Haar and Ackerman, 1971). Because of this early generation, for years researchers considered the YS to be the source of HSCs that colonize further hematopoietic sites. However, the YS origin of HSCs was challenged by chick/quail chimeras construction experiments (quail embryo body grafted into a chicken YS) that showed YS-derived cells are not able either to produce hematopoietic cells sustainably or to give rise to lymphoid cells (Beaupain et al., 1979; Dieterlen-Lievre, 1975; Lassila et al., 1982). Hence, YS progenitors lack of multipotential and long-term maintenance, therefore, the YS is not the initial source of HSCs. In addition, similar chick/quail chimeras experiments showed that HSCs come from the embryo body, precisely the aorta region. In the mouse, Godin et al demonstrated that at embryonic day 9 (E9), the region that contains the developing aorta, known as the paraaortic splanchnopleura (P-Sp), was able to give rise to B cells upon transfer into irradiated mice, whereas the YS precursors could not (Godin et al., 1995). Other groups pointed to the same region named the aorta-gonad-mesonephros (AGM) at slightly later stage (E10.5) as containing stem cells capable of long-term multilineage repopulation in adult recipients (Medvinsky et al., 1996; Muller et al., 1994). The P-Sp and AGM are identical regions at two different development time points and can be referred to as P-Sp/AGM.

The *in situ* origin of HSCs in the mouse dorsal aorta was established through organ culture of the embryonic site that will give rise to the P-Sp/AGM. This part of the embryo (called Splanchnopleura) was isolated at E8, before any hematopoietic cells are generated in the embryo body, and also before blood cells circulate from the YS to the embryo (a connection that occurs at the 4-5 somite [S] stage) (McGrath et al, 2003). *In vitro* and *in vivo* analyses of the hematopoietic cells grown for the Sp-explants and from the corresponding YS showed that hematopoietic progenitors with multilineage potential (including lymphoid) and LTR-activity could develop after organ culture from the Sp region that will later give rise to the P-Sp/AGM, indicating *in situ* generation of HSCs. In contrast, the corresponding YS, similarly treated, only gave rise to erythro-myeloid cells, and had short term (up to 2 month)

erythro-myeloid reconstitution potential *in vivo* (Cumano et al., 1996, 2001). The model of HSCs development during embryonic life is the same in human embryos (Ivanovs et al., 2014; Tavian et al., 2001).

These findings together established the fundamental notion that embryonic hematopoiesis initiates in two independent sites, first in the YS and later in the P-Sp/AGM that is the first place for HSCs emerge (Cumano and Godin, 2007; Cumano et al., 2001; Godin et al., 1999). As a consequence, the YS-derived hematopoiesis is independent on HSCs, and it does not follow the same differentiation processes as in the adult hierarchy (**Fig 1**). I will first give the information about HSCs development, then describe later the details of the development of YS-derived hematopoiesis, which is more related to my thesis project.

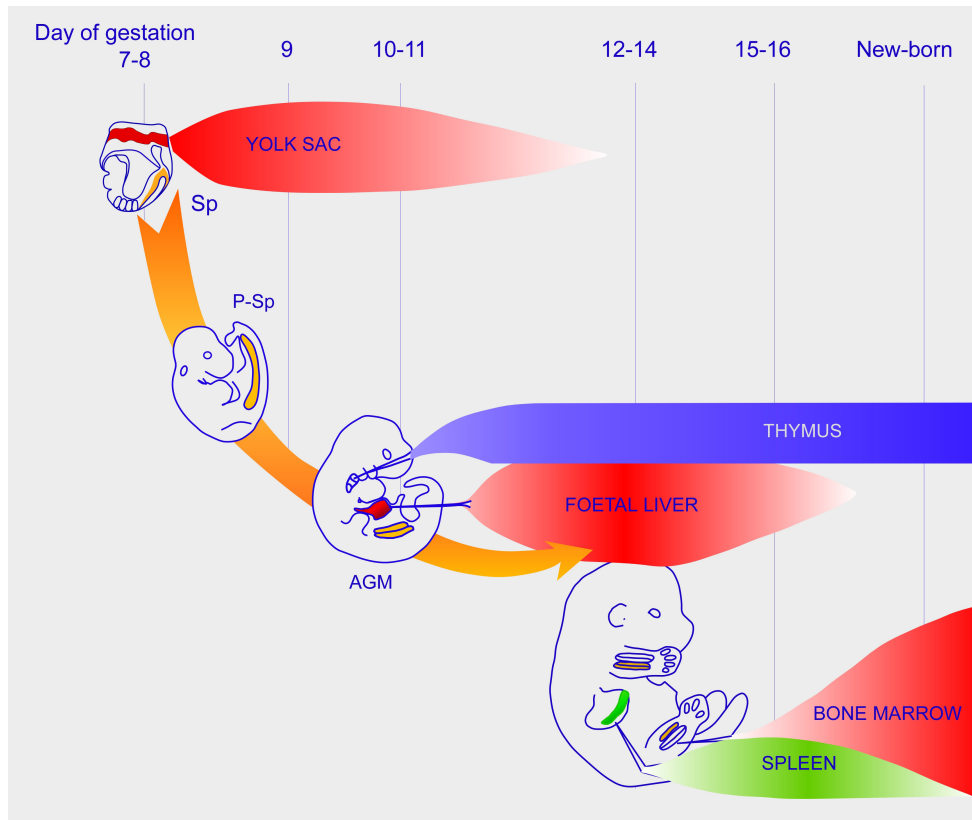


**Figure 3: Schematic representation of the successive hematopoietic sites during mouse ontogeny.**

An illustration of a mouse shows the hematopoietic sites and organs during embryonic development (two independent hematopoietic sites: yolk sac and P-Sp/AGM; intermediate site: fetal liver; hematopoietic organs: the first being the thymus, then the spleen and, finally, the bone marrow; the placenta has not been considered to be a hematopoietic organ.). P-Sp/AGM: paraaortic splanchnopleura/aorta-gonad-mesonephros region.

#### **1.1.4.2. HSCs generation and further contribution to hematopoietic development**

HSCs are generated in the P-Sp/AGM region but do not differentiate *in situ* (Godin et al., 1999; de Bruijn et al., 2000; Kumaravelu et al., 2002; Lancrin et al., 2009). *In vitro* assays revealed that the vast majority of hematopoietic cells in this region remain multipotent

(Godin et al., 1999). In addition, the circulating blood is found to contain multipotent hematopoietic progenitors as early as E10 when the production of HSCs has not reached the maximum level (Delassus and Cumano, 1996). These observations suggest that P-Sp/AGM should be considered as a generation site of HSCs but not a site of hematopoietic differentiation. Moreover, beside the aorta, other arterial regions (vitelline and umbilical vessels) were found to be sites for HSCs emergence (de Bruijn et al., 2000; Inman and Downs, 2007), suggesting a close relationship between the developing hematopoietic and vascular systems.

Intraembryonic HSCs were phenotypically characterized as c-Kit high, CD41 medium, CD45 low to undetectable (Bertrand et al., 2005a). They also share a large number of markers with endothelial cells, such as CD31, CD34, AA4.1, VE-Cadherin, Tie2, etc. Because of the close physical relationship between developing HSCs and the artery wall, and also because HSCs and endothelial cells share so many surface markers and transcription factors (Scf/Tal-1, Lmo2 Runx1, GATA-2) that are important for the production of hematopoietic progenitors, a common progenitors for both lineages was considered (hemangioblast for the YS and hemogenic endothelium for the P-Sp/AGM). The model considered now for HSCs generation, following evidences gathered in zebrafish (Bertrand et al., 2010; Kissa and Herbomel, 2010), chicken (Jaffredo et al., 1998) and mouse (Boisset et al., 2010) models, is that they develop from already differentiated endothelial cells through a mechanism called endothelia to hematopoietic transition.

Once HSCs are generated, they rapidly enter circulation and reach the different hematopoietic organs (**Fig 4**). HSCs activity was found in the mouse placenta starting at E10.5-E11.0 and the placental HSCs pool rapid expands between E11.5 and 12.5 (Gekas et al., 2005). As a result, the placenta harbors significant numbers of HSCs that is over 15-fold more than does the AGM region or the YS, suggesting that the placenta may provide a unique microenvironment for HSC development. Placental HSCs could be generated *in situ* or be colonized by AGM- or FL-HSCs though circulation, or both, which still needs to be comprehensively studied.

The properties of HSCs in each site vary in function, most probably depending on diverse niches that modulate HSCs expansion and/or differentiation and ensure intrinsic characteristics of HSCs at each stage (Cordeiro Gomes et al., 2016; Martinez-Agosto et al., 2007; Wang and Wagers, 2011). The FL is considered as the major site of hematopoietic site during embryonic development, where the size of hematopoietic cell pool largely amplifies to fulfill the requirement of embryonic development (Godin and Cumano, 2002; Mikkola and Orkin, 2006). Exogenous hematopoietic cells colonize the FL to initiate hematopoiesis (Müller et al., 1994; Sánchez et al., 1996; Kieusseian et al., 2012). Considering the limited number of HSCs produced in the P-Sp/AGM (500-1000 cells) (Godin et al., 1999) and the extent of hematopoietic activity observed at early stages in FL, it is likely that the majority of cells that initially colonize the FL are erythroid/myeloid cells from the YS, which has generated numerous hematopoietic cells and establishes the first vascular connections to the FL through vitelline vessels (Cumano and Godin, 2007). HSCs are detected in the FL at E10 (Kieusseian et al., 2012). In contrast to adult BM, where HSCs are largely quiescent (Oguro et al., 2013; Reagan and Rosen, 2016), in the FL, HSCs are actively cycling. Indeed, FL provides an unique microenvironment that allows the rapid expansion of HSCs. HSCs expand in numbers from E12.5 to E16.5 and acquire the final characteristic phenotypic makers that define them in the adult BM around E15 (Morrison et al., 1995). In addition to supporting HSCs expansion, the FL is also the main hematopoietic site for the differentiation of erythrocytes, myeloid cells and lymphocytes (Kieusseian et al., 2012). It is generally stated that FL HSCs migrate to the BM and become the main contributors to adult hematopoiesis. Transplantation assays in mice have demonstrated that FL HSCs start to colonize the BM during late period of gestation (Medvinsky et al., 2011).

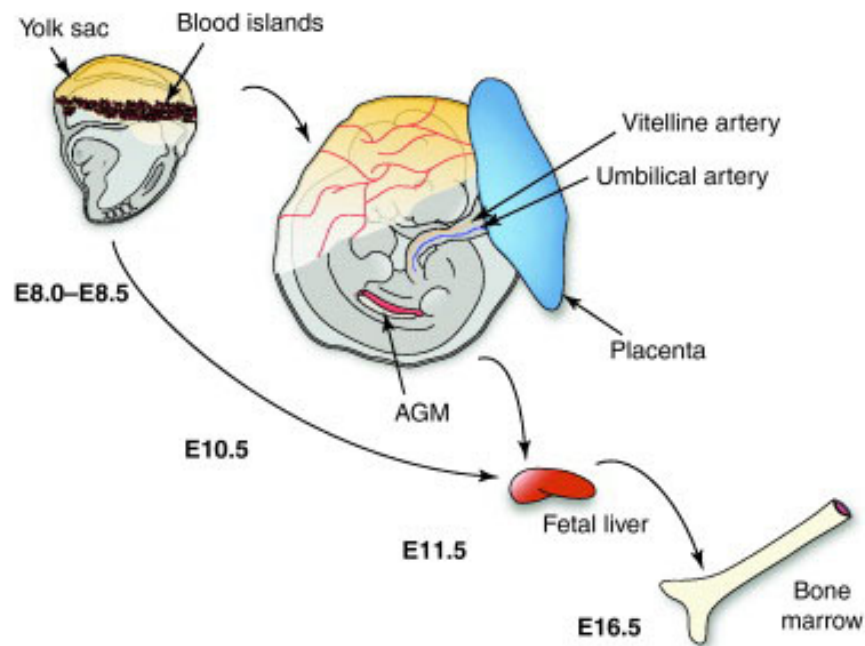


**Figure 4: Migratory and circulatory routes of hematopoietic cells in the murine embryo over developmental time.**

The first hematopoietic progenitors are found in the YS blood islands at E8.0-E8.5. Once circulation is established, blood cells colonize other developing hematopoietic organs through vitelline artery. Around E9.5, the P-Sp/AGM initiate the generation of blood precursors that, together with YS cells, colonize to the FL rudiment. The FL is the major hematopoietic site where blood progenitors expand and/or mature. Finally, the BM is colonized by precursors from the FL before birth and remains the main hematopoietic niche throughout adult life (from Costa et al., 2012).

## 1.1.5. Distinct waves of embryonic hematopoiesis

### 1.1.5.1. The three waves

During embryonic development, the hematopoietic system is established in three successive waves that are temporally and spatially restricted, with each producing specific blood progenitors (**Fig 5**) (McGrath et al., 2016; Palis, 2016; Yoder, 2014). The first wave of blood production is termed “primitive” and initially arises in the blood islands of the developing YS at E7.5 (Palis, 2014). The initial primitive hematopoiesis process is considered to be unilineage, while the adult-type hematopoiesis that is termed “definitive” is multilineage. Studies in the spatial and temporal kinetics of early embryonic hematopoiesis potential indicate that primitive hematopoiesis is restricted to the erythroid, megakaryocyte, and MΦ lineages and does not produce lymphoid cells or HSCs (Palis et al., 1999; Tober et al., 2006, 2008; Yoshimoto et al., 2011). I will give more information on this wave in the following chapter.

The second wave of hematopoiesis occurs in the YS between E8.0 and E8.5 with the appearance of “erythro-myeloid progenitors” (EMp) that continue to be formed until E10.5 (Frame et al., 2013, 2015; Lux et al., 2008; McGrath et al., 2015a). Clonogenic analysis has confirmed that EMp are able to give rise to definitive erythroid cells and megakaryocyte, and to broad myeloid lineage (MΦ, and various types of granulocytes, as well as their common granulo-monocytic [GM] progenitors), but do not contain lymphoid potential (McGrath et al., 2015b), meaning that the primitive and EMp-derived definitive hematopoiesis share erythro-myeloid potential. Contrary to EMp that give rise to the mature cells through a progressive differentiation process with intermediate progenitors (GM and EMk), mature MΦ in the first primitive wave appear to lack of the intermediate progenitors.

Because EMp-derived hematopoiesis wave lacks the long-term repopulating potential and produces mature cells in a differentiation pathway similar to the adult, this wave has been called the “transient definitive” wave, distinguishing it from the earlier primitive

hematopoiesis that is composed of transient wave of monopotent hematopoietic progenitors and the third which is the HSCs-derived definitive wave of hematopoiesis (McGrath et al., 2016). McGrath et al showed that YS-derived EMp have a unique immune-phenotype (McGrath et al., 2015a): at E8.5, EMp express significant c-Kit and CD41 on their cell surface, while primitive erythroid progenitors (primitive erythroid colony-forming cells [EryP-CFCs]) reside in the c-Kit<sup>lo</sup>CD41<sup>lo</sup> population. By E9.5, EMp can be prospectively identified as the surface marker of c-Kit<sup>+</sup>CD41<sup>+</sup>CD16/32<sup>+</sup>, distinguishing from maturing populations of c-Kit<sup>neg</sup> CD16/32<sup>+</sup> CD45<sup>hi</sup> primitive MΦ and c-Kit<sup>neg</sup> CD41<sup>hi</sup> Gp1bβ<sup>+</sup> primitive megakaryocytes. At E10.5, EMp are found to remain present in the YS and the blood circulation, but are more highly enriched in the FL, where they expand and differentiate into multiple cell lineages (McGrath et al., 2015a).

Recent evidences showed that during the second wave of hematopoiesis, B and T lymphoid progenitors also arise from the YS, as well as in the embryo proper around E9.0 (Boiers et al., 2013; Cumano et al., 1996; Yoshimoto et al., 2012). These B or T lymphocyte-restricted progenitors migrate to and differentiate in the early FL, and are thought to provide unique subsets of lymphoid cells that persist in the adult. However, although this wave of hematopoiesis contains erythro-myeloid and lymphoid potential, it is not involved in adult-type HSCs.

The third wave begins at E10.5 with the emergence of HSCs in the AGM regions and in other embryonic arterial vessels (Cumano and Godin, 2007). As mentioned above, these precursors then colonize the FL where they begin to expand in numbers and establish definitive hematopoiesis.

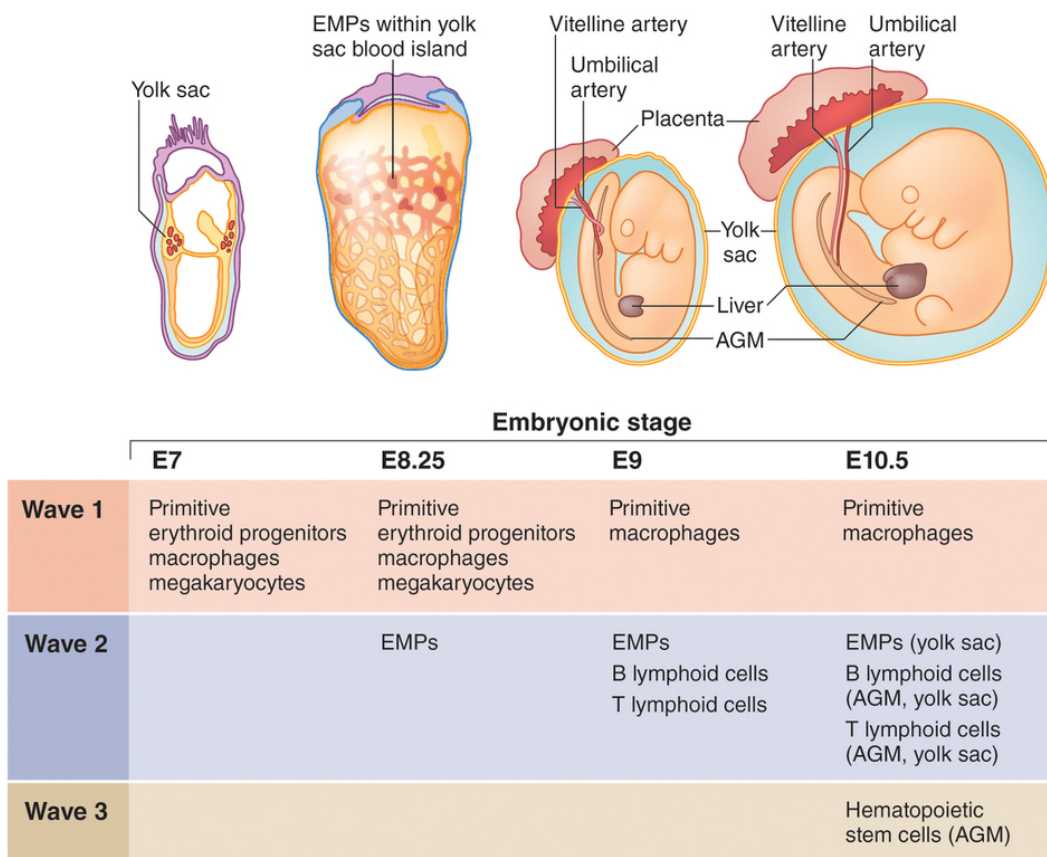


**Figure 5: Different hematopoietic waves during ontogeny.**

The first wave originates primarily in the YS to produce primitive erythrocyte, MΦ and megakaryocytes. A second wave consists of erythroid-myeloid progenitors (EMp) and lymphoid-biased progenitors that can reconstitute lethally irradiated recipients after experimental transplantation, but spontaneously disappear before adulthood in their native environment. The third wave is that conventional fetal HSCs give rise to the quiescent adult HSCs that sustain post-natal hematopoiesis (Yoder, 2014).

### 1.1.5.2. YS-derived waves: erythropoiesis in the primitive and transient definitive waves

Studies of adult hematopoiesis provide an assumption that all circulating blood cells are ultimately generated by HSCs. This paradigm was also applied to the embryonic hematopoiesis in early studies. However, as mentioned above, while the emergence of HSCs begins at E10 in the AGM region of the embryo proper, a functional hematopoietic circulatory system, involving embryonic (primitive) erythroid cells, definitive erythrocytes, as well as platelets and hematopoietic progenitors, has already established in the murine embryo (Palis, 2016). In fact, early erythropoiesis is essential for survival and growth of the murine embryo, as the newly forming bloodstream need to be filled by hemoglobinizing primitive erythroblasts (Baron et al, 2012, 2013; Ferkowicz et al, 2003; Palis et al., 2001). The first few EryP-CFCs appear in the YS blood island of the late streak mouse embryo at E7.25 and produce large, nucleated  $\beta$ H1-globin-expressing erythroid cells. EryP-CFCs transiently expand in numbers by E8.5, and subsequently differentiate into a cohort of primitive erythroblasts in the bloodstream with the onset of the cardiac contractions at E8.25 (Kingsley et al., 2004). Just soon after the appearance of EryP-CFCs, the overlapping wave of definitive erythroid progenitors (burst-forming units-erythroid [BFU-Es]) begins to emerge, also in the YS, accompanied temporally and spatially by megakaryocyte and myeloid cells (Ferkowicz et al, 2003). In contrast with primitive erythroblasts, definitive erythroblasts are smaller, anucleate and express adult globin genes, which are similar to those found later in the FL and adult BM (**Fig 6**) (Baron et al, 2012). BFU-Es increase in numbers by E9.5 within the YS, then transit to the newly forming liver, prior to the HSCs colonization, and rapidly set up the definitive erythropoiesis (McGrath et al., 2011). Thus, continuous production of erythrocytes derived by BFU-Es ensures the requirement of the dramatically growing mid-gestation mouse embryo and provides an essential bridge between transient primitive erythropoiesis and HSC-derived definitive erythropoiesis. Though the primitive and definitive erythropoiesis have been well characterized, little is known about the differences between primitive and definitive megakaryocytes, as well as primitive and definitive M $\Phi$  in terms of specific function for embryonic development.

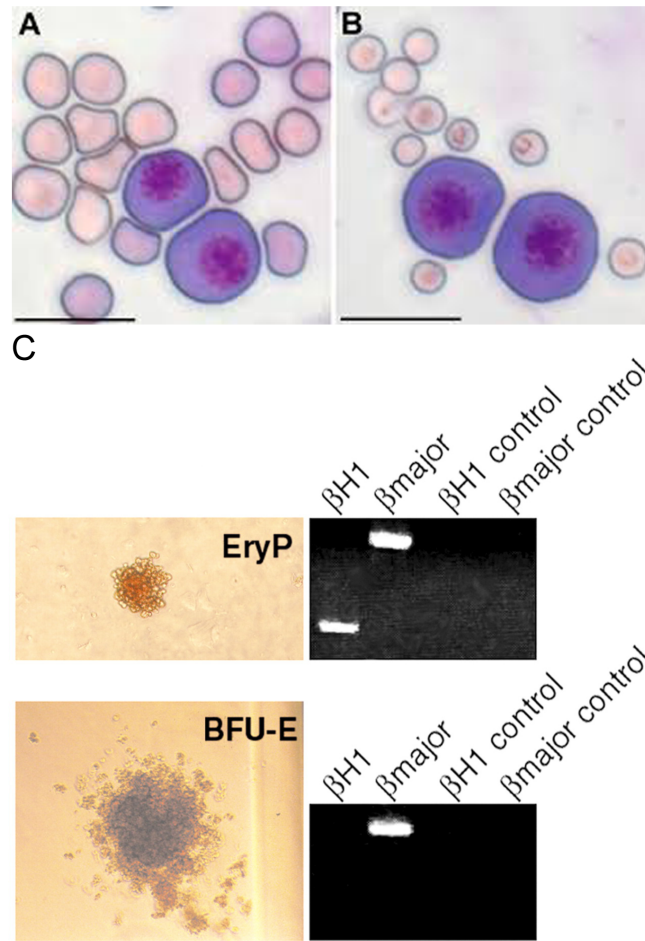


**Figure 6: Comparison between primitive and definitive erythropoiesis.**

(A) Morphology of primitive and definitive erythroblasts. EryP-CFCs (E10.5) were mixed with fetal (E17.5) or (B) maternal peripheral blood erythrocytes. Cytospun cells stained with Giemsa stain. Scale bar: 20  $\mu$ m (Baron et al, 2012); (C) Colony morphology and analysis of hemoglobin mRNA expression. Photomicrograph of an E8.5 yolk sac primitive EryP and a definitive BFU-E. Panels to the right of the photomicrographs depict the results of RT-PCR analysis of plucked erythroid colonies and reveal that EryP contain mRNA for  $\beta$ H1 (embryonic hemoglobin) and  $\beta$  globin major (adult hemoglobin) while BFU-E express mRNA for only  $\beta$  globin major. Negative control samples were tested using no reverse transcriptase (Ferkowicz et al, 2003).

### 1.1.5.3. Early ontogeny of YS-derived MΦ

CX3CR1 is the receptor for chemokine CX3CL1/fractalkine and is prominently expressed in the mononuclear myeloid compartment (Jung et al., 2000). By using a mouse strain model in which the CX3CR1 chemokine receptor gene was replaced by a green fluorescent protein (GFP) reporter gene (referred to as CX3CR1<sup>GFP</sup> mice), Bertrand et al described three different pathways leading to the establishment of MΦ populations in the YS during early embryonic development, according to the correlation of progenitor phenotypes and differentiation potentials (**Fig 7**) (Bertrand et al., 2005b). The first MΦ population detected in the YS is maternally derived-MΦ that colonize the mesoderm layer from E7.5 on and display a mature phenotype (CD45<sup>+</sup>CD11b<sup>+</sup>F4/80<sup>+</sup>). These maternally derived cells transiently contribute to the MΦ population pool and cannot be detected in the YS after E9.5. A first wave of YS-derived MΦ is produced by monopotent MΦ progenitors (YS-MΦ), which appear slightly later at E8 (from the first somite stage). These YS-MΦ display a CD45<sup>-</sup>c-Kit<sup>+</sup> phenotype and generate primitive MΦ population through a differentiation pathway (A1, CD45<sup>+</sup>c-Kit<sup>+</sup>CD11b<sup>+</sup>; A2, CD45<sup>+</sup>c-Kit<sup>lo</sup>CD11b<sup>+</sup>CX3CR1<sup>lo</sup>; A3, CD45<sup>+</sup>c-Kit<sup>-</sup>CD11b<sup>+</sup>CX3CR1<sup>+</sup>F4/80<sup>+</sup>), which is similar to that found in the adult. Later, progenitors displaying erythro-myeloid potential (YS-EMp) give rise to the second YS-derived MΦ wave, which is a transient definitive population, as well as granulocytes and monocytes. These YS-EMp-derived MΦ progenitors arise independently in the YS at around the 5S stage and share a similar phenotype (CD45<sup>-</sup>c-Kit<sup>+</sup>) and MΦ differentiation pathway to the previous one. Consistent with these observations, utilizing the MΦ lineage-tracing approaches, Hoeffel et al (Hoeffel et al., 2015) recently identified two independent YS-derived MΦ waves during the transient definitive stage. A first wave of called “early” EMp-like cells mainly generates MΦ population at E7.5, which might represent primitive MΦ, and the second wave of “late” EMp at E8.25 gives rise to YS MΦ *in situ*. Then these precursors migrate to the FL through blood circulation at E9.5, where they generate progenitors with broader myeloid cell potential, including FL monocytes. Both of these successive YS-derived MΦ populations have potential to contribute to the establishment of

resident tissue M $\Phi$  and participate in embryonic developmental events by their phagocytic nature.

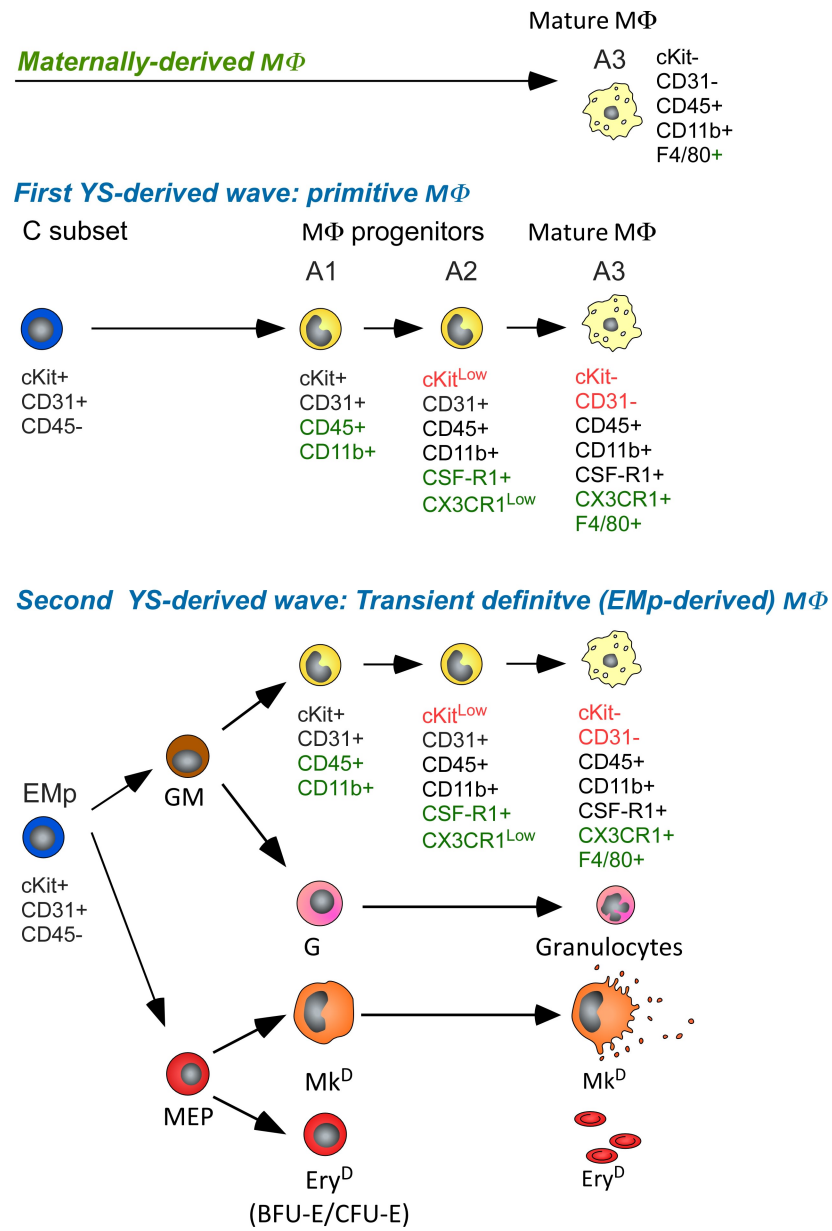


**Figure 7: Developmental stages followed by the 3 distinct M $\Phi$  waves, characterized by their phenotype, origin, differentiation potential, and lineage relationship.**

Ery indicates erythrocytes; Gr, granulocytes (adapted from Bertrand et al., 2005b).

### 1.1.6. The macrophage lineage

MΦ are multifunctional cell types that are found in most tissues in mice and play a central role in tissue homeostasis and repair, as well as immunity (Okabe and Medzhitov, 2016; Wynn et al., 2013; Wynn and Vannella, 2016). During embryonic development, they have mainly been involved in the clearing of dead cell through their phagocytic activity, which make them important for the shaping of the developing embryo (Mosser et al., 2017; Veiga-Fernandes and Pachnis, 2017). But now, they appear to play more specialized functions during development since recent genetic lineage-tracing experiments demonstrated that early HSC-independent hematopoiesis contributes to long-lived tissue-resident MΦ populations such as brain microglia, skin Langerhans cells as well as liver Kupffer and lungs alveolar MΦ, that persist into adulthood (Davies et al., 2012; Gomez Perdiguero and Geissmann, 2015). Most of them are maintained by local self-renewal, without replenishment by adult HSCs, under healthy condition. Thus, both HSC-derived and HSC-independent MΦ compartments are co-existing in the adult blood system. Understanding the unique features of fetal-derived MΦ cells will be necessary to fully decode the intrinsic disease processes involving these MΦ.

#### 1.1.6.1. Tissue-resident macrophages

Tissue-resident MΦ include spleen red-pulp MΦ, lung alveolar MΦ, epidermal Langerhans cells, brain microglia, liver Kupffer cells, large peritoneal MΦ, and F4/80<sup>bright</sup> pancreatic, kidney and cardiac MΦ, etc (**Fig 8**). For ages, it was believed that tissue-resident MΦ were continuously repopulated by blood-circulating monocytes that are produced by HSCs-derived myeloid progenitors in the adult BM. However, in recent years, the knowledge for the origin and maintenance of tissue-resident MΦ has changed dramatically. Several studies have now revealed that except for the mucosal/border tissues such as the intestine, the dermis and the heart, in which circulating monocytes are constantly

replenishing the aging tissue-resident M $\Phi$  pool, the majority of tissue-resident M $\Phi$  populations are embryonically derived and can be self-maintained by local proliferation throughout adulthood, without a contribution from BM-derived precursors in the steady state (Bain et al., 2016; Ensan et al., 2016; Epelman et al., 2014; Gibbings et al., 2017; Hashimoto et al., 2013; Hoeffel et al., 2012; Sheng et al., 2015; van de Laar et al., 2016). The current understanding of tissue-resident M $\Phi$  ontogeny is largely depended on lineage tracing approaches *in vivo* driven by genes generally involved in myeloid differentiation (*Csflr* or *Cx3cr1*) or hematopoietic emergence (*Runx1* or *Tie2*), which provide strong evidences for the source of tissue-resident M $\Phi$  populations from the different hematopoietic waves.

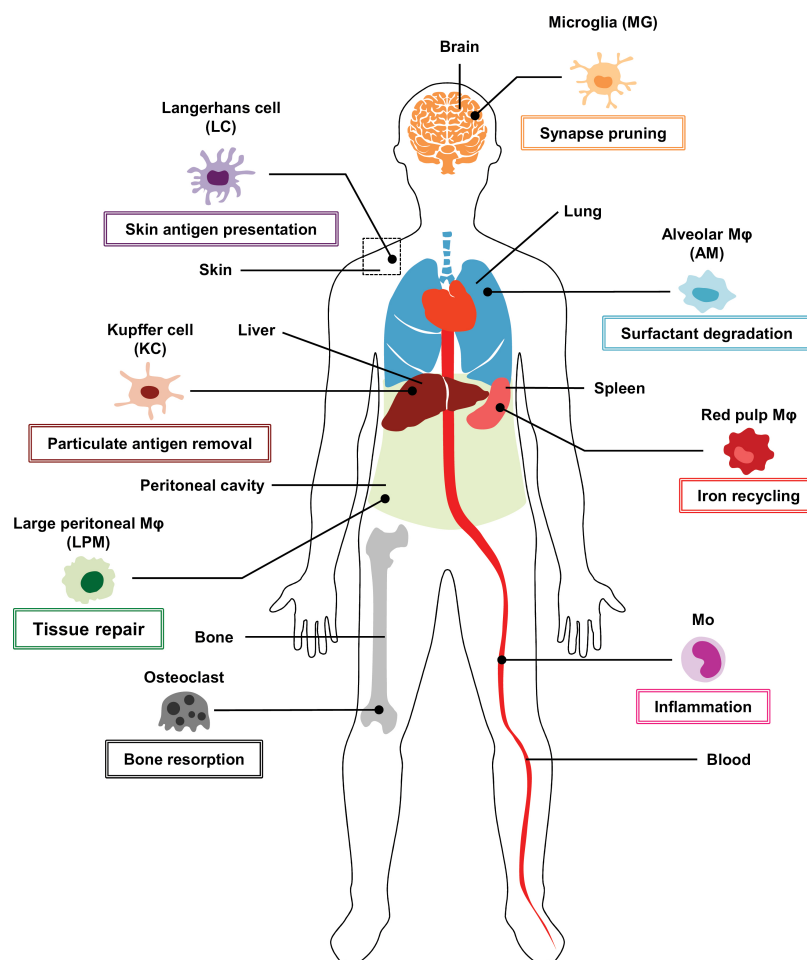


**Figure 8: Localization and functions of macrophage and monocyte subpopulations.**

AM, alveolar macrophage; KC, Kupffer cell; LC, Langerhans cell; LPM, large peritoneal macrophage; M $\Phi$ , macrophage; MG, microglia; Mo, monocyte (Kurotaki et al., 2017).

### 1.1.6.2. Strategies for the fate-mapping system

Despite several shortages for temporal restriction and promoter usage in different hematopoietic waves and their progeny, lineage tracing approach is still a very powerful tool to assess the fate of progenitor cells *in vivo*. Generally, in conditional gene targeting mouse model, Cre is inserted by site-specific homologous recombination into the selected locus through genetic manipulations. The principle of target gene selection is that its expression in mice should be restricted to a particular developmental stage or certain cell lineage, or both. Conditional gene expression has been achieved by engineering loxP-flanked stop sequences located between the promoter and a cDNA gene encoding a fluorescent marker, such as EGFP, tdRFP, EYFP, LacZ, TomatoRed, or another spectral variant (**Fig 9**). The expression of selected target gene is simultaneously activating the Cre-recombinase protein expression that irreversibly removes the loxP-flanked stop codon, resulting in turning on the permanent expression of fluorescent protein. The *Rosa26* locus is one of the commonest targets to be used as a reporter gene driver because of its strong and ubiquitous expression pattern (Zambrowicz et al., 1997). In addition, some specific signature genes of cell type are also widely used as a target reporter, such as *Cx3cr1* in the MΦ lineage (Wolf et al., 2013), *FMS-like tyrosine kinase 3 (Flt3)* in stem cells (Boyer et al., 2011), etc. Because Cre-recombinase is constitutively active, once it is expressed at a particular stage, or in a lineage, all daughter cells will be continuously labelled. For example, because BM LSK precursors have high-level *Flt3* expression, the majority of myeloid and lymphoid lineages progenies are marked in *Flt3*<sup>Cre</sup> knock-in adult mice (Boyer et al., 2012).

Moreover, in order to temporally control Cre activity to study different hematopoietic waves of developing cells, or to be able to study the effects of gene deletion at late development stages or in the adult when the mutant dies at early stage of embryonic development, inducible gene targeting mice model has been created by fusing the ligand-binding domains of steroid hormone receptors, such as estrogen receptor (ER) and modified ER (Mer), to chimeric recombinases (Metzger et al., 1995; Metzger and Feil, 1999). Specifically, in the absence of the inducing agent (tamoxifen; metabolized to 4-hydroxytamoxifen, the active

compound), the heat shock protein Hsp90 forms heterodimers with Cre-recombinase protein in the cytoplasm and prevents Cre from removing the loxP-flanked stop codon to activate reporter gene expression. Under injection of tamoxifen, Cre-recombinase protein is released from the inhibitory complex and translocated into the nucleus, finally leading to heritable labeling of the targeted cell (**Fig 9**).

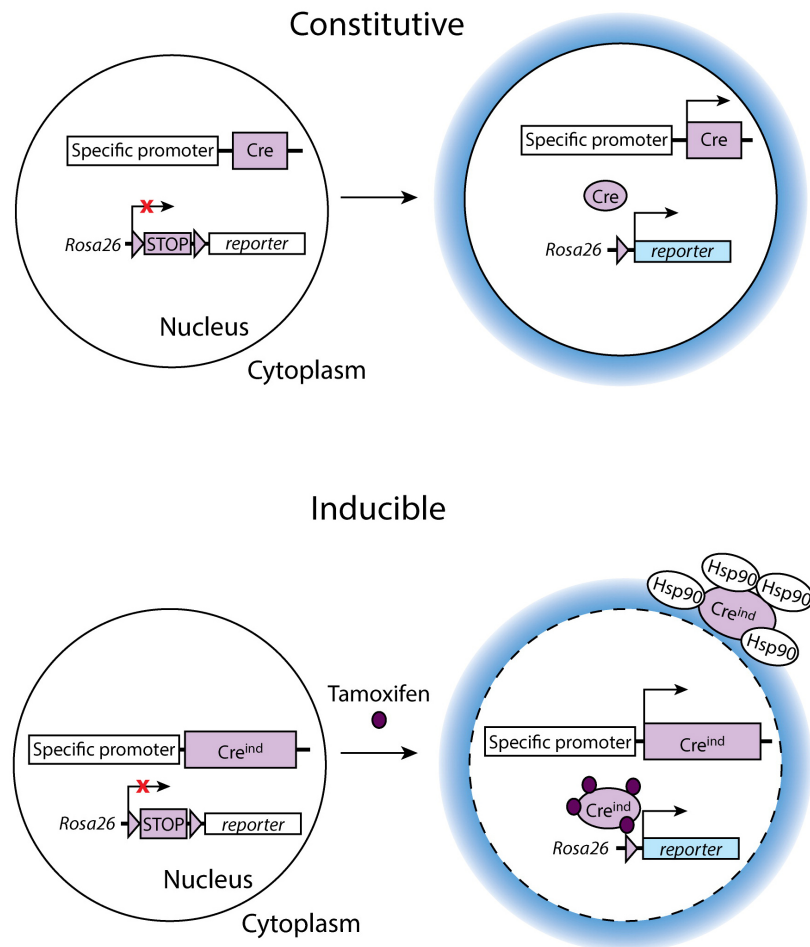


**Figure 9: A Schema of the constitutive and inducible conditional gene targeting approaches.**

(adapted from Hofer et al., 2016)

### 1.1.6.3. Lineage tracing of the origin of macrophage in different tissues

Several transgene mouse models of inducible gene targeting, such as the Runx1-Mer-Cre-Mer, the Tie2-Mer-Cre-Mer (Tie2-iCre) and the c-Kit-Mer-Cre-Mer (c-Kit-iCre) mice, have been exploited for the M $\Phi$  lineage tracing studies, as well as other hematopoietic cells (**Fig 10**) (Ginhoux et al., 2010; Gomez Perdiguero et al., 2015; Sheng et al., 2015). *Runx1* plays a pivotal role for the emergence of embryonic hematopoiesis and loss-of-function *Runx1* is lethal to the embryo (Hirschi, 2012). *Runx1* is first expressed in hematopoietic cells as they emerge in the YS. Therefore, in *Runx1*<sup>MerCreMer</sup> mice (Ginhoux et al., 2010), in which Mer-Cre-Mer recombinase is induced by tamoxifen under the control of *Runx1*, cells labeled in the YS at E7.5, a time when *Runx1* expression is limited to the primitive hematopoiesis, will only give rise to primitive M $\Phi$ , as well as primitive EryP-CFC and megakaryocytes, and tamoxifen application at few hours later can lead to either EMP-derived definitive M $\Phi$  (at E8.5) or HSCs-derived definitive M $\Phi$  (at E9.5) labeling in this system (**Fig 10A**).

In contrast, *Tie2* is expressed on all the endothelial-like precursors of hematopoiesis by E7.5 and then is turned off in hematopoietic cells after they differentiation (McGrath et al., 2015b). Thus, all endothelial cells and their progeny (both non-hematopoietic and hematopoietic cells) will be labeled after tamoxifen injection in the Tie2-iCre model. Consequently, an early tamoxifen injection (at E7.5) will target all hematopoietic waves-derived M $\Phi$  that are produced before the time of analysis, whereas a late injection (at E10.5) will only target the latest HSCs-derived definitive M $\Phi$  (Gomez Perdiguero et al., 2015) (**Fig 10B**).

Moreover, all hematopoietic progenitors, but not endothelial cells, express c-Kit (Ivanova et al., 2002). Thus, an early tamoxifen injection (at E7.5) in the c-Kit-iCre model will restrict the labeling to primitive wave (Sheng et al., 2015). However, progenitors produced by each hematopoietic wave coexist in the embryo after E8.5 and these progenitors still express c-kit. A later tamoxifen injection (at E8.5 and E9.5) might thus result in the cumulative labeling of

undifferentiated primitive M $\Phi$  progenitors and EMP-derived M $\Phi$  precursors, as well as both EMP- and HSCs-derived M $\Phi$  precursors, and their mature progenies (**Fig 10C**).

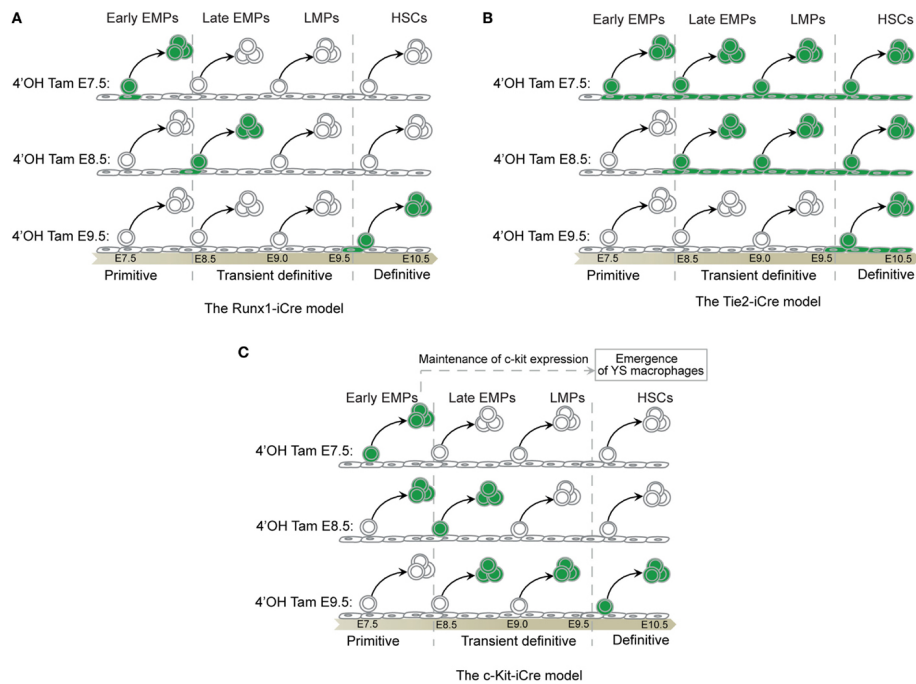


**Figure 10: Fate-mapping systems of macrophages and other hematopoietic cell.**

Green color represents labeling cells (Hoeffel and Ginhoux, 2015).

#### 1.1.6.4. The three models on the origin of tissue resident macrophages

Only recently, by using the fate-mapping system, researchers have proposed three different models for the contribution of embryonic progenitors to adult tissue resident M $\Phi$  populations (**Fig 11**). Using *Tie2*-dependent inducible mice models, Gomez Perdiguero et al (Gomez Perdiguero et al., 2015) suggested that YS-derived EMP are a common origin for the majority of tissue resident M $\Phi$  in liver, brain, epidermis and lung (**Fig 11, Model 1**). The authors found that there is a higher proportion of adult tissue resident M $\Phi$  YFP labeling than that of leukocytes when tamoxifen is injected upon *Tie2-iCre:Rosa26<sup>YFP</sup>* mice at E7.5; a similar YFP labeling proportions of both cell types at E8.5 injection; and a relatively more

frequently YFP labeled in leukocyte populations than tissue resident MΦ from E9.5 injection. These findings, thus, indicated that a progenitor cell type that expresses *Tie2* at E7.5 but not after E9.5, gives rise to the majority of fetal and adult MΦ, and the authors proposed this progenitor to be YS EMP.

In another model, researchers (Hoeffel et al., 2015) proposed that except for brain microglia, which derives from YS MΦ, the most other adult tissue resident MΦ, including skin, liver, kidney, lung, gut and spleen, derive predominantly from fetal monocytes generated by YS *c-myb*<sup>+</sup> EMP (**Fig 11, Model 2**). Using *Runx1*- and *Csf1r*-dependent inducible mice models, as well as *Rosa26*<sup>R26-EYFP/R26-EYFP</sup>, Hoeffel et al (Hoeffel et al., 2015) identified two temporally and functionally distinct waves of EMPs emerging in the YS between E7.5 and E8.5. The first wave of “early” CSF-1R<sup>hi</sup>c-Myb<sup>-</sup> "EMP" emerges in the YS from E7.5 and gives rise mostly to brain microglia. The “late” CSF-1R<sup>lo</sup>c-Myb<sup>+</sup> EMP are produced in the YS from E8.5 and most of these cells migrate into the FL through the blood circulation at E9.5. After colonized the FL, these cells differentiate into multiple lineages, including FL monocytes that give rise to most tissue resident MΦ through a monocytic intermediate.

In the third Model, Sheng et al recently concluded that all adult tissue resident MΦ, such as Kupffer cell, alveolar MΦ, red pulp MΦ, kidney F4/80<sup>hi</sup> MΦ, dermis MHCII<sup>lo</sup>F4/80<sup>hi</sup> MΦ, as well as colon F4/80<sup>hi</sup> MΦ and peritoneum F4/80<sup>hi</sup> MΦ, are progenies of fetal classical HSCs with the exception of microglia and partially epidermal Langerhans cells, which originate from YS progenitors (**Fig 11, Model 3**) (Sheng et al., 2015). The authors have generated a *c-Kit-iCre:Rosa26-loxP-STOP-loxP-eYFP* mice model in which the administration of tamoxifen induces irreversible tagging of c-Kit expressing cells, as well as their progenies. In this fate-mapping system, researchers found that adult microglia and partial epidermal Langerhans cells can be robustly labeled when tamoxifen is injected at E7.5, but other tissue resident MΦ, as well as peripheral hematopoietic cells, are labeled very poorly. In contrast, tamoxifen injection at E8.5 or E9.5 efficiently labels all adult peripheral hematopoietic cells including adult tissue resident MΦ (about 40%-60%). These results therefore led to the hypothesis that definitive fetal HSCs give rise to all the adult tissue

resident MΦ, with the exception of microglia and, partially, epidermal Langerhans cells, which arise from YS-derived primitive MΦ progenitors.

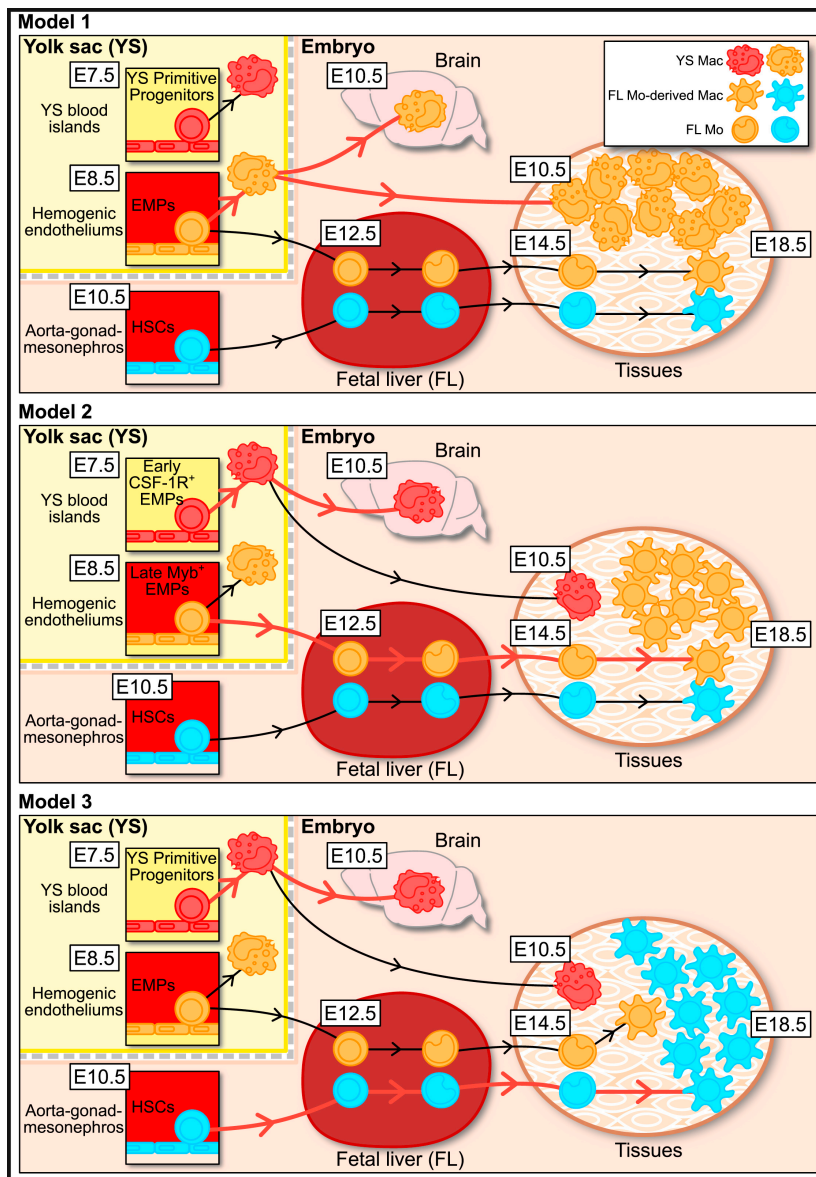


**Figure 11: Three Different Models of Fetal Macrophage Ontogeny.**

The Model 1 corresponds to the work of Gomez Perdiguero et al. (2015), the Model 2 to the work of Hoeffel et al. (2015), and the Model 3 to Sheng et al. (2015). Red arrow indicates the proposed major path of ontogeny and differentiation in each model. Cell colors are matched to their proposed origins (Ginhoux and Guilliams, 2016).

#### 1.1.6.5. The origin of embryonic microglia

Microglia are CNS resident MΦ that play pleiotropic functions in the normal and pathological brain. Impaired microglial development and function are thought to be involved in the onset and development of various neurodevelopmental and neurodegenerative diseases (Colonna and Butovsky, 2017; Prinz and Priller, 2014). Thus, understanding of the origin of microglia may provide new therapeutic approaches for the treatment of these diseases. In fact, studies in the past decades have been carried out to dissect the origin of microglia (Alliot et al., 1999; Epelman et al., 2014; Ginhoux et al., 2010; Gomez Perdiguero et al., 2015; Hashimoto et al., 2013; Hoeffel et al., 2015; Kierdorf et al., 2013; Schulz et al., 2012). As stated above, although there is a controversy for the origin of some tissue MΦ, all fate mapping experiments agreed that microglia originates from early YS-derived MΦ. Similarly, by combining vital staining with in situ hybridization, Herbomel et al found that, in zebrafish embryos, early MΦ (equivalent to primitive MΦ in mice [Herbomel et al., 1999]; for a review on hematopoietic cell development in the zebrafish embryo, see Bertrand and Traver, 2009) colonize the brain and differentiate into microglia through a CSF1R-dependent invasive process (Herbomel et al., 2001). Rossi et al further demonstrated that in the zebrafish, it is the *slc7a7*<sup>+</sup> primitive MΦ subset produced early during development in the anterior lateral plate mesoderm region that will give rise to embryonic microglia (Rossi et al., 2015).

However, in contrast to zebrafish embryos, in which primitive and definitive hematopoiesis are separated by temporally and spatially (Bertrand and Traver, 2009), in mice, primitive and EMP-derived MΦ subsets appear overlapped and coexist in the YS so that their respective contribution to microglia was naturally questioned. Primitive hematopoietic populations have been characterized as independent of *c-Myb*-expression for their development, contrary to their definitive counterpart (McGrath et al., 2015b; Gomez Perdiguero and Geissmann, 2013; Tober et al., 2008). The normal amount of microglial cells found in mice lacking the *c-Myb* transcription factor argues for a primitive origin of microglia progenitors (Kierdorf et al., 2013; Schulz et al., 2012). Additionally, Ginhoux et al. reached a similar conclusion because

the induction of *Runx1* expression at E7.25-7.5 that leads to microglia labeling, targets progenitors present at the latest E8.5 (Ginhoux et al., 2010), when EMP-derived MΦ progenitors are not yet produced. However, this protocol leads to 30-40 % microglia labeling, and although this level is likely to be underestimated, an additional contribution from a slightly later source, namely EMP-derived MΦ progenitors, might be considered (Ginhoux et al., 2010). Conversely, two sets of investigations suggested that EMP-derived definitive MΦ population provide microglia (Gomez Perdiguero et al., 2015; Kierdorf et al., 2013). Sorted c-Kit<sup>+</sup>CD45<sup>low</sup> progenitors from E8-YS were shown to give rise to erythro-myeloid cells *in vitro* and to microglial cells upon culture on microglia-depleted hippocampal slice cultures (Kierdorf et al., 2013). In the second study (Gomez Perdiguero et al., 2015), the induction of *csf-1r<sup>Cre</sup>* at E8.5 resulted in the labeling of c-Kit<sup>+</sup>CD45<sup>low</sup> MΦ progenitors in E9.5 YS and of head MΦ at E10.5. However, EMP and primitive MΦ progenitors share the same c-Kit<sup>+</sup>CD45<sup>low</sup> phenotype and are both present in the YS at the stages analyzed (Bertrand et al., 2005b), so that in both instances, the identification of the MΦ/microglia progenitors is still unclear (McGrath et al., 2015b). The question of the respective contribution of primitive and EMP-derived definitive MΦ progenitors to the developing microglia thus remained open.

## 1.2. Development and function of microglia in mice

### 1.2.1 Myeloid cell types in the central nervous system

The central nervous system (CNS) contains a heterogeneous class of myeloid populations that play distinct roles in maintaining tissue homeostasis and pathological response in different tissue compartments during development and adulthood (Prinz et al., 2011; Ransohoff and Cardona, 2010). According to their localization, morphology, as well as surface-marker expression and *in vitro* responses, the myeloid cells of the CNS have been characterized and classified into five groups: parenchymal microglia, non-parenchymal meningeal M $\Phi$  (mM $\Phi$ ), CNS perivascular M $\Phi$  (pvM $\Phi$ ), M $\Phi$  of the choroid plexus (cpM $\Phi$ ) and disease-associated monocytes (**Fig 12**) (Prinz et al., 2017). Specifically, microglia are the only myeloid cell type present in the CNS parenchyma where they are surrounded by neurons, astrocytes and oligodendrocytes; subdural mM $\Phi$  are in close proximity to meningeal fibroblasts; pvM $\Phi$  are located between the laminin<sup>+</sup> endothelial and glial basement membranes; cpM $\Phi$  are mainly found on the apical side of the choroid plexus epithelium facing the cerebrospinal fluid and in the stroma (Prinz and Priller, 2014; Ransohoff and Cardona, 2010).

In addition, CNS M $\Phi$  have been recently shown to possess a unique feature: In most organs, such as the heart, spleen, lungs and intestine, tissue M $\Phi$  are regularly replaced by blood-derived monocytes (Goldmann et al., 2016). In contrast, except cpM $\Phi$ , other CNS M $\Phi$ , including microglia, mM $\Phi$  and pvM $\Phi$ , have been shown to originate entirely from embryonic YS-precursors without any significant input from the circulating blood cells or BM-derived monocytes during adulthood (Goldmann et al., 2016). In these locations, M $\Phi$  are maintained by their longevity and capacity of self-renewal (Soucie et al., 2016). Interestingly, these M $\Phi$  have unique phenotypes in the healthy CNS, in addition to M $\Phi$ -related surface markers common among the resident M $\Phi$ , such as Iba-1, F4/80, CD11b, CX3CR1 and MERTK. Microglia display a down-regulated phenotype with a low expression of the transmembrane tyrosine phosphatase CD45, of Fc receptors and major

histocompatibility complex class II (MHC class II) compared to other CNS MΦ. Several microglia-specific genes such as *P2ry12*, *Fcrls*, *Hexb*, *Tmem119*, *Tgfbr1* and *Sall1* have also been identified in large gene-expression studies (Bennett et al., 2016; Buttgerit et al., 2016; Gautier et al., 2012; Gosselin, et al., 2014; Lavin et al., 2014). Furthermore, mMΦ and pvMΦ selectively express the endocytic pattern-recognition receptor CD206 (Goldmann et al., 2016). Moreover, pvMΦ, as well as part of mMΦ and cpMΦ, were found to express the scavenger receptor CD163 (Goldmann et al., 2016). Recent single-cell RNA-sequencing studies further showed that pvMΦ specifically express *Cd163*, *Hpgd*, *Mrc1*, *Slc40a1* and *F13a1* (Goldmann et al., 2016; Mass et al., 2016; Zeisel et al., 2015). The discovery of specific expression signatures in the various MΦ subsets in the CNS may be due to the profound effect of the local microenvironment, pointing to the different roles of CNS MΦ in homeostasis and defence. In this part, I will focus on recent findings in regulation of microglia development and the role of microglia during neurodegenerative disease.

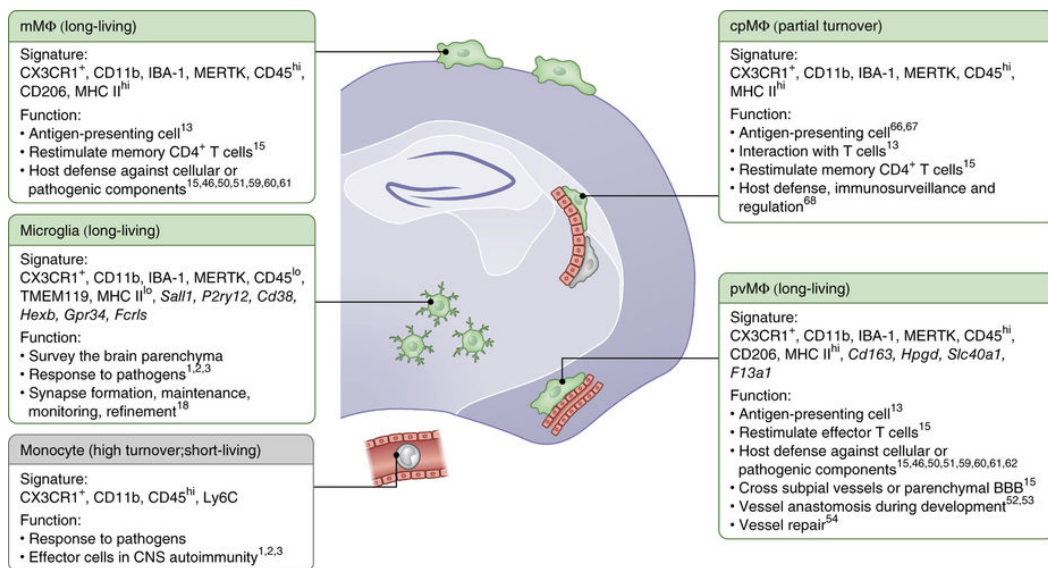


**Figure 12: The localization and genetic signature of CNS macrophages.**

CNS MΦ can be distinguished from monocytes by the expression of Ly6C, a marker present on monocytes but not on CNS MΦ (Prinz et al., 2017).

### 1.2.2. The development of microglia

The population of parenchymal microglia in the adult murine CNS accounts for 5% to 12% of the total number of glial cells and varies in the different brain regions analyzed (from 22 to 165 cells/mm<sup>2</sup>) (Aguzzi et al., 2013). Contrary to neurons and glia that derive from the neuroectoderm, microglial cells originate from the YS mesoderm. By crossing the *Runx1*<sup>iCre</sup> mice with floxed *Rosa26* reporter mice and performing tamoxifen-mediated induction at different time points Ginhoux et al (Ginhoux et al., 2010) strongly demonstrated that the YS-derived primitive MΦ population that is initially present at E7.5 is the major source of the resident adult microglia (**Fig 13**). The transcription factor *c-Myb* is required for the development of definitive hematopoiesis (Tober et al., 2008), and for the maintenance and renewal of HSC-derived myeloid cells (Schulz et al., 2012). Nevertheless, the microglial pool is unaffected in *c-Myb*-deficient embryos, confirming that they derive from the earlier YS population (Schulz et al., 2012). It was further proved that the development of *c-Myb*-independent microglia requires the transcription factor *Pu.1*, as well as *Csf1r* (Ginhoux et al., 2010; Kierdorf et al., 2013).

Microglia populate the CNS during early embryogenesis: MΦ progenitors are initially found in the neuroepithelium of mice at E8.5-10, with substantial numbers being detected in the fourth ventricle at E10.5. From E11.5, they start to invade the cortex (Swinnen et al., 2013). Specifically, MΦ/microglia cells cluster in the pial surface of the cortex and within the lateral ventricles at E12.5, the onset of this migration process. Afterwards, they become randomly distributed throughout the cortical wall, except for the cortical plate region in later embryonic ages (Swinnen et al., 2013). However, to date, little is known about how microglial migration, recruitment and positioning into the cortex are regulated during embryonic CNS development. Recent studies showed that the ablation of the basal progenitors that express the chemokine SDF1/Cxcl12<sup>+</sup> in the subventricular zone affects CX3CR1<sup>+</sup> microglia recruitment into the ventricular/subventricular zone (Arnò et al., 2014), suggesting that neural progenitor cells may orchestrate the migration and positioning of

microglia into the cortex during embryonic development. Moreover, researchers recently found that in zebrafish, neuronal apoptosis attracts committed microglial precursors into the brain via specific routes in a blood circulation-independent fashion (Casano et al., 2016; Xu et al., 2016), further confirmed the regulatory roles of neural cells in microglial colonization.

Following migration, the number of microglial cells present in the cortex significantly increased up to E17.5 and they continuously proliferate until postnatal (P) days P14 (Nikodemova et al., 2015; Swinnen et al., 2013). It has been reported that the number of microglia increase 20-fold during the period extending from P0 to P11 (Prinz and Priller, 2014). Interestingly, after an initial increase during the first two weeks, microglial numbers in mouse brain were found to decline from P15 and the pool of microglia was reduced by half by 6 weeks of age (Nikodemova et al., 2015). During this period, microglia also undergo morphological transformation, characterized by the transition from an amoeboid to a ramified morphology (Zusso et al., 2012). In general, ramified cells have small somas and extensive arborized processes that are necessary for the active surveillance function of microglia. Following this step, the density of microglial cells remained remarkably stable in the vast majority of brains areas by the spatial and temporal coupling of proliferation and apoptosis, with little change from the young (4-6 months) to the aged (18-24 months) mice (Askew et al., 2017). The adult microglia population was found to possess the potential for efficient self-renewal without the contribution of peripheral myeloid cells (Askew et al., 2017). Using a new *Cx3cr1*<sup>CreER</sup>-based system to conditionally deplete the microglial cells in adult mice, Bruttger et al. recently found that the microglial compartment could reconstitute within 1 week following depletion. This restorative processes, which was independent from BM-derived precursors, relied on the proliferation of CNS-resident microglia, mediated by the interleukin-1 receptor (IL-1R) signaling pathway (Bruttger et al., 2015).

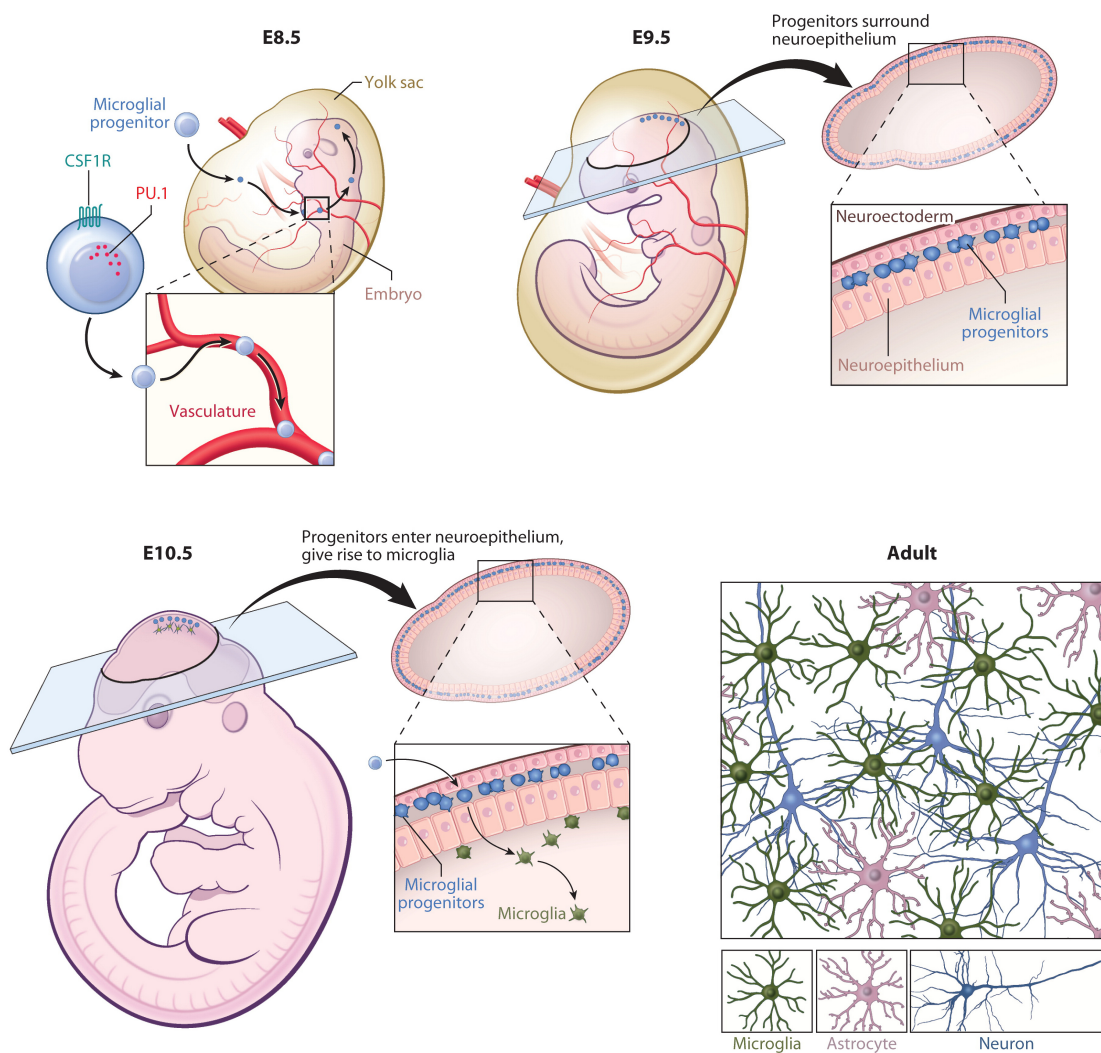


**Figure 13: Microglial origin and development.**

Microglia originate from primitive M $\Phi$  progenitors that are generated by the embryonic YS during development (prior to E8.5) and enter the brain rudiment via the circulatory system. These progenitors surround the neuroepithelium of the developing brain around E9.5 and one day later enter the neuroepithelium and begin to colonize the CNS parenchyma. Microglia at this stage of development have an amoeboid rather than a ramified morphology. Microglia become completely ramified throughout the brain by postnatal day 28. *c-Myb*-independent microglia are *Pu.1* and *Csfl-r* dependent (Nayak et al., 2014).

### 1.2.3. Factors that regulate the development of microglia

During embryonic development, YS-derived MΦ progenitors colonize to the brain and give rise to parenchymal microglia. The developmental program of microglial cells has been shown to be controlled by various molecules, including transcription factors, growth factors, and chemokines, among others (**Table 2**). For example, signaling via CSF1R plays essential roles in microglial development. CSF1R (Colony Stimulating Factor 1 Receptor) is a tyrosine kinase transmembrane receptor that is expressed on mononuclear myeloid cells throughout the body (Chitu and Stanley, 2006). The deficiency of *Csf1* or *Csf1r* results in the dramatic reduction in the number of microglia (Ginhoux et al., 2010). Moreover, microglial pool is more profoundly affected by the absence of CSF1R than by the absence of CSF1, suggesting the presence of the complementary ligand for CSF1R. Of note, IL-34, which is principally produced by neurons, has recently been identified as a second ligand for CSF1R. Wang et al showed that the mutation of IL-34 results in a 20% of reduction of brain microglia. Interestingly, the most notable reduction of microglia populations was observed in the cerebral cortex, hippocampus, and corpus callosum, suggesting a regional heterogeneity of CSF1 and IL-34 expression (Wang et al., 2012). RUNX1 interacts with the CCAAT enhancer-binding protein to regulate the expression of *Csf1r*, promoting the development of MΦ, including microglia (Zhang et al., 1996). Besides this, a recent study uncovered a novel function of RUNX1 in postnatal microglia by showing that it not only controls the proliferation but also the activation and maturation of postnatal microglia (Zusso et al., 2012).

The transcription factor Interferon Regulatory Factor 8 (IRF8) also has a direct impact on microglial development. A recent study linked IRF8 to microglia development, finding that the number of microglia is strongly reduced during adulthood in IRF8<sup>-/-</sup> mice due to a defect in the survival and maturation of YS-derived myeloid progenitors during embryonic development (Kierdorf et al., 2013). Thus, it is conceivable that IRF8 participates in the development of microglia, at least partly, by regulating apoptosis-related genes.

The transcription factor PU.1 is also an indispensable regulator of microglial development during ontogeny in mice. Indeed, the differentiation and maturation of YS-derived progenitors were found to be dependent on the presence of PU.1, since mice deficient in PU.1 completely lack MΦ, including the microglia population (Kierdorf et al., 2013).

**Table 2: Microglia phenotypes in animals lacking specific molecules** (Prinz and Priller, 2014)

Absent molecule	Microglia morphology	Microglia number
CSF1	↓	↓
CSF1 receptor	↓	↓
DAP12	ND	↓
Interleukin-34	ND	↓
IRF8	↓	→ or ↓
Transcription factor PU.1	NA	↓
RUNX1	↓	ND

↓ indicates a either dysmorphic or reduced number of microglia; → indicates no change. CSF1, colony-stimulating factor 1; DAP12, DNAX-activation protein 12; IRF8, interferon regulatory factor 8; NA, non-applicable; ND, not determined; RUNX1, runt-related transcription factor 1.

#### 1.2.4. Physiological roles of microglia

As the resident MΦ of the CNS, microglial cells are known to be indispensable for normal brain development and defects in microglia function is thought to play a roles in the development of neuropathologies. In addition, major recent discoveries have revealed that microglia actively interact with neurons during both embryonic and postnatal development and can modulate the fate and functions of synapses in the adult CNS (Colonna and Butovsky, 2017; Wake et al., 2013; Wu et al., 2015). Disruption of the interactions between microglia and neurons has been shown to result in a severe negative impact on CNS development and function. Thus, microglial cells originating from YS-derived myeloid

precursors contribute to the establishment and maintenance of the normal nervous system by phagocytosis, removing dying or dead neuronal cells, as well as potentially influencing the formation and maturation of neuronal networks (**Fig 14**).

#### **1.2.4.1 Phagocytosis**

During both embryonic and postnatal development, the CNS undergoes a massive programmed cell death, which is necessary for the maintenance of tissue homeostasis and for the formation of proper neuronal circuits. The clearance of apoptotic neural cells is achieved by microglia, which engulf the cells debris. Importantly, during neurogenesis, this process occurs without initiating an inflammatory response (Hristova et al., 2010; Marín-Teva et al., 2004; Takahashi et al., 2005). This phagocytosis process is mediated by so-called “find-me” and “eat-me” signals (**Fig 14A**). Apoptotic neurons release several “find-me” signals, including the lipid lysophosphatidylcholine, CXCL12, sphingosine 1 phosphate, as well as the nucleotides ATP and UTP, to recruit microglia to actively participate in phagocytosis. Once microglia cells have migrated to the source of the “find-me” signals, they are stimulated by “eat-me” signals that are usually exposed ligands on apoptotic cells. The phosphatidylserine is the most evolutionary conserved “eat-me” signal, which prompts phagocytes to engulf the cells. Other “eat-me” signals for microglia have been well described in details such as soluble fractalkine (CX3CL1) and lysophosphatidylcholine. Moreover, the hydrolyzate of UTP, UDP, was shown to directly bind P2Y6 microglial receptors and facilitate phagocytosis. Microglia were also found to induce the programmed cell death of neuronal cell by releasing mediators during development (**Fig 14A**). An example of this was observed in the retina of the developing chick eye, where retinal nerve cells became apoptotic due to microglia-induced release of nerve growth factor (Frade and Barde, 1998). Additionally, programmed cell death of neurons in the developing murine hippocampus was found to be triggered by microglia. In this region, microglia released reactive oxygen species

in a CD11b-dependent and DNAX activation protein of 12 kDa (DAP12)-dependent manner that induces neuronal death (Wakselman et al., 2008).

#### **1.2.4.2 Maintenance of neuron survival**

In addition to the elimination of dying or dead cells, microglia also contribute to promotion of neuronal survival by releasing neurotrophic factors to the surrounding cellular milieu. By using Cd11b-DTR mice and CX3CR1 knockout mice, Ueno et al (Ueno et al., 2013) recently evidenced that insulin-like growth factor-1 (IGF-1) released by activated microglia promotes the survival of cortical neurons (layer V) at early postnatal stages (**Fig 14D**). Immunohistochemical analyses revealed that early after birth (postnatal days 1 to 7), microglia accumulate along subcerebral and callosal axon fibers and that either IGF-1 inhibition or the depletion of microglia promoted cell death of cortical neurons on the trajectory of layer V pyramidal cell axons (Ueno et al., 2013). In addition, CX3CR1 deficiency or IGF-1 inhibition in microglial cells similarly led to death of layer V cortical neurons (Ueno et al., 2013), suggesting that the supportive role of microglia for neural survival may be mediated partly by fractalkine signaling (i.e., CX3CL1-CX3CR1) and IGF-1 release.

#### **1.2.4.3 Control of synaptic function**

Other trophic factors secreted by microglia including basic fibroblast growth factor, hepatocyte growth factor, epidermal growth factor, platelet-derived growth factor, nerve growth factor, and brain-derived neurotrophic factor (BDNF). These factors were shown to play significant roles in neuronal development, maintenance, and function throughout life (Coull et al., 2005; Tong et al., 2012). For example, the formation and functional maturation of synapses function depends on trophic factors and synaptogenic signals derived from microglia (**Fig 14C**). Lim et al (Lim et al., 2013) found that microglial IL-10 can promote

the formation of new synapses in cultures. Moreover, under conditional removal of BDNF specifically in microglial of *CX3CR1<sup>CreER</sup>* mice, Parkhurst et al (Parkhurst et al., 2013) evidenced that microglial BDNF facilitates learning-related synapse formation, increases neuronal tropomyosin-related kinase receptor B phosphorylation and controls the expression of synaptic proteins, suggesting an important role for microglial BDNF in regulation of synaptic plasticity and function.

#### **1.2.4.4 Synaptic pruning**

During postnatal development, microglial phagocytic activity is also crucial for synaptic homeostasis. The stripping of neuronal synapses by microglia is achieved through several mechanisms. The complement system appears to be involved in the processes of synaptic pruning by microglial cells (**Fig 14B**). The complement protein cascade, C1q and C3, are expressed in neurons and localizes to unused synapses for microglia recognition via C3 receptors (CR3; a heterodimer of CD11b and CD18) or for direct lysis via the complement cascade. Mice lacking CR3 or C3 showed defects in synaptic elimination, resulting in sustained synaptic connectivity (Stevens et al., 2007). The fractalkine signaling (CX3CR1-CX3CL) also plays important roles in microglia-mediated synaptic pruning (Rogers et al., 2011; Zhan et al., 2014). CX3CL is a transmembrane glycoprotein expressed on the neuronal surface that can also be released as a soluble molecule after proteolytic cleavage. By following the fate of representative pre- and postsynaptic proteins, Paolicelli et al found that the engulfment of PSD95-immunoreactive postsynaptic densities was significantly decreased in CX3CR1 deficient mice (Paolicelli et al., 2011).

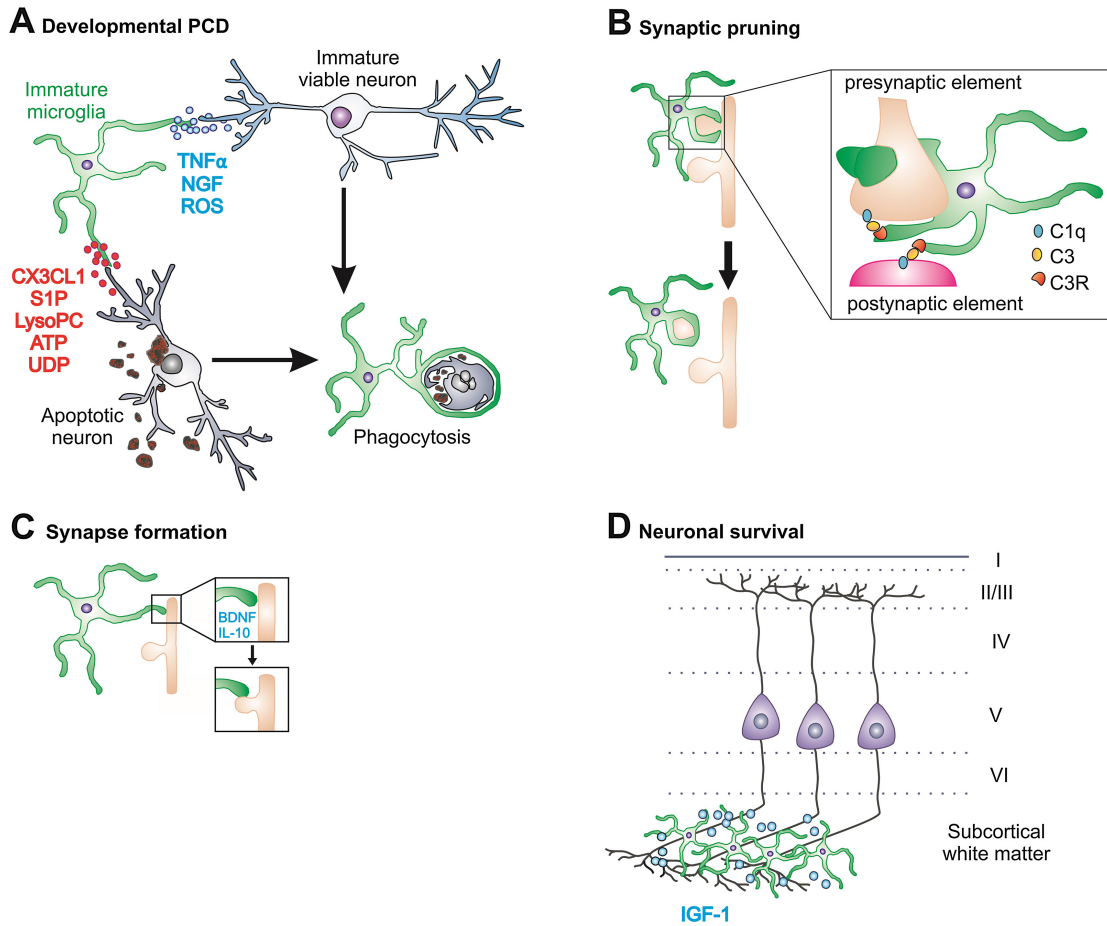


**Figure 14: Main microglial functions during CNS development.**

(A) Phagocytosis of apoptotic neurons expressing “eat-me” signals (red) and induction of neuronal apoptosis through different signaling pathways (blue). (B) Pruning of supernumerary weak synapses tagged by proteins of the complement cascade. (C) Formation of new synapses mediated by BDNF or IL-10 signaling. (D) Survival of layer 5 pyramidal neurons through the release of IGF-1 in the white matter (adapted from Mosser et al., 2017).

### **1.2.5 Microglial dysfunction is involved in neurodevelopmental defects**

Owing to the fact that microglial cells actively contribute to the establishment and functional maturation of neuronal networks during development, microglia dysfunction may have long-term consequences on the structure and function of these networks, and thereby contribute to the risk for neurodevelopmental disorders. Neurodevelopmental disorders are a group of behavioral disorders whose onset occurs early in life. These disorders mainly comprise autism and schizophrenia spectrum disorders, intellectual disability, and attention deficit hyperactivity and obsessional compulsive disorders.

#### **1.2.5.1 Autism spectrum disorders**

Autism spectrum disorder (ASD) arises during the early childhood with a heterogeneous presentation that is typically associated with repetitive behaviour and significant lifelong cognitive, social skills and communication impairments for the individual. The deficiency in the synaptic pruning during synaptic maturation has been investigated and may explain some of the behavioural and circuit-level deficits found in autism. Mice lacking the CX3CR1 receptor displayed a superabundance of weak excitatory synapses due to impaired elimination of immature synaptic connections during the second and third postnatal weeks (Paolicelli et al., 2011). CX3CR1 deficiency in adult mice also affected synaptic multiplicity, functional long-range connectivity, social behavior, together with increased repetitive-behavior phenotypes, suggesting that primary defects in the microglial cells may result in circuit-level deficits across neurodevelopmental disorders, including autism (Zhan et al., 2014).

### **1.2.5.2 Rett syndrome**

Rett syndrome is an X-linked ASD that caused by mutations in the X chromosomal gene *methyl-CpG-binding protein 2 (MeCP2)*. Loss of function of MeCP2 increased the production and release of glutamate in microglia, resulting in the neurotoxicity *in vitro*. In the Rett syndrome mouse model, Derecki et al (Derecki et al., 2012) reported that transplantation of wild-type bone marrow into lethally irradiated *Mecp2*-null mice led to the arrestment of disease progression, due to the restoration of microglial phagocytic activity against apoptotic targets. The reduction of Rett syndrome pathology mediated by wild-type microglia was attenuated when the phagocytic activity was inhibited, suggesting the important role of microglial phagocytic activity in Rett syndrome. However, whether BM transplantation is a potentially effective therapeutic approach for patients with autism is a matter of debate. Wang et al (Wang et al., 2013) replicated and extended the BM transplantation experiments in three different Rett syndrome mouse models, but found that despite robust microglial engraftment, BM transplantation from wild-type donors failed to arrest early death or ameliorate neurological deficits.

### **1.2.5.3 Obsessional compulsive disorders**

Obsessional compulsive disorders (OCD) are characterized by persistent thoughts and repetitive behaviors. In the mouse, OCD can be studied by examining grooming behavior that serves diverse physiological functions (Weingarden and Renshaw, 2015). The gene *Hoxb8* was first found to be necessary for normal grooming behavior in mice (Greer and Capecchi, 2002). By specifically deleting the *Hoxb8* gene, Greer and Capecchi found that the resultant knockout mice display excessive (pathological) grooming behavior in an obsessive-compulsive behavioral pattern that lead to hair loss and self-inflicted skin lesions (Greer and Capecchi, 2002). In addition, they further demonstrated that, within the CNS, *Hoxb8* is expressed only by a subset of microglia (or their progenitors). Moreover, this aberrant behavioral pattern could be partially corrected by a reconstitution therapy involving

the transplantation of wild type bone marrow cells into irradiated *Hoxb8*<sup>-/-</sup> mice (Chen et al., 2010). These results pointed to a crucial role for microglia in the development of neuro-behavioural defects and to the existence of microglia subsets controlling specific neuronal circuits. It also confirmed the capacity of bone marrow-derived progenitors to complement the microglia pool under pathological conditions.

## 1.3. Transcription factor Lyl-1 in hematopoiesis

### 1.3.1 Lyl-1 function in leukemia

The *Lyl1* gene, which encodes a bHLH transcription factor, was originally identified at chromosomal translocation loci [t(7;19)(q35;p13)] from some cases of T-cell acute lymphoblastic leukemia (T-ALL) (Mellentin et al 1989). Lyl-1 is a Class II bHLH protein that is expressed in a tissue-specific manner. Its homologous bHLH motif is shared with other family members and it is responsible for protein-protein, as well as protein-DNA interactions (Jones, 2004). Unlike Class I bHLH proteins, Class II bHLH transcription factors activate or repress transcription by binding to target gene sequences as heterodimers with E-proteins (Wang and Baker, 2015). Lyl1 has been shown to form heterodimers with the E-protein E2A/TCF3 (Miyamoto et al, 1996).

The involvement of Lyl-1 in leukemia has been extensively documented. 30% of Lyl-1 overexpressing transgenic mice displayed a T- or B-cell malignant lymphomas after an average latent period of 352 days, providing direct evidence that an aberrant expression of *Lyl1* plays a role in lymphomagenesis (Zhong et al., 2007). Moreover, the fact that overexpression of *Lyl1* in mouse BM cells resulted in T-cell expansion in the peripheral blood further evidenced that *Lyl1* has the potential to induce leukemia development (Lukov et al., 2011). Lmo2 protein is an oncogenic transcription factor that is frequently overexpressed in T-ALL and its binding capacity to DNA sequences depends on the recruitment of Lyl-1 (Wadman et al., 1994). By using the Lmo2-transgenic mice lacking Lyl-1 in the thymus, McCormack et al (McCormack et al., 2013) found that Lyl-1 is required for the leukemic activity of Lmo2, including aberrant self-renewal of thymocytes, and subsequent generation of T-cell leukemia, suggesting that Lyl-1 is the critical bHLH cofactor for Lmo2 in leukemia. Additionally, Zohren et al (Zohren et al., 2012) indicated a distinct mechanism for the involvement of Lyl-1 in T-ALL, via the control of the T-progenitor pool. The production of lymphoid-primed multipotent progenitors (LMPP), CLPs and early T lineage progenitors (ETPs) were severely inhibited in Lyl-1 knockout adult mice.

Lyl-1-deficient ETPs and thymocyte progenitors at the CD4-CD8-double-negative 2 stage displayed more apoptosis, blocked differentiation and impaired population expansion. CHIP assays performed in the mouse HPC-7 hematopoietic progenitor cell line, further showed that Lyl-1 directly binds to an enhancer located 35 kilobases upstream of *Gfi1*. Lyl-1 regulation of *Gfi1* expression at the LMPP and ETP stages was shown to promote T cell lymphopoiesis (Zohren et al., 2012).

In addition to its involvement in T-ALL induction, Lyl-1 was also found to be a potential oncogenic factor for acute myeloblastic leukemia (AML) formation. *Lyl-1* was highly expressed in most AML cell lines and in CD34+ AML cells. Moreover, overexpressing *Lyl-1* in K562 and U937 cell lines led to an increased growth rate and clonogenic potential (Meng et al., 2005). In addition, forced expression of *Lyl-1* in K562 cells resulted in enhanced spontaneous and hemin-induced erythroid differentiation but blocked spontaneous as well as PMA-induced megakaryocytic differentiation. By performing the antibody supershifting experiments, San-Marina et al (San-Marina et al., 2007) found that Lyl-1 indirectly interacts with the cyclic AMP receptor element binding protein 1 (CREB1) that is a widely-expressed transcription factor and a suspected oncogene in AML. Lyl-1 can alter the expression of CREB1 target genes, suggesting a direct role in the malignant phenotype by occupying different promoters. San-Marina et al (San-Marina et al., 2012) further identified that those two suspected oncoproteins, CREB1 and Lyl-1, can co-regulate the expression of Stathmin (STMN1) by directly binding to its promoter regions. STMN1 is a microtubule destabilizing protein with a key role in cell cycle progression and cell migration that is over-expressed in AML. It is therefore suggested that the interactions between CREB1-LYL1-STMN1 may contribute to the malignant phenotype.

### 1.3.2 Functional roles of Lyl-1 in hematopoiesis

So far, two *Lyl-1* allele mutant transgenic mice models have been generated to investigate the role of Lyl-1 in hematopoiesis (**Fig 15**). The first *Lyl-1* knockout mouse model (*Lyl-1<sup>LacZ</sup>*) was generated through homologous recombination (Capron et al., 2006). In these mice, part of *Lyl-1* coding region was replaced by the LacZ reporter gene. The LacZ gene was inserted within the sequence encoding the first helix of Lyl-1 HLH domain, in exon four. Consequently, this *Lyl-1<sup>LacZ</sup>* allele encodes a C-terminally truncated Lyl-1 protein fused to  $\beta$ -Galactosidase ( $\beta$ -Gal) (Capron et al., 2006). As *Lyl-1<sup>LacZ</sup>* keeps all the 5' cis-regulatory region of *Lyl-1*, the detection of  $\beta$ -Gal expression and/or activity in any cells is likely to reveal the transcriptional activation of the *Lyl-1* locus in wild-type mice. The second *Lyl-1* knockout mouse model was generated by replacing the entire coding region of *Lyl-1* with a lox-P-flanked Neo cassette (refer to as *Lyl-1<sup>Mg</sup>*) (Souroullas and Goodell, 2011).

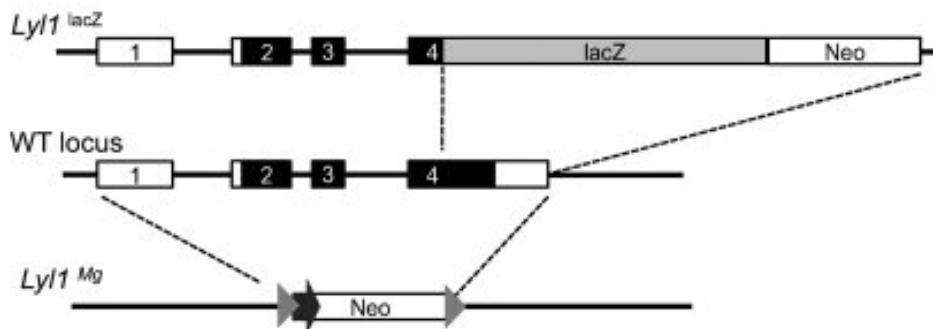


**Figure 15: Schematic comparison of the two targeted alleles of Lyl1.**

The *Lyl-1<sup>LacZ</sup>* mouse model has a LacZ/Neo cassette inserted into the fourth exon of the gene, disrupting the HLH and C-terminus, whereas the *Lyl-1<sup>Mg</sup>* allele eliminates the entire coding region (Souroullas and Goodell, 2011).

As stated above (§1.3), the loss-of-function of Scl/Tal-1, Lyl-1 paralogous transcription factor, resulted in the embryonic lethality at E9.5 due to the absence of hematopoietic cell

generation. In contrast, both *Lyl-1<sup>LacZ/LacZ</sup>* null homozygous (targeting HLH domain) mice and *Lyl-1<sup>Mg/Mg</sup>* (targeting full coding sequence) mice were viable and fertile, with no obvious developmental defects. However, adult HSCs from both strains displayed a defective self-renewal, as well as a block in B cells differentiation (Capron et al., 2006; Souroullas and Goodell, 2011). By using the *Lyl-1<sup>LacZ</sup>* knockout mice, Capron et al (Capron et al., 2006) found that Lyl-1 is not involved in the specification of HSCs. However, both FL- and adult BM-HSCs from *Lyl-1<sup>LacZ/LacZ</sup>* animals displayed a severely impaired long-term reconstitution capacity, an observation that was further confirmed in *Lyl-1<sup>Mg/Mg</sup>* knockout mice (Souroullas and Goodell, 2011). Furthermore, although Lyl-1 does not compensate for Scl/Tal-1 in HSC specification processes, Souroullas et al (Souroullas et al., 2009) showed, using Scl/Lyl-1 conditional double knockout mouse models, that *lyl-1* and Scl/Tal-1 shares some level of functional redundancy in HSC survival and that Lyl-1 plays a critical role in adult HSC maintenance.

Lyl-1 was also shown to play definite, but distinct, roles in BM- and spleen-derived erythropoiesis (Capron et al., 2011). The BM and spleen erythroblasts had a quite different *Lyl-1* expression pattern. In the spleen, *Lyl-1* was expressed at a very high level in immature erythroblasts, but its expression level was decreased during differentiation, whereas in the BM, erythroblasts expressed low level of *Lyl-1* gene in immature erythroblasts, while this expression increased during differentiation. Moreover, in the BM, Lyl-1 deficiency resulted in decreased erythropoiesis with a partial block in the differentiation, and an enhanced apoptosis associated with decreased Bcl-x<sub>L</sub> expression. In contrast, erythroid progenitor and precursor cells were significantly increased in the spleen of *Lyl-1<sup>LacZ/LacZ</sup>* mice.

### **1.3.3 The expression pattern of Lyl-1 during hematopoietic ontogeny**

During ontogeny, Scl/Tal-1 is required for hematopoietic cell generation, both in the YS and in the intra-embryonic compartment. Considering the similarities between Lyl-1 and

*Scl/Tal-1*, our group investigated the expression pattern of *Lyl-1* in mouse embryos from E7 to E14 using *in situ* hybridization, as well as  $\beta$ -Gal expression in *Lyl-1<sup>LacZ</sup>* knock-in embryos and meanwhile compared *Lyl-1* expression pattern with that of *Scl/Tal-1*, with particular emphasis given to developmental hematopoiesis (Giroux et al., 2007).

Overall, *Lyl-1* was shown to be specifically expressed by derivatives of the hemangioblastic mesoderm, as it is only expressed by endothelial, endocardial and hematopoietic cells during embryonic development. Additionally, a comparison between the expression patterns of *Lyl-1* and *Scl/Tal-1* revealed a largely overlapping pattern, in the developing vasculature and endocardium and, within the developing hematopoietic system, in the sites of emergence of intra-embryonic HSCs, in the FL and spleen, and the absent expression in the thymus.. However, the expression patterns of these two genes differed in several instances: (1) unlike *Scl/Tal-1*, the *Lyl-1*/ $\beta$ -Gal protein was not expressed in YS-blood islands during vasculogenesis and primitive erythropoiesis, so that the endothelial expression of the *Lyl-1*/ $\beta$ -Gal protein was restricted to the intra-embryonic compartment and allantois; (2) *Lyl-1* did not share *Scl/Tal-1* neuronal expression (van Eekelen et al., 2003). Altogether, these data suggested that *Lyl-1* most probably plays roles in the development of hematopoiesis that was further investigated in our team. My research project focused on the first steps of this hematopoietic development, investigating *Lyl-1* function in YS hematopoiesis.

## **2 RESULTS**

### **Functions of the transcription factor Lyl-1 in the development of the macrophage lineage**

## 2.1. Summary

The majority of the results presented here are developed and illustrated in the paper to be submitted. The data that are not presented in this article will be detailed in the second part of the result section and are referred to as additional data.

### 2.1.1. *Lyl-1* expression characterizes primitive macrophage progenitors from the first of YS-derived wave.

During embryogenesis, there is a conserved program of HSC-independent hematopoiesis that precedes HSC function and is required for embryonic survival. This early, HSC-independent, hematopoiesis consists of two waves to produce hematopoietic cells. The first wave of hematopoiesis contains primitive erythroid, megakaryocyte and M $\Phi$  progenitors that arise in the YS at E7-7.5, well before HSC formation. A second wave of multi-potential EMP also arises in the YS. EMP first emerge at E8.25-E8.5 and increase in numbers in the YS by E9. Because progenitors from these two waves are mixed in the systemic circulation, their relative contribution to embryonic hematopoiesis remains elusive. *Lyl-1* is a bHLH transcription factor that is closely related to *Scl/Tal-1*. *Scl/Tal-1* is proved to be required for specification of YS hematopoiesis, as well as definitive HSCs. Moreover, by using the *Lyl-1<sup>lacZ</sup>* strain, we previously showed that *Lyl-1* expression pattern during ontogeny largely overlaps with that of *SCL/Tal-1*, indicating that *Lyl-1* may play a role during developmental hematopoiesis.

To investigate this hypothesis, we first assessed whether *Lyl-1* plays a role in YS hematopoietic cells development. We submitted to clonogenic assay *Lyl-1<sup>LacZ/LacZ</sup>*, *Lyl-1<sup>WT/LacZ</sup>* and wild type E8-YS, which were organ cultured for 1 day (OrgD1). Because the YS is dissected before circulation is established, this culture system also to specifically analyze progenitors originating from the YS. Moreover, the organ culture step allows the

development of progenitors from the two YS waves, making this culture system adapted for initial investigation on gene deletion effect. We found that *Lyl-1* disruption significantly increased the production of MΦ progenitors, while the yield of other progenitors types, including GM progenitors and EMp, was not modified. The size of *Lyl-1<sup>LacZ/LacZ</sup>* and *Lyl-1<sup>WT/LacZ</sup>* MΦ colonies as well as the cell morphology was similar to those observed in wild type colonies.

We next investigated whether *Lyl-1* invalidation similarly affected the MΦ population derived from the differentiation of intra-embryonic HSC. At E10-10.5, the AGM contains newly generated HSC and YS-derived hematopoietic cells that have colonized the intra-embryonic compartment through the blood flow. These YS-derived cells include mature MΦ, as well as progenitors endowed with MΦ potential, such as committed MΦ, GM and EMp progenitors. To specifically assess the differentiation potential toward the MΦ lineage from AGM-HSC, wild type, *Lyl-1<sup>WT/LacZ</sup>* and *Lyl-1<sup>LacZ/LacZ</sup>* AGM cells were cultured on OP9 to allow their differentiation. After 4 days of culture, the number and type of progenitors produced was further characterized through clonogenic assays. Contrary to what was observed for E8-OrgD1-YS, wild type and *Lyl-1* mutant AGM gave rise to similar numbers of MΦ progenitors, as well as GM and EMp. Moreover, the amount of CD11b<sup>+</sup> and F4/80<sup>+</sup> MΦ produced was similar in the three genotypes at various time points of the culture. These data together suggested that *Lyl-1* does not regulate MΦ production from intra-embryonic HSC, as it does in the early YS (See additional data).

During YS development, MΦ develop from c-Kit<sup>+</sup>CD31<sup>+</sup>CD45<sup>-</sup> progenitors (C subset), which subsequently acquire CD11b and CD45 expression (A1 subset). Further MΦ differentiation is characterized first by c-Kit down-regulation (A2 subset), then by the concomitant down-regulation of CD31 and up-regulation of CX3CR1 and F4/80 (A3 subset). Because of the effects on YS-MΦ production we found in *Lyl-1<sup>LacZ</sup>* mice, I analyzed the phenotype and relative distribution of the MΦ subsets in WT and *Lyl-1* mutant E8-OrgD1 and in E9-YS by cytometry analysis. I also used FACS-Gal assay, as a reporter for *Lyl-1* expression, this assay allows the flow cytometry characterization of cells that display a β-Gal

activity using its fluorescent substrate (FDG). I showed that mutant E8-OrgD1 or E9-YS harbored a large  $CD45^{neg/low}$  subset within the  $CD11b^+CD31^+$  (A1-A2 progenitors) population. This subset was absent from WT E9-YS and was no longer observed after E9.5 in the three *Lyl-1* genotypes. Importantly, this transient C to A1 intermediate subset was demonstrated to be 100% Lyl-1 positive.

Previous results showed that YS generates two MΦ waves: the first YS-derived MΦ wave, also called primitive MΦ, originates from monopotent MΦ progenitors that appear at E7.5-E8, in the absence of upstream progenitors, such as GM and EMp, and the second wave of YS-derived MΦ is that EMp give rise to the definitive MΦ. MΦ from the first and second YS-derived waves cannot be distinguished by their phenotype. Moreover, they rapidly mix within the YS, and soon after within the systemic blood flow. Consequently, the specific features of primitive MΦ have not yet been characterized in detail. So I first assessed *Lyl-1* expression in MΦ progenitors at E9, a few hours before EMp emerge, using FACS-Gal assay. I found that the vast majority of  $c-Kit^+CD45^+CD11b^+$  primitive MΦ progenitors expressed Lyl-1. Interestingly, few hours later (E9-9.5), Lyl-1 negative MΦ progenitors were also detected in the YS, suggesting that two distinct MΦ progenitors pool can be discriminated by *Lyl-1* expression.

As stated above, Lyl-1 deficiency only affects MΦ production in the early YS (E8 OrgD1 and E9), but does not do that in the intra-embryonic HSC population. Moreover, the YS generates two MΦ waves, so that E9-9.5 YS harbors both primitive MΦ progenitors from the first wave and MΦ progenitors from the second wave, which originate from the myeloid differentiation of GM and EMp. A substantial Lyl-1/FDG expression in MΦ progenitors was detected from *Lyl-1<sup>LacZ/LacZ</sup>* E8-OrgD1-YS (C-A1) or E9-YS (C-A1-A2), whereas only a subset of MΦ progenitors from E9-E9.5 YS expressed Lyl-1. Therefore, we proposed that these Lyl-1 positive MΦ progenitors might represent the primitive ones that are present at earlier stages. Unfortunately, MΦ progenitors of the first and second YS waves cannot be discriminated by their phenotype, so that the only possible way to assess whether Lyl-1 HLH deletion specifically targets one MΦ progenitors population was to use their different

kinetics of appearance, despite the reduced number of progenitors present. The first GM and EMP appear in the YS at the 3-5S-stage. We therefore analyzed  $\beta$ -Gal activity in *Lyl-1*<sup>WT/LacZ</sup> E8-YS, at the 0-5S stage. We found that at a stage when the YS only harbors primitive M $\Phi$  progenitors within the myeloid lineage, all CD11b<sup>+</sup>CD31<sup>+</sup> primitive M $\Phi$  progenitors expressed Lyl-1. Additionally, we also sorted the Lyl-1/FDG positive and negative fractions from *Lyl-1*<sup>WT/LacZ</sup> E8-YS and submitted to clonogenic assays. We found that most hematopoietic progenitors were included in the FDG negative fraction. However, nearly all M $\Phi$  progenitors were consistently present in the FDG positive fraction. The clonogenic assays also showed that less than one GM and EMP progenitor per YS were detected at the 0-5S-stage, in both wild type and mutant YS, confirming that the assay was performed at a time when it is possible to discriminate primitive M $\Phi$  progenitors from M $\Phi$  progenitors derived from the second, EMP-derived, YS wave. We also observed in each experiment a 2-3-fold increase in the percentage (and absolute number per YS) of primitive M $\Phi$  colonies obtained from both *Lyl-1*<sup>WT/LacZ</sup> and *Lyl-1*<sup>LacZ/LacZ</sup> YS compared to wild type.

To get stronger evidence, I tested the hematopoietic potential of Lyl-1 positive progenitors versus that of negative progenitors from later developmental stage. Specifically, FDG<sup>+</sup>/Lyl-1<sup>+</sup> and FDG<sup>-</sup>/Lyl-1<sup>-</sup> c-Kit<sup>+</sup>CD45<sup>+</sup>CD11b<sup>+</sup> progenitors were sorted from *Lyl-1*<sup>WT/LacZ</sup> E10-YS and submitted to clonogenic assay. Their progeny was compared to that of E9 WT and *Lyl-1*<sup>WT/LacZ</sup> YS that only harbors primitive M $\Phi$  progenitors. I found that progenitors from E9-YS nearly exclusively produced M $\Phi$  colonies, while E10 YS also generated GM and G colonies. Moreover, the majority of FDG<sup>+</sup>/Lyl-1<sup>+</sup> progenitors only gave rise to M $\Phi$  colonies, whereas FDG<sup>-</sup>/Lyl-1<sup>-</sup> progenitors also produced GM or granulocyte colonies, which characterize their definitive type.

The results of the three approaches undertaken here correlate to show that Lyl-1 expression discriminates the YS-derived primitive and definitive M $\Phi$  progenitors. Moreover, we find that Lyl-1 function during normal development seems to negatively regulate the generation and expansion of the primitive M $\Phi$  lineage, as shown by the increased production of C to A1 transition subset as well as the increased recovery of M $\Phi$  progenitors in *Lyl-1*<sup>LacZ/LacZ</sup> YS.

To further develop the results I gained from the *in vitro* and flow cytometry analyzes mentioned above, we decided to perform RNA-Seq analyses to (1) determine the specific features of primitive MΦ, compared to definitive MΦ from older embryos; (2) assess what is the effect of Lyl-1 inactivation on the poorly known primitive MΦ population. The information gathered from this RNA-Seq assay might provide long sought after information on primitive MΦ population, and might shed a new light on the regulation of the properties of embryonic hematopoietic progenitors. The overall experimental strategy and aims of this ongoing RNA-Seq are shown in additional data.

### **2.1.2. Lyl-1 expressing primitive MΦ give rise to embryonic microglia.**

The progeny of Lyl-1-expressing primitive MΦ progenitors may contribute to various MΦ populations of the developing embryo. So I next questioned the contribution of Lyl-1 positive MΦ progenitors to the mature MΦ compartment, focusing on E10.5-YS, E10.5-FL, as well as developing brain.

The relative contribution of primitive and transient definitive YS waves to the first steps of FL development is still unclear. Using facs-Gal assay, I found that the E10.5-FL contain two distinct MΦ progenitors discriminated by their Lyl-1 expression, confirming that primitive MΦ population also colonize the FL during early embryonic development (See additional data).

It was recently established through fate mapping experiments that microglia originates from early YS-derived MΦ. However, as stated above, primitive and EMp-derived MΦ lineages coexist in the YS so that their respective contribution to microglia was naturally questioned. However, EMp and primitive MΦ progenitors share the same c-Kit<sup>+</sup>CD45<sup>low</sup> phenotype and are both present in the YS at the stages when fate map experiments were performed, so that the respective contribution of primitive and EMp-derived definitive MΦ progenitors to the developing microglia remains unclear. Using FACS-gal assay, I found that compared to

E10.5-YS that comprised both  $FDG^+/Lyl-1^+$  and  $FDG^-/Lyl-1^-$  M $\Phi$  progenitors, the brain rudiment from the same embryos harbored mostly  $FDG^+/Lyl-1^+$  M $\Phi$  progenitors. Moreover, F4/80<sup>+</sup> M $\Phi$  from E10.5-YS also contained both  $FDG^+/Lyl-1^+$  and  $FDG^-/Lyl-1^-$  population, while in E10.5 brain at, mature M $\Phi$  were exclusively  $FDG^+/Lyl-1^+$ . These data strongly suggest that the initial source for microglia development is YS-derived Lyl-1 positive primitive M $\Phi$ .

As mentioned before, primitive hematopoiesis is preserved in embryos lacking the expression of *c-Myb*, and the primitive wave is considered as *c-Myb*-independent for its development. Moreover, the expression of *c-Myb* has been shown to be dispensable for the development of microglia. Thus, to strengthen our conclusion about the primitive origin for microglia, I performed qRT-PCR analyses to detect whether there is a discrepancy in *c-Myb* transcript between Lyl-1 positive and negative M $\Phi$  progenitors population. The results showed that YS- $FDG^-/Lyl-1^-$ -myeloid progenitors displays similar *c-Myb* levels as FL definitive progenitors. In contrast, *c-Myb* levels in YS- $FDG^+/Lyl-1^+$  and brain/head M $\Phi$  progenitors were similar to that of E9-YS primitive M $\Phi$  progenitors, strengthening their primitive status and lineage relationship.

### **2.1.3. Lyl-1 inactivation impairs M $\Phi$ maturation at early embryonic stage.**

To obtain information on Lyl-1 function during M $\Phi$  development, I first used *Cx3cr1*<sup>WT/GFP</sup> mice to sort A1, A2 and A3 M $\Phi$  subsets from both E10.5-YS and brain and analyze Lyl-1 transcript levels during M $\Phi$  differentiation. I found that *Lyl-1* mRNA levels were similar in the YS and brain for each M $\Phi$  subset. The expression of Lyl-1 is maintained throughout differentiation with a reduction from A1 to A3, implying different Lyl-1 requirement during M $\Phi$  maturation.

I also built up *Cx3cr1*<sup>GFP</sup>*Lyl-1*<sup>LacZ</sup> double mutant strain mice to more accurately check the influence of Lyl-1 inactivation during M $\Phi$  differentiation. I had initially observed that the

size of the whole MΦ population appeared similar in the three genotypes. But, using the newly developed strains (*Cx3cr1<sup>GFP/WT</sup>Lyl-1<sup>WT/WT</sup>*; *Cx3cr1<sup>GFP/WT</sup>Lyl-1<sup>LacZ/WT</sup>*; *Cx3cr1<sup>GFP/WT</sup>Lyl-1<sup>LacZ/LacZ</sup>*), I observed a reverse distribution of A1, A2 and A3 subsets in the YS and brain, the YS containing mainly A1 and A2 progenitors, while the brain contains mostly mature MΦ. This suggests that the early brain is a favorable environment for MΦ maturation. The data also revealed that compared to *Cx3cr1<sup>GFP/WT</sup>Lyl-1<sup>WT/WT</sup>* mice, there were more A1 progenitor and less A3 mature MΦ in both YS and brain of *Cx3cr1<sup>WT/GFP</sup>Lyl-1<sup>LacZ/LacZ</sup>* mutant mice. Thus, the results together suggest that *Lyl-1* inactivation impairs MΦ maturation.

#### **2.1.4. *Lyl-1* controls embryonic microglia pool at two developmental stages.**

Previous evidence showed that the microglia compartment is established at around E11.5 and maintained by local proliferation without circulating monocyte input under health condition. So to detect whether *Lyl-1* expression was maintained in microglia development, I measured *Lyl-1* mRNA levels in sorted microglia from wild type and *Lyl-1<sup>LacZ/LacZ</sup>* mutant mice, as well as LacZ activity by FACS-gal assay, at 6 time points (E12, 14, 16, P0, 15 and 42). *Lyl-1* expression level increased following embryonic development and was highly enriched at P15 and 42 in wild type microglia. *Lyl-1* expression was also maintained in microglia throughout embryonic development in *Lyl-1<sup>LacZ/LacZ</sup>* mutant mice. However, LacZ activity significantly decreased at P15 and was only barely detected at P42 in mutant microglia.

To assess the effect of *Lyl-1* on microglia development, I next investigated the kinetics of microglia in wild type, *Lyl-1<sup>WT/LacZ</sup>* and *Lyl-1<sup>LacZ/LacZ</sup>* mice from E9.5 to E14.5. Specifically, the total number of brain cells was counted. Then the percentage of microglia was further characterized through FACS analysis. Finally, the number of microglia per brain was estimated by using the total numbers and percentages. I found that wild type and *Lyl-1<sup>WT/LacZ</sup>*

mice show similar trend of microglia growth. Contrary to what was observed for wild type and *Lyl-1<sup>WT/LacZ</sup>*, *Lyl-1<sup>LacZ/LacZ</sup>* brains initially (E10.5-11.5) displayed an excess ( $CD31^+CD45^+CD11b^+$ ) microglia progenitors population, but these progenitors rapidly resumed a normal distribution afterwards and steadily decreased after E14.5. In terms of mature microglia, I found a significant reduction of  $F4/80^+$  microglia in the brain of *Lyl-1<sup>LacZ/LacZ</sup>* mutant mice at E12 (See additional data), whereas the amount of microglia was not influenced before E11, suggesting again that *Lyl-1* inactivation impairs the proliferation of microglia, but not of brain colonization. Although reduced microglia numbers were still present in the mutants at E14, the population pool seemed to recover by itself. By using the similar method, a reduced number of microglia in *Lyl-1* mutants was also found at P0-3.

To better understand the regulation mechanism of *Lyl-1* in microglia development, I then assessed microglia survival and expansion in wild type and mutant brain at these defective time points. Analysis of the incorporation of the thymidine analog BrdU into microglia at E12 showed more such incorporation in wild type subsets examined than in their mutants counterparts, suggesting a lower proliferation rate in mutant microglia. In addition, analysis of the binding of AnnexinV to microglia showed a similar frequency of apoptosis between wild type and mutant cells at E12 and P0-3. Interestingly, the frequency of apoptotic cells was lower in *Lyl-1<sup>LacZ/LacZ</sup>* mutants at E14. This finding might be one of explanations for recovery of microglia pool in mutants after E12.

Combination of genetic depletion strategy and transcriptomic analysis suggested that microgliogenesis is tightly regulated during development. As mentioned before, the differentiation and proliferation of microglia are required for the CSF-1 receptor, which plays roles through two ligands, CSF-1 and IL-34. Also, evidences have also showed that the development of microglia is dependent on the transcription *Pu.1* and *Irf8*, etc. To further define the *Lyl-1* function during microglia development, I performed qRT-PCR on embryonic (E12, 14, 16), postnatal (P0-3, 15) and adult microglia (P42). I quantified transcripts from genes that are known to be involved in M $\Phi$ /microglia development and differentiation (*Cx3cr1*, *Irf8*, *Csf1-r*, *Mafb*, *Runx1*, *Pu.1*), as well as regulators of

developmental hematopoiesis (*Scl/Tal-1*, *Lmo2*) and related factors (*Tcf3/E2A*, *Tcf4/E2.2*). By analyzing genes regulated differentially in *Lyl-1*-deficient microglia compared to control wild type, I found that several of the previously described microglia development-dependent genes were down-regulated at specific stage following *Lyl-1* deletion, such as *Cx3cr1* at E12, *lmo2*, *Csf1-r* and *Irf8* at both E12 and P0. More interestingly, I found that the expression level of *Mafb*, which controls microglia self-renewal in the adult, was significantly decreased in mutant cells around birth. One possible explanation is that microenvironment drives activation of microglia self-renewal through down-regulation of *Mafb* to compensate the microglia defects around birth. Notably, the stages which genes were modified were consistent to the stages of impaired number of microglia.

### **2.1.5. *Lyl-1*-defective microglia induce social anxiety disorders**

Microglia are thought to play key roles in brain development, homeostasis and function. During development, they monitor and scavenge dying cells, pathogens and molecules, engulf synaptic material to shape the synapse network through a pruning mechanism. So that, impaired microglia function is considered to be involved in many neurodegenerative diseases such as autism, schizophrenia or obsessive-compulsive disorders. Knockout of chemokine receptor *Cx3cr1* in mice leads to a transient reduction of microglia during the early postnatal period and a disruption in microglia -mediated synaptic pruning, resulting in impaired functional brain connectivity and social behaviour. Considering that microglia play key roles in neurogenesis, we wanted to know whether *Lyl-1* disruption in microglia could impair neurodevelopmental processes.

It is well documented that microglia produce and secrete cytokines, including ILs, tumor necrosis factors (TNFs) and so on, that are involved in cellular communication, regulate inflammation and immune responses, and cell growth, survival and differentiation. I checked the transcript levels of three important cytokines genes (*IL-1 $\beta$* , *IL-6* and *TNF- $\alpha$* ) in

microglial cells from wild type and Lyl-1 mutants mice at P0 and P15. The qPCR results showed that the gene expression levels of these three cytokines are much lower in the Lyl-1 mutants at P15, suggesting impaired functions in Lyl-1 deficiency microglia (See additional data).

We also set collaboration with Marco Prinz's group in University of Freiburg, Germany, to further understand the consequence of Lyl-1 inactivation in adult mouse. My part in this collaboration was to prepare the tissue samples for the analyses performed in Marco Prinz's group. The counting iba+ microglia cell number on brain slices correlated with our quantification by cytometry analysis to show a reduced microglia number in the newborn, but not in E14.5 and adult mutants. Moreover, they evidenced that newborn microglia is dysmorphic. Their major discovery came from behaviour analyses of adult mutants that evidenced impaired social behaviour. Lyl-1 implication in autism syndrome disorder was further confirmed by functional magnetic resonance imaging experiments, showing that Lyl-1 mutant show hyperactivity in the various brain area involved in social anxiety.

### **2.1.6. Possible involvement of Lyl-1 defects in other neurologic diseases**

We have been collecting information from bibliographic and database to assess whether Lyl-1 is also involved in human microglia in normal and pathological condition. The information so far obtained confirmed the expression of Lyl-1 in human microglia, but did not so far provide clear-cut evidences for Lyl-1 involvement in autism syndrome disorders, as well as in Alzheimer's disease. It however points to Lyl-1 implication in neuro-inflammatory processes (See additional data).

## **2.2. Result 1: Lyl-1 links microglia development to neuropsychiatric disease (Article in preparation)**

Shoutang Wang<sup>1\*</sup>, Thomas Blank<sup>4\*</sup>, Anna-Lila Kaushik<sup>1,\*</sup>, Katrin Kierdorf<sup>3</sup>, Deshan Ren<sup>1</sup>, Gabriel Matherat<sup>1</sup>, Yann Lécluse<sup>2</sup>, Hana Raslova<sup>1</sup>, Isabelle Plo<sup>1</sup>, Marco Prinz<sup>3#</sup>, Isabelle Godin<sup>1#</sup><sup>✉</sup>

\*, # Equal contributions; ✉ Corresponding Author

### ***Summary***

Microglia are tissue macrophages of the central nervous system that control tissue homeostasis, and are crucially important for organ integrity. Neuropsychiatric diseases are hallmarked by neuronal dysfunction and associated glial activation. Whether microglial activation is causative or secondary in neurodevelopmental disorders is currently unclear. Microglia are long-living cells entirely acquired during ontogeny from HSC-independent yolk sac progenitors. Factors impairing YS development may thus eventually lead to neuropsychiatric abnormalities. We show that the transcription factor Lyl-1 marks YS-derived primitive macrophage progenitors that produce the entire microglia pool. Lyl-1 disruption alters the development of primitive macrophage and microglia, resulting in a functionally impaired adult microglia. The synaptic pruning is disrupted leading to neuronal disconnectivity, causing impaired social interactions with anxiety like behavior. We thus identify Lyl-1 as a novel and critical regulator of primitive macrophage development, which disruption impacts microglia development and functionality, leading to the development of a distinct neuropsychiatric phenotype.

## INTRODUCTION

Microglial cells play pleiotropic functions in the normal and pathological brain. During development, they are involved in the shaping of the synapse network through a pruning mechanism, so that impaired microglial function is thought to be involved in the development of disorders such as autism, schizophrenia or obsessive-compulsive disorders (*Prinz and Priller, 2014; Zhan et al., 2014*). Fate map studies from several groups including ours demonstrated that microglia develops from progenitors originating from the YS (*Ginhoux et al., 2010; Schulz et al., 2012; Kierdorf et al., 2013; Gomez Perdiguero et al., 2015*), thus confirming a developmental model that we had previously put forward (*Alliot et al., 1999*).

Blood cell production in the developing embryo results from the contribution of sequential waves of haematopoietic progenitors, independently generated (*Cumano and Godin, 2007*). Blood cells arise first from the yolk sac (YS) that rapidly supplies the embryo with erythroid and myeloid cells from embryonic day (E) 7-7.5. The generation of progenitors for these lineages occurs prior to the production of haematopoietic stem cells (HSC) in two distinct waves.

Considering the macrophage ( $M\Phi$ ) lineage, the first YS-derived  $M\Phi$  wave, called primitive ( $M\Phi^{\text{Prim}}$ ), originates from monopotent  $M\Phi$  progenitors that appear at E7.5-E8, in the absence of upstream progenitors as defined in the adult haematopoietic hierarchy (*Palis et al., 1999; Bertrand et al., 2005b*), namely erythro-myeloid progenitors (EMp), then granulo-monocytic progenitors (GM) that later constitute the forefathers of MF progenitors. These EMp and GM progenitors emerge slightly later (E8.25) and give rise to the second YS-wave, called transient definitive, by producing definitive  $M\Phi$  ( $M\Phi^{\text{Def}}$ ), as well as

granulocytes (McGrath et al., 2015). M $\Phi$  from the first and second YS waves, which cannot be distinguished by phenotype, rapidly mix within the YS, and soon after within the systemic blood flow, so that the specific features of M $\Phi$ <sup>Prim</sup> remain poorly characterized. Consequently, whereas it is now clearly established that microglia entirely derives from YS-derived M $\Phi$  progenitors, the contribution of primitive vs. EMP-derived MF progenitors remains a matter of debate.

Haematopoietic progenitors features, such as cell fate decision, progenitor maintenance and differentiation, etc. are regulated by a transcription factor network that comprises Tal-1/SCL, Lmo2, Runx1 and GATA-2, the major regulators of haematopoietic progenitors development during ontogeny (Pina and Enver, 2007; Wilson et al., 2010). Tal-1/scl, lmo2 and gata-2 belong to a transcriptional complex, which also includes the basic helix-loop-helix (bHLH) transcription factor lymphoblastic leukaemia-derived sequence 1 (Lyl-1). Like its paralog tal-1/scl, lyl-1 was initially identified in chromosomal translocations leading to paediatric T-cell acute lymphoblastic leukaemia, but contrary to Tal-1/SCL, which is mandatory for the specification of all haematopoietic progenitors in the embryo (Curtis et al., 2012), Lyl-1 functions during developmental haematopoiesis remains largely unknown.

Analysing YS Haematopoiesis in *Lyl-1<sup>LacZ</sup>* mice, we discovered that Lyl-1 expression discriminates M $\Phi$ <sup>Prim</sup> from EMP-derived M $\Phi$ <sup>Def</sup> progenitors. These Lyl-1-expressing M $\Phi$ <sup>Prim</sup> progenitors were found to gives rise to the entire microglia, Lyl-1 transcripts being expressed in primary microglia and not in other CNS cells. Lyl-1 inactivation leads to an increased production of M $\Phi$ <sup>Prim</sup> progenitors in the YS, and to a decreased production of microglia at two development time points (E12.5 and P0-3). Remarkably, Lyl-1 inactivation in microglia

impacts neurodevelopmental processes, as behavioural investigations pointed to social anxiety disorder in *Lyl-1* deficient mice.

***Primitive MΦ progenitors, discriminated from EMP-derived MΦ progenitors by *Lyl-1* expression, gives rise to the entire microglia pool***

Targeting *lyl-1* HLH domain (*Lyl-1<sup>LacZ</sup>* strain (Capron *et al.*, 2006)) or the full coding sequence (Souroullas and Goodell, 2011) leads to impaired self-renewal of adult HSC, defective lymphoid differentiation (Capron *et al.*, 2006; Souroullas *et al.*, 2009; Zohren *et al.*, 2012), as well as impaired endothelial cells maturation (Pirot *et al.*, 2014). *Lyl-1* expression pattern during ontogeny essentially overlaps that of *Tal-1/SCL*: both factors are similarly expressed in the developing cardiovascular and haematopoietic systems, suggesting that *Lyl-1* may play a role during developmental haematopoiesis (Giroux *et al.*, 2007). A requirement for functional *lyl-1* during developmental processes was also suggested by significantly decreased litter size and increased perinatal lethality in *lyl-1<sup>LacZ/LacZ</sup>* compared to Wild Type (WT) strains (Extended data Fig. 1a).

The effect of *Lyl-1* invalidation on YS haematopoiesis was first probed using E8-YS maintained in organ culture for 1 day (E8-OrgD1-YS), a culture system that allows the development progenitors from both primitive and transient definitive waves of YS, and also avoids the contamination by progenitors of intra-embryonic origin (Cumano *et al.*, 1996) that occurs after E8.25 (4-5 somite-stage (S)) (McGrath *et al.*, 2003). The production of MΦ progenitors was increased from *lyl-1<sup>WT/LacZ</sup>* and *lyl-1<sup>LacZ/LacZ</sup>* E8-OrgD1-YS compared to WT, while the yield of other progenitors types, including EMP and GM was unmodified (Fig. 1a).

During YS development, both  $M\Phi^{Prim}$  and  $M\Phi^{Def}$  develop from  $c\text{-Kit}^+CD31^+CD45^-$  progenitors (C subset), which subsequently acquire CD11b and CD45 expression (A1 subset). Further  $M\Phi$  differentiation is characterized first by c-Kit down-regulation (A2 subset), then by the concomitant down-regulation of CD31 and up-regulation of F4/80 and CX3CR1 (A3 subset) (Bertrand *et al.*, 2005b) (Fig. 1b). Further analysis of the phenotype and relative distribution of  $M\Phi$  progenitors subsets (Extended data Fig. 1b) showed that  $lyl\text{-}1^{lacZ/LacZ}$  E8-OrgD1 or E9-YS harboured a large  $CD45^{neg/low}$  subset within the  $CD11b^+CD31^+$  (A1-A2 progenitors) population that was no longer observed in WT YS at E9, and in mutant YS after E9.5 (Extended data Fig. 1c). This transient  $CD11b^+CD31^+CD45^{neg/low}$  C to A1 transition subset was also characterized by Lyl-1 expression (Extended data Fig. 1d), assessed using Facs-Gal assay, whereby the  $\beta$ -Galactosidase activity reporting Lyl-1 expression is detected using its fluorescent substrate FDG.

Interestingly, Facs-Gal assay also evidenced that, while the entire  $M\Phi$  progenitors population from E9-YS expressed Lyl-1 (Fig. 1c, Extended data Fig. 1b), E8-OrgD1-YS (data not shown) and E9.5-YS harboured two distinct  $M\Phi$  progenitors subsets discriminated by their FDG/Lyl-1 expression. As stated above, the YS cumulates  $M\Phi^{Prim}$  progenitors from the first YS wave and  $M\Phi$  progenitors from the second wave, which originate from the differentiation of EMp, then GM progenitors. Because only a subset of  $M\Phi$  progenitors from E8-OrgD1- or E9.5-YS expressed Lyl-1, while the entire population expressed it at E9, we hypothesized that  $lyl\text{-}1$  may mark and regulate the  $M\Phi^{Prim}$  wave. As  $M\Phi^{Prim}$  and  $M\Phi^{Def}$  progenitors cannot be discriminated by phenotype, we relied on the earliest stage of  $M\Phi^{Prim}$  progenitors production to assess  $lyl\text{-}1$  expression and function (Fig. 1d).

Since the first EMP and GM progenitors appear in the YS after the 3-5S-stage (*Palis et al., 1999; Bertrand et al., 2005b*), Facs-Gal assay was performed at E8 (0-5S stage), when only  $M\Phi^{Prim}$  are present. The CD11b population comprised two subsets, maternal  $M\Phi$  (CD11b+CD31-CD45+F4/80+ CD31-), which are present at this stage (*Bertrand et al., 2005b*) and a CD11b<sup>+</sup>CD31<sup>+</sup> CD45<sup>neg/low</sup> subset similar to the C to A1 transition subset observed at E9. FDG/Lyl-1 expression was only observed in the C to A1 transition subset. Notably, most cells (69.27%  $\pm$  0.33%) within the FDG/Lyl-1<sup>+</sup> gate co-expressed CD11b and CD31, thus qualifying as  $M\Phi^{Prim}$  progenitors. Conversely, the bulk of CD11b<sup>+</sup>CD31<sup>+</sup>  $M\Phi^{Prim}$  progenitors were found to display FDG/Lyl-1 expression. Additionally, the Lyl-1<sup>+</sup>  $M\Phi^{Prim}$  progenitors subset was consistently larger in *lyl-1<sup>WT/LacZ</sup>* than in WT YS, correlating with the increased production of  $M\Phi$  progenitors observed in *lyl-1<sup>WT/LacZ</sup>* E8 OrgD1-YS (**Fig1d**).

In clonogenic assays (**Fig. 2b**), we consistently observed a 2-3-fold increase of  $M\Phi$  progenitors production in *lyl-1<sup>WT/LacZ</sup>* and *lyl-1<sup>LacZ/LacZ</sup>* YS compared to WT, despite the limited number of  $M\Phi^{Prim}$  colonies (2-3 per YS). Moreover, when FDG/Lyl-1<sup>+</sup> and FDG/Lyl-1<sup>-</sup> fractions sorted from *lyl-1<sup>WT/LacZ</sup>* E8-YS were submitted to clonogenic assays, most haematopoietic progenitors derived from FDG/Lyl-1 negative cells. In contrast, the FDG/Lyl-1<sup>+</sup> subset consistently produced  $M\Phi$  progenitors (72.78  $\pm$  9.65%; n=3). These  $M\Phi$  progenitors amounted 1-4 per YS, a value consistent with published data (*Palis et al., 1999; Bertrand et al., 2005b*).

Contrary to  $M\Phi^{Prim}$  that differentiate from monopotent progenitors,  $M\Phi^{Def}$  arise from EMP progenitors that concomitantly generate GM progenitors and granulocytes (*McGrath et al., 2015*). To check whether Lyl-1 expression strictly characterize  $M\Phi^{Prim}$  progenitors,

cKit+CD45+CD11b+ myeloid progenitors from E10-YS, that cumulates both primitive and transient definitive lineages, were separated into FDG/Lyl-1 positive and negative subsets and submitted to clonogenic assay (*Fig. 1e*). Non-myeloid contaminants, such as EMk and EMP were recovered in similar amounts in all samples. Within myeloid colonies, E9-YS nearly exclusively produced M $\Phi$  colonies, while E10 YS also generated GM and G colonies. The E10-YS FDG+/Lyl-1+ colony output overlapped with that of E9-YS, in accordance with a restriction of lyl-1 expression to M $\Phi$ <sup>Prim</sup> progenitors. Furthermore, the FDG/Lyl-1 negative fraction gave rise to GM, G and M $\Phi$  colonies, confirming their definitive status.

Altogether, these data correlate to show that YS-derived M $\Phi$ <sup>Prim</sup> progenitors express Lyl-1, and that, in the early embryo, Lyl-1 expression discriminates M $\Phi$ <sup>Prim</sup> and M $\Phi$ <sup>Def</sup> progenitors. It is generally accepted that the production of primitive progenitors in the early YS is transient. Due to the increased production of M $\Phi$  progenitors in mutant YS, we may put forward the hypothesis that, during normal ontogeny, Lyl-1 negatively regulate the commitment, expansion and/or timing of production of M $\Phi$ <sup>Prim</sup> progenitors.

We next questioned the contribution of Lyl-1 expressing M $\Phi$  progenitors to the mature M $\Phi$  compartment, focusing on E10 YS and developing brain, since fat mapping analyses established that resident M $\Phi$  in this tissue exclusively arise from the YS (*Hoeffel et al., 2015; Sheng et al., 2015; Askew et al., 2017*). As stated above, M $\Phi$ <sup>Prim</sup> and EMP-derived M $\Phi$ <sup>Def</sup> progenitors subsets coexist in the YS so that their respective contribution to microglia was naturally questioned. Primitive haematopoietic populations have been characterized as independent of c-Myb-expression for their development, contrary to their definitive counterpart (*Tober et al., 2008; Gomez Perdiguero and Geissmann, 2013; McGrath et al.,*

2015). The normal amount of microglial cells found in mice lacking the c-Myb transcription factor argues for a primitive origin of microglia progenitors (Schulz et al., 2012; Kierdorf et al., 2013). Ginhoux et al. reached a similar conclusion because the induction of Runx1 expression at E7.25-7.5 that leads to microglia labeling, targets progenitors present at the latest at E8.5, when EMP-derived M $\Phi$  progenitors are hardly produced. However, this protocol leads to 30-40 % microglia labeling (Ginhoux et al., 2010) and although this level is likely to be underestimated, an additional contribution from a later source, namely EMP-derived M $\Phi$  progenitors, could be considered. Conversely, EMP-derived M $\Phi$ <sup>Def</sup> progenitors were also considered as providing microglia (Kierdorf et al., 2013; Gomez Perdiguero et al., 2015). Sorted c-Kit+CD45<sup>low</sup> progenitors from E8-YS were shown to give rise to erythro-myeloid cells *in vitro* and to microglial cells upon culture on microglia-depleted hippocampal slice cultures (Kierdorf et al., 2013). Also, the induction of *csf-1r*<sup>Cre</sup> at E8.5 resulted in the labeling of c-Kit+CD45<sup>low</sup> M $\Phi$  progenitors in E9.5 YS and of head M $\Phi$  at E10.5 (Gomez Perdiguero et al., 2015). However, c-Kit+CD45<sup>low</sup> M $\Phi$ <sup>Prim</sup> progenitors and EMP being both present in the YS at the stages analyzed (Bertrand et al., 2005b), the identification of the M $\Phi$ /microglia progenitors was still open (McGrath et al., 2015). Consequently, the respective contribution of M $\Phi$ <sup>Prim</sup> and EMP-derived M $\Phi$ <sup>Def</sup> progenitors to the developing microglia remains unclear.

We addressed this issue by FACS-Gal analysis (Fig. 1g) and observed that while the E10 YS comprised both FDG<sup>+</sup>/Lyl-1<sup>+</sup> and FDG<sup>-</sup>/Lyl-1<sup>-</sup> M $\Phi$  progenitors, the brain/head from the same embryos harboured mostly FDG<sup>+</sup>/Lyl-1<sup>+</sup> progenitors, although FDG<sup>-</sup>/Lyl-1<sup>-</sup> M $\Phi$  progenitors could also be present, probably due to the brain contamination with non-neuronal tissues at

these early developmental stages. Similarly, while F4/80+ MΦ from E10-YS were also sub-divided into FDG<sup>+</sup>/Lyl-1<sup>+</sup> and FDG<sup>-</sup>/Lyl-1<sup>-</sup> subsets, in the E10-brain/head, they were exclusively FDG<sup>+</sup>/Lyl-1<sup>+</sup>, suggesting that they arise from Lyl-1-expressing MΦ<sup>Prim</sup> progenitors. This conclusion was strengthened by qRT-PCR analyses of cMyb expression levels in sorted FDG/Lyl-1 positive and negative A1 progenitors (cKit<sup>+</sup>CD45<sup>+</sup>CD11b<sup>+</sup>) from *lyl-1*<sup>WT/LacZ</sup> E10-YS. Indeed, FDG/Lyl-1 negative A1 progenitors displayed cMyb levels similar to Sca1<sup>+</sup>cKit<sup>+</sup> progenitors from E12.5 foetal liver, as a positive control for definitive, cMyb dependent progenitors. In contrast, FDG<sup>+</sup>/Lyl-1<sup>+</sup> YS progenitors, as well as MΦ progenitors from E10 brain/head expressed cMyb levels similar to that of E9-YS MΦ<sup>Prim</sup> progenitors, strengthening their primitive status and lineage relationship (**Fig. 1h**). These results indicate that Lyl-1-expressing MΦ<sup>Prim</sup> progenitors colonize the brain and give rise to the entire microglia pool.

### ***Lyl-1-inactivation impairs microglia development at two development stages (E12 and P0)***

A maintained expression of Lyl-1 throughout MΦ/microglia differentiation, with a level decreasing from A1 to A3 subsets was evidenced in both E10 YS and brain/head by qRT-PCR analyses performed in a WT context, at E10 when A1-A2-A3 subsets are all sizeable (**Extended Fig. 2b**). To characterize the effect of Lyl-1 mutation, we assessed the distribution of A1-A2 and A3 MΦ subsets in E10-YS and brain/head using the *CX3CRI*<sup>GFP/GFP</sup>;*Lyl-1*<sup>LacZ/LacZ</sup> double mutant strain we developed to this end. The size of the whole MΦ population appeared similar in the three genotypes, with A1 progenitors predominating in the YS and A3 mature MΦ prevailing in the brain. In both locations, the A1

to A3 distribution was highly impacted by Lyl-1 mutation that led to an increased A1 pool and a reduced A3 pool. A2 MF progenitors were also reduced in  $CX3CRI^{WT/GFP}Lyl-1^{LacZ/LacZ}$  E10-YS, but not in the brain/head (**Fig. 2a**). It thus appears that, beside its function in the regulation of the size of the MΦ progenitors pool, Lyl-1 also appears involved in the regulation of the differentiation towards mature MΦ/microglia.

Having defined Lyl-1 implication in the initial steps of microglia settlement in the brain, which is achieved by E11.5 (*Sheng et al., 2015; Matcovitch-Natan et al., 2016*), we turned to latter stages of microglia development. Cytometry and confocal analyses (**Extended data Fig. 2c, d**), as well as qRT-PCR (**Fig. 2e**) and database analyses (*Matcovitch-Natan et al., 2016*), evidenced the maintenance of Lyl-1 expression in microglia until adulthood. We therefore examined the impact of Lyl-1 inactivation on the kinetic evolution of microglia pool size during development (*see methods*). The MΦ progenitors pool (CD31+CD11b<sup>+</sup>) that was initially (E10-11.5) enlarged in  $Lyl-1^{LacZ/LacZ}$  brain rapidly resumed a normal distribution afterwards, steadily decreasing after E14.5 (**Extended data Fig. 3a**), as previously reported in a WT context (*Kierdorf et al., 2013*).

By comparing the kinetic of microglia development in WT and  $Lyl-1^{LacZ/LacZ}$  brains, we identified E12.5 as the first step impacted by the mutation (**Fig. 2b**). Microglia content in  $lyl-1^{LacZ/LacZ}$  brain stopped its increase at this stage, due to reduced proliferation (**Fig. 2c**), and not to increased Apoptosis (Data not shown). Interestingly, after this stage, the microglia population resumed a growth paralleling that of WT and  $lyl-1^{+/LacZ}$  microglia, a recovery that may partly be accounted for a highly reduced apoptosis level observed  $lyl-1^{LacZ/LacZ}$  microglia compared to WT at E14.5 (**Extended Fig. 3b**).

Both cytometry analyses and counting of iba-1–positive microglia on brain sections correlated to identify P0-P3 as a second developmental stage altered in *lyl-1<sup>LacZ/LacZ</sup>* mice, as evidenced by a reduced size of the microglia population (**Fig. 2d**). At this stage, the recovery of CD11b+ cells from *lyl-1<sup>LacZ/LacZ</sup>* brains for cytometry analyses was reproducibly lower ( $87.18 \pm 0.37 \times 10^3$ ; n=9) than in WT brain ( $140.96 \pm 0.91 \times 10^3$ ; n=9). Consequently, despite an increased percentage of CD11b+ microglia within mutant brains, the estimated microglia number correlated with microglia count *in situ* and confirmed the reduction of microglia population. The reduction of total brain cells count in *lyl-1<sup>LacZ/LacZ</sup>* mice, in frame with a trophic function of microglia on CNS cells (*Antony et al., 2011; Ueno et al., 2013*), may therefore involve Lyl-1 in the regulation of neuronal growth. Moreover, an altered microglia development at P0-P3 was also evidenced by its dimorphic morphology characterized by a decreased ramification numbers (**Fig.2e**). The reduction of the microglia pool size at perinatal stages appeared transient, since a normal amount of microglia was observed in the adult through both cytometry and iba-1+ cell counting (**Extended data Fig. 3c**). Such transient decrease of microglia pool size occurs during normal development, during the 2<sup>nd</sup> and 3<sup>rd</sup> postnatal weeks (*Zhan et al., 2014*), but also in CX3CR1 mutant during the 1st postnatal weeks (*Paolicelli et al., 2011*). This highly dynamic control of microglia pool size during key steps of neural development is probably achieved through changes in cell cycle status and niche occupancy.

The identification of E12.5 and P0-P3 as key stages for Lyl-1 function in microglia development was further confirmed by qRT-PCR analyses of the expression of a set of genes essential for MF (PU.1, CSF1-R, Mafb) and/or microglia (Runx1, CX3CR1, irf8)

development and function, as well as known regulators of developmental hematopoiesis (Tal1, lmo2, Runx1) and related factors (Tcf3/E2A, Tcf4/E2.2) (**Fig. 2f, g**). Overall the temporal evolution of this set of genes correlated with previous reports (*Kierdorf et al., 2013*; *Matcovitch-Natan et al., 2016*) (NCBI-GEO accession number GSE79812). This time course analyses highlighted CSF-R1, Irf8 and lmo2 down-regulation in *lyl-1<sup>LacZ/LacZ</sup>* microglia at both E12.5 and P0-P3, while CX3CR1 level was decreased only at E12.5. Interestingly, Lyl-1 expression was unmodified in CX3CR1<sup>GFP/GFP</sup> mutants, suggesting that Lyl-1 may regulate CX3CR1 expression in microglia. Indeed, CX3CR1, as well as irf8 and lmo2, belong to Lyl-1 potential targets genes (*Wilson et al., 2010*). Mafb expression level in *lyl-1<sup>LacZ/LacZ</sup>* microglia transiently decreased at P0-P3 and afterwards resumed a WT expression level. As Mafb represses self-renewal in resident MF (*Soucie et al., 2016*), this transient decrease might be linked to the recovery of a normal microglia amount in the adult. The expression levels of PU.1, Tcf3/E2A and Tcf4/E2.2 were unmodified in *lyl-1<sup>LacZ/LacZ</sup>* microglia whatever the studied stages, while Runx1 expression was only affected after birth. The expression of Tal-1 was decreased at E14 and increased after birth, suggesting that this Lyl-1 paralog (*Curtis et al., 2012*) does not compensate for Lyl-1 deficiency during embryonic stages of microglia development, but may do so during post natal stages (**Extended data Fig. 3d**).

### ***The lack of Lyl-1 impairs microglia identity in the adult brain.***

Amongst brain cell types, Lyl-1 expression was restricted to microglia, as evidence in primary culture of brain cells types (**Fig. 3c**), result also confirmed from RNA-Seq database analyses (*Zhang et al., 2014*), which also evidenced lower levels of Lyl-1 expression by

endothelial cells that are known to express Lyl-1 (*Giroux et al., 2007; Pirot et al., 2010*). Lyl-1 expressing microglial cells in adult brains were also detected upon b-Gal immuno-labeling of *Lyl-1<sup>WT/LacZ</sup>* brain (**Fig. 3b**). Interestingly, Lyl-1 expression was also detected in the human microglia from healthy adult frontal cortex (*Wehrspaun et al., 2015*).

More data on microglia immunohistochemistry (Iba-1, MHC class II, CD68 etc.) and on microglia morphology (Imaris-based) will be provided by M.Prinz/T.Blank.

RNA-seq of microglia (P42) with heat map (hierarchical clustering), GO analysis, mostly induced genes. Data will be provided by M.Prinz/T.Blank

***Disruption of Lyl-1 leads to an altered social behavior and reduced neuronal connectivity in Lyl-1 deficient animals.***

We next questioned the long-term impact of these microglial alterations on brain development, with a focus on behavioural changes. *Lyl-1<sup>LacZ/LacZ</sup>* mice showed no obvious differences in depressive-like behaviour, general anxiety, or grooming behaviour when compared to WT mice (**Fig. 4a**). In contrast, in the three-chamber test, *lyl-1<sup>LacZ/LacZ</sup>* mice showed no elevated tendency to spend more time with another rodent (social approach) or with a novel intruder (**Fig. 4b**) more so than with a familiar one (social novelty), which indicates social anxiety. From control experiments, we concluded that the observed differences were not due to impaired olfactory sensory function or defects in novel object recognition (**Fig. 4c**). These data collectively indicate that the severe behavioural changes found in *lyl-1<sup>LacZ/LacZ</sup>* mice are typical for social anxiety disorders (SAD).

To examine to what extent these striking behavioural changes correlates to specific changes in brain activity, we also performed functional magnetic resonance imaging (fMRI) of WT and *Lyl-1<sup>LacZ/LacZ</sup>* mice under resting conditions. Our data (**Fig. 4d**) indicate that *Lyl-1<sup>LacZ/LacZ</sup>* mice exhibit heightened functional connectivity between the basolateral amygdala and various brain regions including hippocampus, thalamus, caudoputamen, orbital area of the isocortex and anterior cingulate cortex, all of which have been implicated in SAD (*Bruhl et al., 2014*).

Correlation matrices from fMRI and superposition of the most prominent fMRI BOLD correlations between brain regions will be provided by M.Prinz/T.Blank.

***Decreased spine density in cinguli gyrus pyramidal cells and reduced field potential in the absence of Lyl-1.***

As stated before, the relationship between impaired pruning and ASD development is now well established. CX3CR1 deficiency has been shown to lead to both impaired pruning and ASD development (*Paolicelli et al., 2011; Zhan et al., 2014*). Considering the link between CX3CR1 and Lyl-1 uncovered during the gene expression analyses, we first compared neuronal morphology (axonal and dendritic arborization and spines) by performing Golgi-Cox staining (*Zaqout and Kaindl, 2016*) at P15 and P60 in vibratome sections from WT and *Lyl-1<sup>LacZ/LacZ</sup>* brain.

Defective synaptic pruning in *Lyl-1<sup>LacZ/LacZ</sup>* mice was established in P15 and P42 *Lyl-1<sup>LacZ/LacZ</sup>* mice through golgi stainings of pyramidal cells and quantification of spines. Data will be provided by M.Prinz/T.Blank.

Electrophysiological recordings are being performed. The data will be provided by M.Prinz/T.Blank.

## ***DISCUSSION***

Overall, we here identify Lyl-1 as a marker for primitive YS-derived MΦ progenitors that will give rise to the entire pool of microglia in the embryo. We also show that Lyl-1 controls microglia development and that a defective Lyl-1 impairs neuro-developmental processes leading to the development of behavior defects belonging to the autism spectrum disorders.

So far, Lyl-1 is the first marker that discriminates MΦ progenitors from the primitive and transient definitive (EMp-derived) YS waves. From our results, it appears that during normal development, Lyl-1 controls the size of MΦ<sup>Prim</sup> progenitor pool and/or the duration of this production, which is though to be transient. This seems achieved through the negative regulation of mesoderm commitment towards this primitive lineage, as evidenced by the net increase -and duration of- production of the CD11b<sup>+</sup>CD31<sup>+</sup>CD45<sup>neg/low</sup> C to A1 transition subset. This novel finding opens a way to better understand the mechanisms underlying the differences between these two MΦ waves, leading in fine to a leap forward in the investigations regarding other HSC-independent lineages. This will be particularly relevant to the Embryonic Stem Cells/iPS domain in which the production of definitive cells types is complicated by the poor discrimination between primitive and definitive populations.

Analyzing the contribution of Lyl-1+ MΦ<sup>Prim</sup> progenitors, we focused on the developing brain, which is the only tissue harboring resident MΦ exclusively of YS origin, and found that the entire microglia in the embryo develops from these MΦ<sup>Prim</sup> progenitors. The contribution of Lyl-1+ MΦ<sup>Prim</sup> progenitors to other tissues was not investigated here, but we consider likely that they provide other resident MΦ populations.

E12.5 and P0-P3 were identified as key stages of microglia development impacted by Lyl-1 invalidation. These stages correspond respectively to the end of "early" (E9-E12.5) and "pre-microglia" (E14.5-P9) stages of recently defined stepwise microglia development program (*Matcovitch-Natan et al., 2016*). In this program, pre-microglia stage (E14.5-P9) was related to processes involved in synaptic pruning and neural maturation. The impaired synaptic pruning and associated defective behavior, evidenced here, most probably stem from Lyl-1 defect at this stage (P0-P3). The long-term consequences of the defect caused at E12.5 by Lyl-1 inactivation remains to be determined.

Beside being involved in neurodevelopmental processes, CX3CR1 also plays pleiotropic function during adulthood, and its deregulation is found in neuro-inflammatory and neurodegenerative diseases, as established in murine models of Alzheimer's and Parkinson's disease and amyotrophic lateral sclerosis, as well as neuropathological conditions, such as neuropathic pain and cerebral ischemia (See (*Wolf et al., 2013*) for a review). Considering the maintained expression of Lyl-1 in microglia during adulthood, and the down-regulation of genes essential for microglia function in E12.5 and P0-P3 Lyl mutants, we think highly probable that the deregulation of Lyl-1 might be involved in the development other neurodegenerative/neuroinflammatory diseases and possibly in the development of brain tumors, as suggested by database analysis of deregulated genes in various mouse models (develop ?). Moreover, a few data highlight the relevance of lyl-1 deregulation to human neurodevelopmental and neurodegenerative diseases (*Colangelo et al., 2002; Thomas et al., 2006; McCallum et al., 2016*).

Altogether, the data presented here knowledge acquired during the implementation of this fundamental multi-disciplinary effort is required to cross current limits of developmental hematopoiesis and molecular neuroscience and to achieve new insights into neuronal diseases and help to define novel therapeutic targets that can potentially have major socio-economic consequences.

## **MATERIAL AND METHODS**

### **Mice and embryos**

Mice were housed in the animal facilities of Institut Gustave Roussy ("Plate-forme d'évaluation préclinique", animal facility licence # E 94-076-11). All animal experiments were conducted in compliance with French regulations (Transposition of Directive 2010/63), under authorized project # 2016-030-5798 (2016062214256796) approved by officially accredited Ethical committee n°26.

We used the following mouse strains:

1- C57BL/6 mice from Harlan or Charles Rivers Laboratories, France, referred to as wild type (WT);

2- *lyl-1*<sup>LacZ</sup> mice, genotyped as described before (*Capron et al., 2006*). *lyl-1*<sup>LacZ/LacZ</sup> males were crossed with WT or *lyl-1*<sup>LacZ/LacZ</sup> females to respectively generate *lyl-1*<sup>WT/LacZ</sup> or *lyl-1*<sup>LacZ/LacZ</sup> embryos. This breeding scheme avoided the detection of FDG/*lyl-1* expression in maternally derived MF in the expression analyses performed in *lyl-1*<sup>WT/LacZ</sup> embryos;

3- CX3CR1<sup>GFP</sup> (*Jung et al., 2000*). CX3CR1<sup>GFP/GFP</sup> males were crossed with C57BL/6 to generate CX3CR1<sup>WT/GFP</sup> mice/embryos or to *lyl-1*<sup>LacZ/LacZ</sup> females to generate CX3CR1<sup>WT/GFP</sup>:*lyl-1*<sup>WT/LacZ</sup> mice/embryos.

4-The CX3CR1<sup>GFP/GFP</sup>:*lyl-1*<sup>LacZ/LacZ</sup> double mutant strain was developed from CX3CR1<sup>WT/GFP</sup>:*lyl-1*<sup>WT/LacZ</sup> crosses. CX3CR1<sup>WT/GFP</sup>:*lyl-1*<sup>WT/LacZ</sup> and CX3CR1<sup>WT/GFP</sup>:*lyl-1*<sup>LacZ/LacZ</sup> mice/embryos were obtained by crossing CX3CR1<sup>GFP/GFP</sup>:*lyl-1*<sup>LacZ/LacZ</sup> males to C57BL/6 or *lyl-1*<sup>LacZ/LacZ</sup> females, respectively. To exclude maternal/placental cell contamination, the CX3CR1 transgene was always inherited from the

male parent.

The day of vaginal plug observation was considered as E0.5. Pregnant females were sacrificed by cervical dislocation. Pre-somite embryos were staged according to [Downs et al. \(1993\)](#). From E8 to E10.5, embryos were staged by somite counting and thereafter according to morphological landmarks.

### **Tissues preparation**

YS (E7.5-E10.5) were dissected as described before ([Bertrand et al., 2005a](#)). To perform cytometry analyses of the developing brain, the whole brain of E9-E11 embryos were dissected and dissociated as previously described ([Alliot et al., 1999](#)) and further cleaned from the surrounding ectoderm. Because some contaminating tissues, mostly perineural vessels remained present in E9-E10.5 brain explants, they are referred to as Brain/head at these stages. From E12.5 to adult stages, microglia was recovered following Percoll (P1644, Sigma) separation, according to ([Mildner et al., 2007](#)). E12.5 and E14.5 brains were also mechanically dissociated as for E9-E11 brains to estimate the number of microglia cell per brain from E9 to E14.5.

To obtain the kinetics evolution of microglia number during development (E9-E14.5), the total number of cells per WT and *Lyl-1<sup>LacZ/LacZ</sup>* brain was counted after whole brain mechanical dissociation. The percentage of microglia per brain suspension was obtained following flow cytometry analysis, gating on CD45<sup>+</sup>CD11b<sup>+</sup>F4/80<sup>+</sup> cells. The numbers of microglia per brain was estimated by multiplying the total numbers of cell by the percentage of microglia per

brain. For E12.5, E14.5, E16.5, P0-P3 and P42, we compared the percentage CD45<sup>+/Low</sup> CD11b<sup>+</sup>F4/80<sup>+</sup> microglia from Percoll purified WT and *Lyl-1<sup>LacZ/LacZ</sup>* brains.

### **In vitro culture**

**Organ culture:** YS explants were placed into plates containing "Complete OptiMEM medium", i.e. OptiMEM with Glutamax (51985-042), 1% Penicillin-streptomycin, 0.1%  $\beta$ -mercaptoethanol (all from ThermoFisher) and 10% fetal calf serum (Hyclone). YS explants were maintained in organ culture at 37°C, 5% CO<sub>2</sub> for 1 days and are referred to as OrgD1-YS.

**Clonogenic assay:** Cells were plated in triplicate at 3.10<sup>3</sup> cells/ml in Methocult® M3234 (StemCell Technologies Inc) supplemented with Stem Cell factor (50 ng/ml), EPO (3 U/ml), IL-3 (10 ng/ml), all from Peprotech, IL-6 (10 ng/ml, a gift from Sam Burstein, Maryville IL, USA) CSF-1 (10 ng/ml) and TPO (10 ng/ml, provided by Kirin Brewery, Tokyo, Japan). Cultures were maintained in a humidified incubator at 37°C, 5% CO<sub>2</sub> and colonies were scored at day 5 for primitive erythrocytes (Ery<sup>P</sup>) and day 7 for the other progenitors types.

### **Flow cytometry, FACS-Gal assay and apoptosis assays**

CD31 (Clone Mec13.3), F4/80 (Clone BM8), CD45 (Clone 30F11), CD11b (Clone M1/70) and c-Kit (Clone 2B8) antibodies (*Supplementary Table X*) were used to characterize myeloid cells. Dead cells were excluded by adding 1  $\mu$ g/ml 7-amino actinomycin or DAPI (Sigma) before acquisition. Acquisitions were performed on Canto II cytometers and cell

sorting using FACS-Aria III or Influx (All from Becton Dickinson). Data were analyzed using FlowJo (Treestar) software.

**FACS-Gal assay** (*Fiering et al., 1991; Guo and Wu, 2008*): this assay, used as a reporter for Lyl-1 expression, allows the flow cytometry characterization of cells that display a  $\beta$ -Gal activity, using its fluorescent substrate (Fluorescein di- $\beta$ -galactopyranoside = FDG; F2756; Molecular probe; ThermoFisher).

**Apoptosis assays:** For apoptosis analysis, microglia was stained with anti-CD45-PECy7, anti-CD11b-APC-eFluor® 780 and anti-F4/80-APC, washed and incubated with Annexin V-FITC. 7AAD was added before acquisition.

**Proliferation assay: BrdU incorporation:** Pregnant WT and *Lyl-1<sup>LacZ/LacZ</sup>* females at E12.5 were injected with with BrdU (10  $\mu$ M) and sacrificed 2 hours later. The microglia was isolated and further stained with CD45-PECy7, CD11b-APC-eFluor® 780 and F4/80-PE antibodies. Cells were fixed, permeabilized and treated with DNase (1 hour at 37°C) according to kit instruction. BrdU was revealed with anti-BrdU-APC.

**Brain imaging** Further information will be provided by M.Prinz/T.Blank.

***Brain preparation***

***Immunohistochemistry***

***Iba+ cell counting in brain section***

***Immunofluorescence –bGal stainings***

***Pruning experiments***

### **qRT-PCR analyses**

Total RNA was extracted from sorted CD11b<sup>+</sup>F4/80<sup>+</sup>CD45<sup>low</sup> microglia using Trizol (ThermoFisher). After cDNA synthesis using a SuperScript™ VILO™ Master Mix reverse transcriptase (Invitrogen), quantitative PCR was performed using SYBR Premix Ex Taq II (Tli RNase H Plus, Takara Bio). Gene expression was normalized to the value obtained from E12.5 WT microglia and relative gene expression levels were determined by the  $\Delta\Delta C_t$  method. Gene expression was considered undetectable if the Ct values were > 35 cycles. The sequences of the primers used are provided in *(Supplementary Table Y)*. Further information will be provided by M.Prinz/T.Blank.

Further information will be provided by M.Prinz/T.Blank. for the following items:

**RNA-Seq**

**Behaviour assessment.**

**fMRI.**

**Statistical analysis** Further information will be provided by M.Prinz/T.Blank.

The statistical significance (p value) of the experiments was analyzed using unpaired Student's t test. Statistical significance is indicated as \*p < 0.05, \*\*p < 0.01, and \*\*\*p < 0.001.

## **FIGURE LEGEND**

**Figure 1: *Lyl-1* regulates the production of primitive MΦ from the early YS that will give rise to microglia**

**a.** Left panel: *Lyl-1* invalidation leads to an increased production of MΦ progenitors in the early YS: Clonogenic potential of E8 (0-5 Somites) OrgD1-YS cells: The production of MΦ progenitors (CFU-M) is increased in *lyl-1<sup>LacZ/LacZ</sup>* OrgD1-YS (3-5 independent experiments, each sample cumulating 3 to 6 YS). The size of *lyl-1<sup>WT/LacZ</sup>* and *lyl-1<sup>LacZ/LacZ</sup>* MΦ colonies as well as the cell morphology was similar to those obtained from WT (Data not shown).

Right panel: The distribution of other progenitors endowed with myeloid potential recovered from *lyl-1<sup>LacZ/LacZ</sup>* E8 OrgD1-YS is similar to that of wild type. Abbreviations: GM: granulo-monocytic progenitors; EMp: Erythro-myeloid progenitors.

**b.** Schematic representation of the MΦ differentiation pathways during YS development: MΦ develop from c-Kit<sup>+</sup>CD31<sup>+</sup>CD45<sup>-</sup> progenitors, a phenotype shared by the C subset in the primitive wave and EMp in the transient definitive wave). The MΦ progenitors are first characterized by the expression of CD11b and CD45 (A1 subset), then by c-Kit down-regulation (A2 subset). The differentiation to mature MΦ is characterized by the concomitant down-regulation of CD31 and the up-regulation of F4/80 and CX3CR1 (A3 subset) (*Bertrand et al., 2005b*). While in the primitive wave, the C-subset directly provides the A1 population, in the transient definitive one, the production of A1 progenitors depends of the production of EMp-derived granulo-monocytic (GM) progenitors.

c. While in E9-YS all MΦ progenitors express FDG/Lyl-1, E9.5-YS harbours two populations discriminated by their FDG/Lyl-1 expression. Lyl-1 expression in MΦ progenitors was analysed by FACS-Gal assay whereby the β-Gal fluorescent substrate FDG is used as a reporter for Lyl-1 expression (*See extended data Fig. 2a for the gating strategy*). The contour plots in WT samples indicate the level of non-specific β-Gal activity.

d. Primitive MΦ progenitors express Lyl-1, which regulates their production:

Upper panel: Flow cytometry profiles of wild type (left) and *lyl-1<sup>WT/LacZ</sup>* (middle left) E8-YS (0-3 somites). CD11b<sup>+</sup>CD31<sup>-</sup> MΦ (top gate) corresponds to maternal MΦ. The CD11b<sup>+</sup>CD31<sup>+</sup> MΦ progenitors subset (lower gate), which display FDG/Lyl-1 expression was enlarged in *lyl-1<sup>WT/LacZ</sup>* YS (right panel; 3 independent experiments). Lower panel: Within the FDG<sup>+</sup>/Lyl-1<sup>+</sup> population from *lyl-1<sup>WT/LacZ</sup>* E8-YS (Left) most cells co-expressed CD31 and CD11b<sup>+</sup> (middle). Conversely, CD11b<sup>+</sup>CD31<sup>+</sup> MΦ progenitors displayed FDG<sup>+</sup>/Lyl-1 expression (left). Plain grey histogram indicates non-specific background β-Gal activity/FDG levels in WT samples.

e. Clonogenic assay: Less than one EMP and/or GM progenitor per E8-YS were detected in WT and mutant samples, confirming that the assay was performed at a time when EMP-derived MΦ progenitors are absent. The majority of the 25-30 colonies per YS were Ery<sup>P</sup> (60 to 80% in the 3 genotypes). Similarly to what is observed in E8-OrgD1 YS (Right), the number of MΦ progenitors amongst the colonies obtained from E8-YS (0-3 somites) was increased in *lyl-1<sup>WT/LacZ</sup>* and *lyl-1<sup>LacZ/LacZ</sup>* compared to wild type (left). Few other progenitors were occasionally and randomly found in the *lyl-1<sup>WT/LacZ</sup>* FDG/Lyl-1<sup>+</sup> fraction including EMP (0.81% ± 0.66; n=3). Note that expression and functional assays performed in E8- and

OrgD1-YS point to an intermediate phenotype between WT and *lyl-1<sup>LacZ/LacZ</sup>* YS. Each sample cumulated 5 to 10 YS, in the 3-5 independent experiments performed. The genotype colour code applies to all the sets in the figure.

**f.** Lyl-1 expressing and Lyl-1 negative myeloid progenitor produce a distinct progeny: The type of progenitors produced by sorted cKit+CD45+CD11b+ myeloid progenitors was determined using clonogenic assays in E9 (<18 somites; n=7) YS from WT and *lyl-1<sup>WT/LacZ</sup>*, as well as in WT E10-YS (n=15), each in 3 independent experiments. At E10, myeloid progenitors from *lyl-1<sup>WT/LacZ</sup>* YS were subdivided into FDG/Lyl-1 negative (n=15) and positive (n=12) fractions (5 independent experiments). In all instances, samples are biological replicates cumulating YS from 6 to 8 embryos. 100 to 150 cKit+CD45+CD11b+ cells per condition were plated in clonogenic assays in triplicate. Lyl-1 positive progenitors mostly produce MΦ colonies, while FDG/Lyl-1 negative progenitors also produce GM and G colonies, thus belonging to the transient definitive wave.

**g.** Lyl-1 expressing MΦ<sup>Prim</sup> progenitors give rise to microglia: Representative profiles from 3 independent samples preparation, each cumulating 3-4 YS and brain from the same embryos (*See extended data Fig. 2a for the gating strategy*).

Left panel: While E10 YS harbours both FDG+/Lyl-1+ and FDG-/Lyl-1- MΦ progenitors, in the corresponding brain, MΦ progenitors only express FDG/Lyl-1.

Right Panel: FDG+/Lyl-1+ and FDG-/Lyl-1- mature MΦ coexist in E10-YS, while in the brain all F4/80+ cells (A3 subset) express FDG+/Lyl-1+. Note that at these early stages, the brain preparations are often contaminated with non-neuronal tissues.

**h.** A1 progenitors E9-YS, E10 brain/head, and FDG/Lyl-1+ A1 subset from E10-YS express similar c-Myb<sup>Low/Neg</sup> levels that characterize the primitive YS-wave, In contrast, FDG/Lyl-1 negative fraction in the YS express c-Myb, a hallmark of transient definitive (EMP-Derived) wave. qRT-PCR quantification of c-Myb expression levels in cKit+CD45+CD11b+ A1 progenitors sorted from WT E9-YS, WT and *lyl-1*<sup>WT/LacZ</sup> E10-YS and brain/head, as well as FDG/Lyl-1 positive and negative A1 progenitors fractions from *lyl-1*<sup>WT/LacZ</sup> E10-YS and Lin-Sca+c-Kit+ (LSK) progenitors from WT E12 foetal liver (FL). c-Myb expression levels are shown on a Log<sup>2</sup> scale, normalized to the mean expression value obtained for WT E10-YS, considered as 1.

Figure 1B

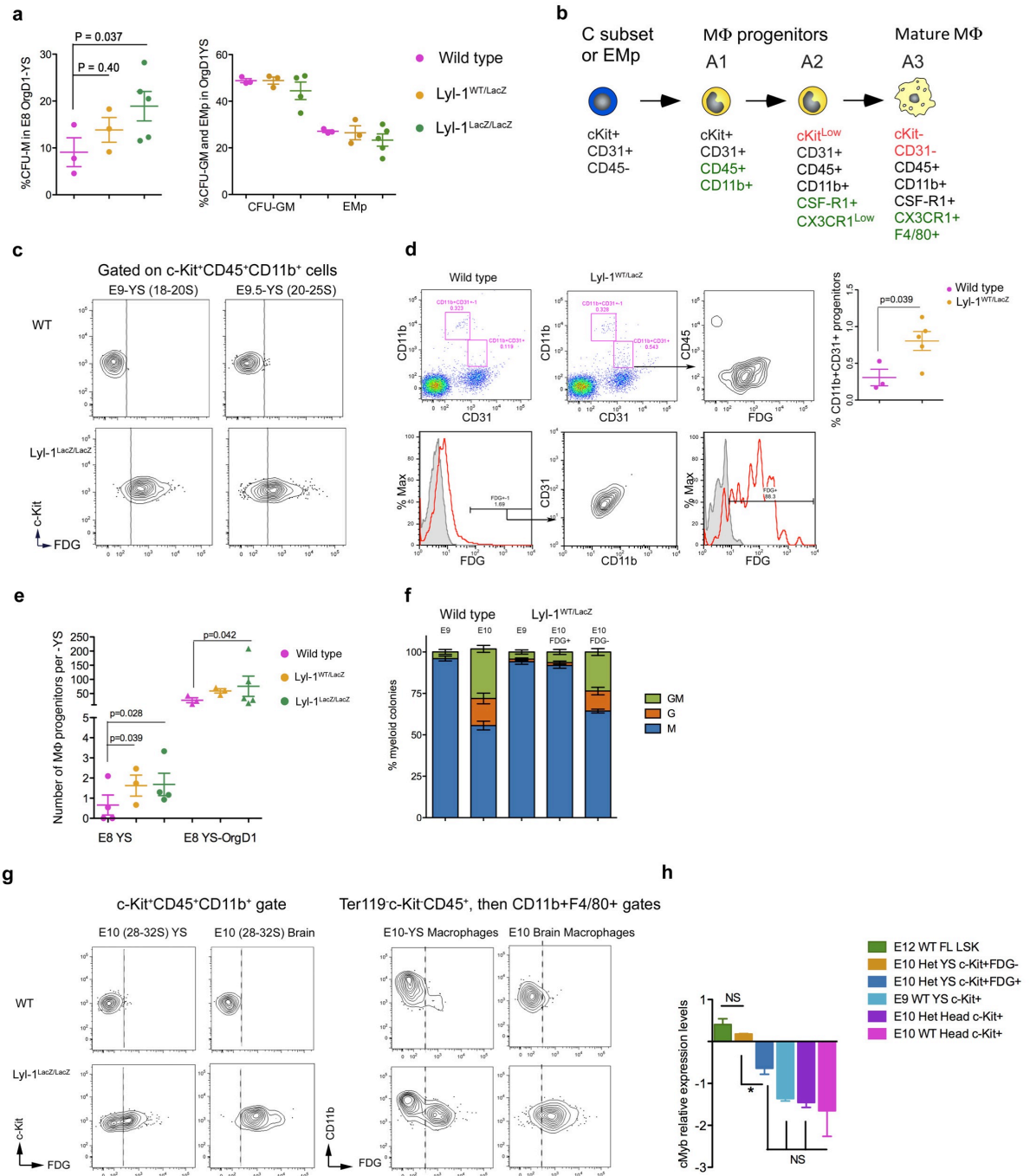


**Figure 2: *Lyl-1* deficiency leads to an increased production of  $M\Phi^{Prim}$  progenitors and to a reduction of the microglia pool at E12.5 and P0-P3**

**a.** Distribution of A1-A2 and A3 MF subsets E10-YS (left) and brain (right) from  $CX3CR1^{WT/GFP};lyl-1^{WT/WT}$ ,  $CX3CR1^{WT/GFP};Lyl-1^{WT/LacZ}$  and  $CX3CR1^{WT/GFP};Lyl-1^{LacZ/LacZ}$  embryos. The size of the whole  $M\Phi$  population appears similar in the three genotypes in both YS and brain (Top panel), but the distribution of the  $M\Phi$  subsets (Middle and lower panel) is modified upon *Lyl-1* invalidation that leads to an increased size of the A1 subset and to a reduced A3 pool (5-12 independent analyses, each sample cumulating 6-8 YS or brain. Plots show the mean  $\pm$  s.e.m).

**b.** Kinetic evolution of  $CD11b^{+}F4/80^{+}CD45^{-/low}$  microglia estimated number (*see methods*) in wild type,  $lyl-1^{+/LacZ}$  and  $lyl-1^{LacZ/LacZ}$  brain (right panel). Microglia was quantified on whole brain preparation (for WT,  $lyl-1^{WT/LacZ}$  and  $lyl-1^{LacZ/LacZ}$  respectively n=: E9: 6, 7, 4; E10: 9, 9, 5; E11: 6, 5, 7; E12: 6, 6, 6; E14: 8, 6, 6). Microglia development in  $lyl-1^{WT/LacZ}$  embryos is similar to that of wild type embryos. At E12.5, microglia content in  $lyl-1^{LacZ/LacZ}$  brain was reduced two fold in  $lyl-1^{LacZ/LacZ}$  brains compared to WT and  $lyl-1^{WT/LacZ}$  brains. Afterwards, it recovered a growth rate similar to that of wild type and  $lyl-1^{WT/LacZ}$  microglia. Quantification performed on percoll purified brain preparations (right) confirmed the decreased size of the microglia pool at E12.5.

**c.** A reduced microglia proliferation may account for the reduced microglia number at E12.5, as shown by the two folds decrease (right) in BrdU-labelled cells in  $lyl-1^{LacZ/LacZ}$  (middle) compared to wild type (left) brain.

- d.** At P0-P3, the count of iba-1+ microglia in *lyl-1<sup>LacZ/LacZ</sup>* midbrain section was lower than in wild type (Left), while in cytometry analyses the percentage of CD11b<sup>+</sup>F4/80<sup>+</sup>CD45<sup>low</sup> microglia from percoll purified whole brain appeared increased. However, the estimated number of CD11b<sup>+</sup>F4/80<sup>+</sup>CD45<sup>-/low</sup> microglia recovered from P0-P3 *lyl-1<sup>LacZ/LacZ</sup>* brains was reduced, due to a significant and reproducible lower cell recovery from *lyl-1<sup>LacZ/LacZ</sup>* brains (n=9).
- e.** Immuno-histochemical iba-1 labeling of P1 microglia evidenced a reduced number of ramifications in microglial cells in *Lyl-1<sup>WT/LacZ</sup>* brain sections.
- f.** Kinetic evolution of Lyl-1 expression levels in WT microglia from embryonic stages to adulthood. An increased expression of Lyl-1 from embryonic stages to adulthood was also inferred from (*Matcovitch-Natan et al., 2016*) timeline RNA-Seq data (GEO accession number GSE79812).
- f.** Quantitative RT-PCR analyses also point to E12.5 and P0 as key development stages regulated by Lyl-1: CD11b<sup>+</sup>F4/80<sup>+</sup>CD45<sup>low</sup> microglia was isolated at sequential development stages. Bar graphs show the kinetic of expression of a selected set of genes and its modification upon Lyl-1 invalidation (Arrowheads), normalized to the mean expression value in WT E12.5 microglia (n=3). Error bars indicate s.e.m.

Figure 2B

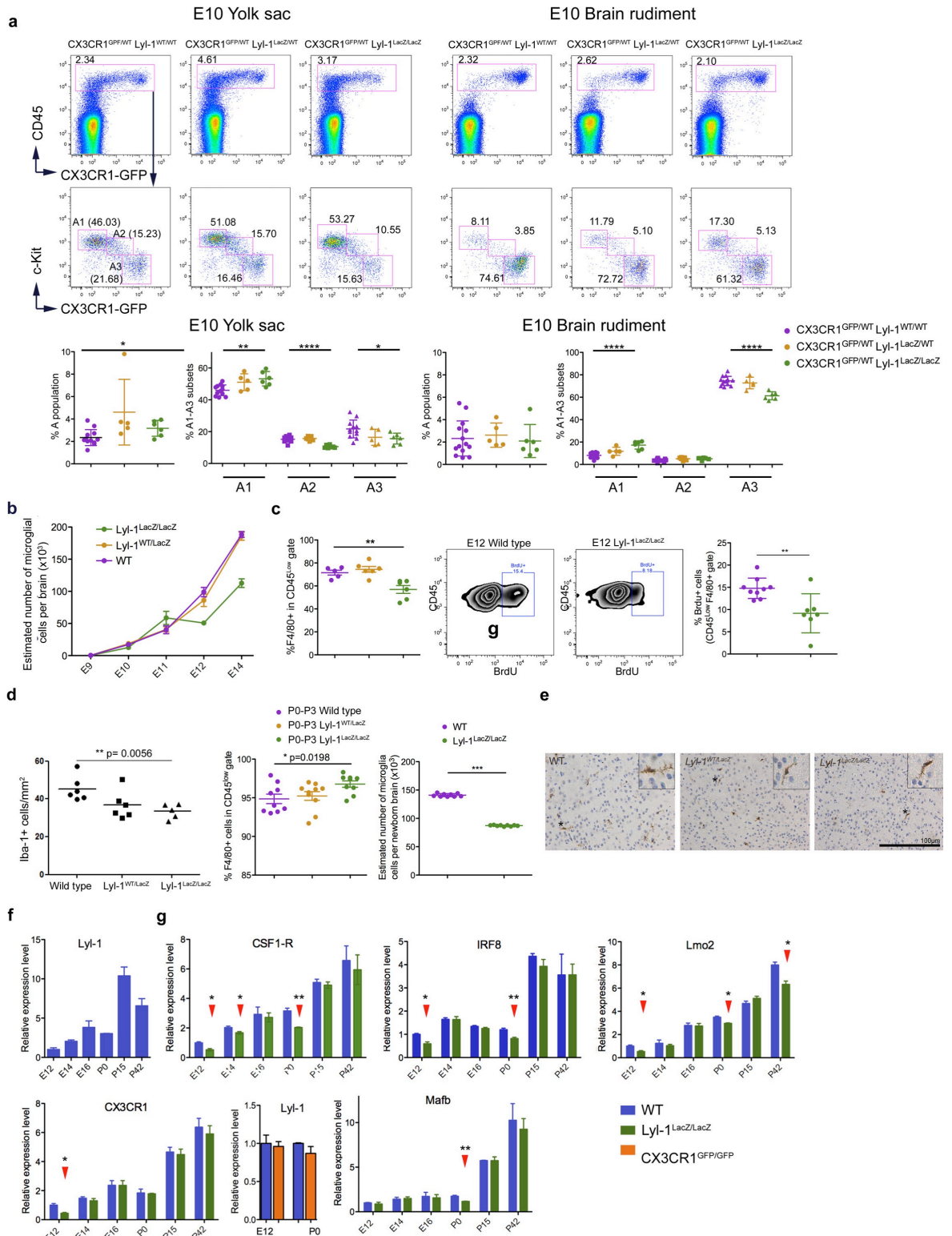


**Figure 3: Lack of *Lyl-1* impairs microglia identity in the adult brain.**

- a.** In the brain, *Lyl-1* expression is restricted to microglia: qRT-PCR quantification of *Lyl-1* expression levels in brain cell types (neurons, primary microglia, astrocytes and oligodendrocytes). *Lyl-1* is expressed by microglia and not by other brain cell types. Search performed on (*Zhang et al., 2014*) RNA-Seq database ([http://web.stanford.edu/gate2.inist.fr/group/barres\\_lab/brain\\_rnaseq.html](http://web.stanford.edu/gate2.inist.fr/group/barres_lab/brain_rnaseq.html)) confirmed our conclusion and also evidenced low levels of *Lyl-1* expression in endothelial cells.
- b.**  $\beta$ -Gal immuno-labeling of adult *Lyl-1*<sup>WT/LacZ</sup> brain. Microglia, characterised by Isolectine B4 expression (Red), also display  $\beta$ -Gal/*Lyl-1* expression (green) in adult brain.
- c.** RNA-Seq P42: Further information will be provided by M.Prinz/T.Blank.

Figure 3

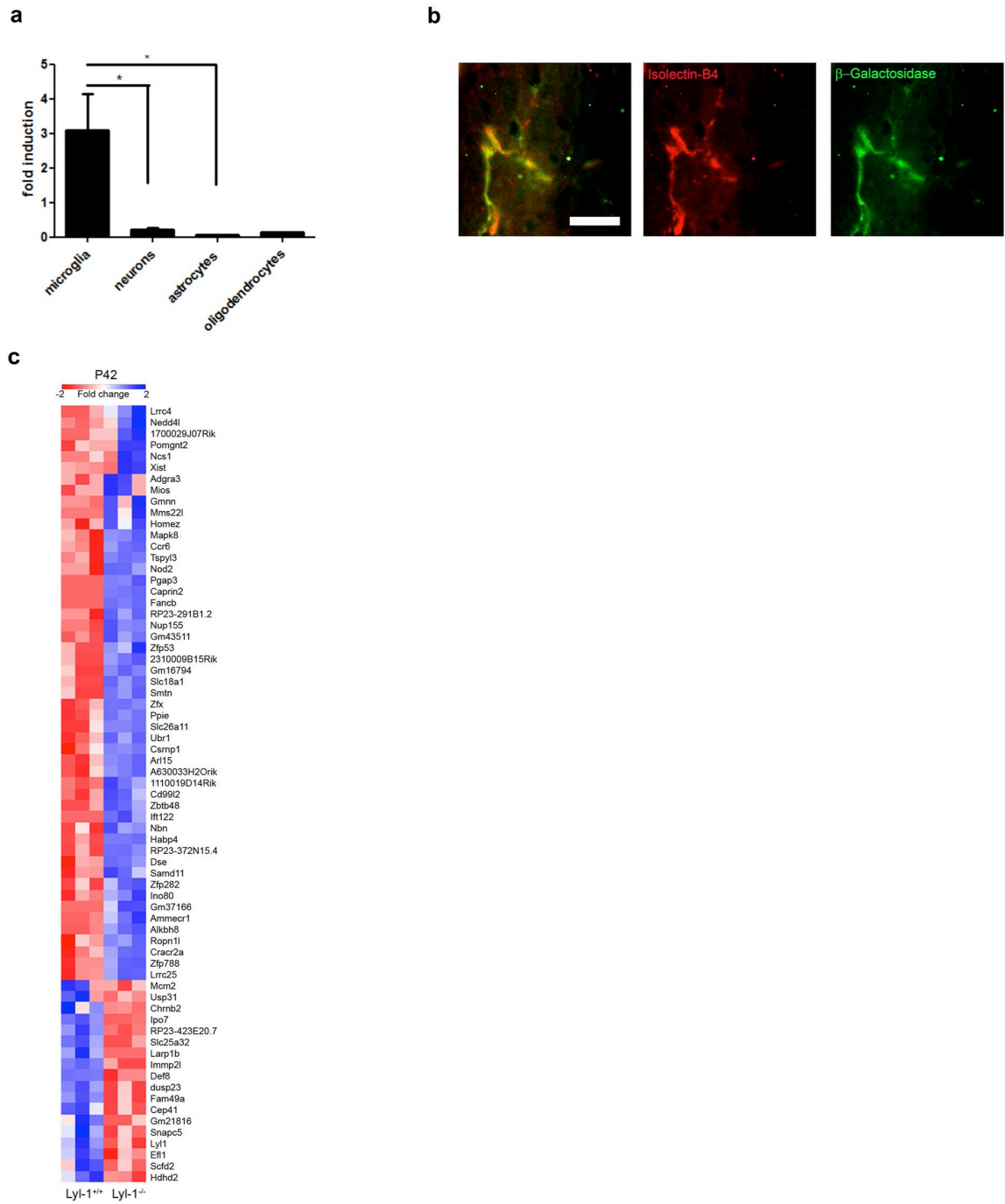


**Figure 4: *Lyl-1* invalidation elicits altered social behavior and reduced neuronal connectivity**

**a.** In the forced swim test (FST: left panel) and the elevated plus maze (EPM: middle panel) test, *lyl-1<sup>LacZ/LacZ</sup>* mice show no difference compared to WT mice. *Lyl-1<sup>LacZ/LacZ</sup>* mice and WT mice spend similar time in self-grooming (Right panel).

**b.** Three-chamber experiment: Whereas WT mice spend more time in the chamber housing a stranger mouse (M) than the chamber housing an empty cage (E), *Lyl-1<sup>LacZ/LacZ</sup>* mice have no preference for either chamber (left panel).

Whereas wild type mice spend more time in the chamber housing a novel mouse (M2) than in a chamber housing a familiar mouse (M1), *Lyl-1<sup>LacZ/LacZ</sup>* mice have a preference for a chamber housing a familiar mouse (M1) (Right panel).

**c.** Olfactory avoidance test (left panel). There was no difference in the olfactory avoidance time between *Lyl-1<sup>LacZ/LacZ</sup>* and wild type mice.

In the novel object recognition test (middle panel), *Lyl-1<sup>LacZ/LacZ</sup>* mice had normal recognition memory for a preconditioned object (F: Familiar), which was presented 24 h before the test, so that they spent more time with the novel object (N: Novel).

Discrimination index (right panel): the normalized ratio of time spent with the familiar object divided by time spent with the novel object, shows that there is no difference between *Lyl-1<sup>LacZ/LacZ</sup>* and wild type mice for novel object recognition ability.

**d.** Functional MRI from *Lyl*-competent (left) and deficient (right) mice indicating strongly enhanced functional connectivity between the basolateral amygdala and various brain regions that are known to be important for social anxiety.

Figure 4

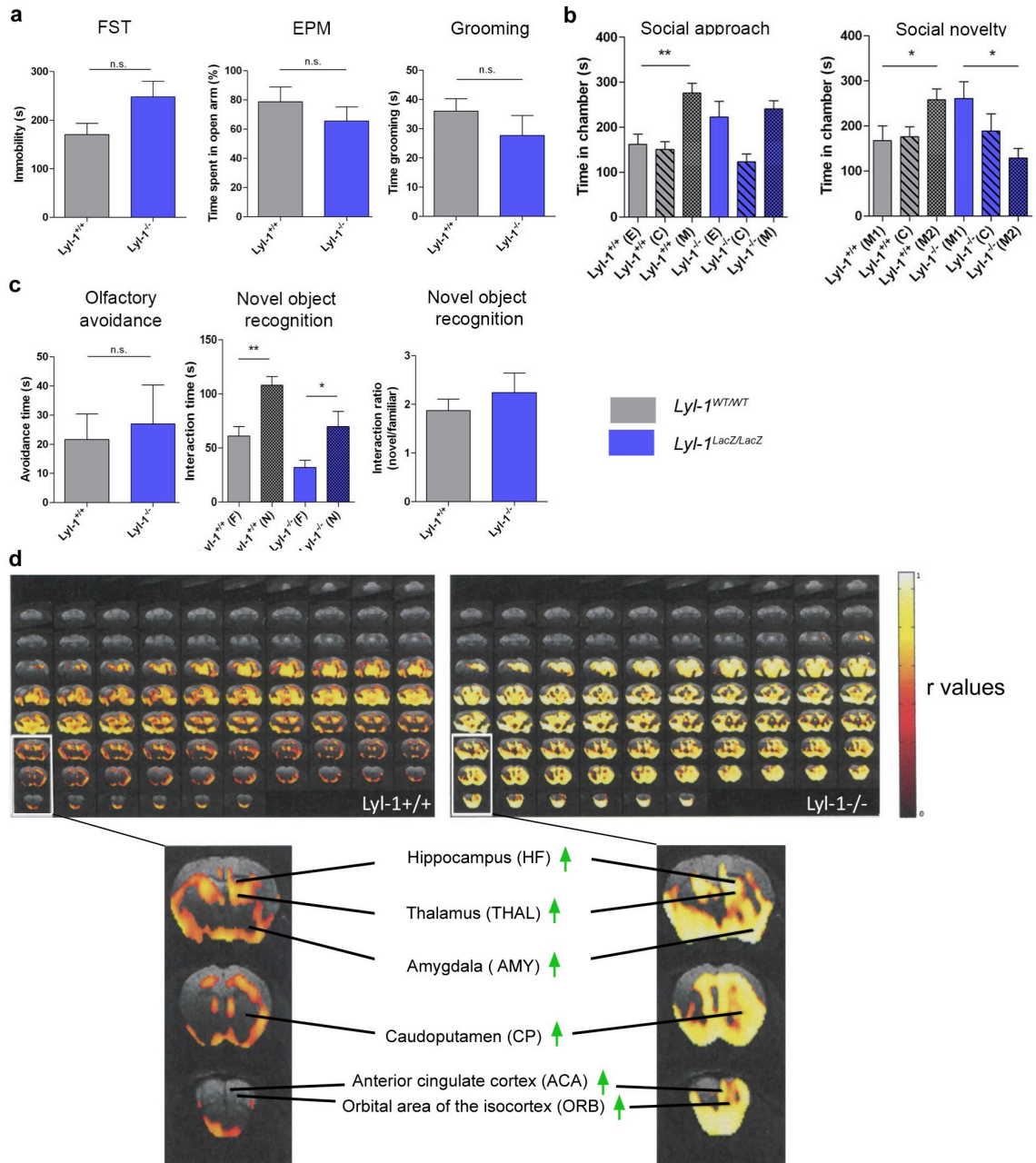


**Figure 5: *Lyl-1* deficiency leads to defective synaptic pruning**

Further information will be provided by M.Prinz/T.Blank.

**EXTENDED DATA**

**Extended Figure 1, related to figure 1:**

**a.** *Lyl-1* deficiency leads to an increased perinatal lethality: Left panel: The number of embryo per litter is unmodified at E14. Middle panel: *Lyl-1* deficiency leads to a reduced number of live new-borns. Right panel: The number of weanlings is further reduced in *Lyl-1<sup>LacZ/LacZ</sup>* mutants, neonatal lethality being significantly increased up to P15, with a main occurrence between P1 and P5 (data not shown). Notably, *Lyl-1* deficiency did not lead to unbalanced sex ratio (data not shown). The numbers of E14.5 embryos, new-borns and weanlings obtained from WT x *lyl-1<sup>LacZ/LacZ</sup>* and WT x WT crosses were similar.

Tuckey box plot; E14.5: n = WT: 35; *Lyl-1<sup>WT/LacZ</sup>*: 35; *Lyl-1<sup>LacZ/LacZ</sup>*: 29.

Newborn and weanlings: n = WT: 150; *Lyl-1<sup>WT/LacZ</sup>*: 95; *Lyl-1<sup>LacZ/LacZ</sup>*: 284.

**b.** Gating strategy used to characterize MΦ progenitors in E8 OrgD1-, E9 and E9.5 YS from WT, *lyl-1<sup>WT/LacZ</sup>* and *lyl-1<sup>LacZ/LacZ</sup>* embryos, related to extended figure 1c, d.

**c.** Phenotype and relative distribution of MΦ progenitors subsets in *lyl-1<sup>WT/LacZ</sup>* *lyl-1<sup>lacZ/LacZ</sup>* and WT E8-OrgD1-, E9- and 9.5-YS *Lyl-1* expression in MΦ progenitors. Mutant E8-OrgD1- and E9-YS harbours a large CD45<sup>neg/low</sup> subset (Arrowhead) within CD11b+ CD31+ A1-A2 progenitors population. This subset, present to a lesser extent in WT E8-OrgD1-YS samples, is no longer observed in WT YS at E9, and in *lyl-1<sup>WT/LacZ</sup>* and *lyl-1<sup>LacZ/LacZ</sup>* YS after E9.5.

Right panel: Quantification of the C to A1 transition subset.

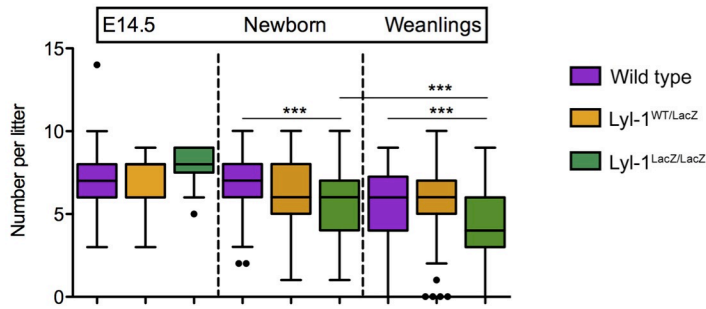
This C to A1 transient population probably corresponds to an intermediate step of MΦ progenitors differentiation, as suggested by the presence of CD31 and lack of CD45 expression and the fact that it is only present at the earliest stage of YS MΦ development.

**d.** Within the CD11b<sup>+</sup> CD31<sup>+</sup> MΦ progenitors gate, both the CD45<sup>neg/low</sup> C to A1 transition subset and CD45<sup>+</sup> cells express FDG/Lyl-1. Lyl-1 expression was analysed by Facs-Gal assay whereby the β-Gal fluorescent substrate FDG is used as a reporter for Lyl-1 expression.

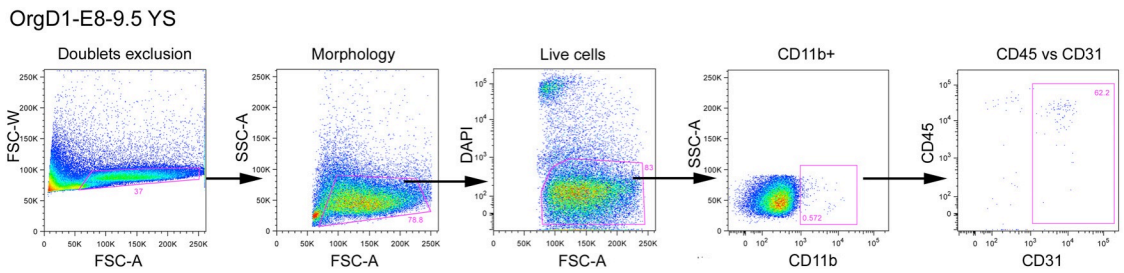
The contour plots in WT samples indicate the level of non-specific β-Gal activity.

Extended figure 1B, related to figure 1

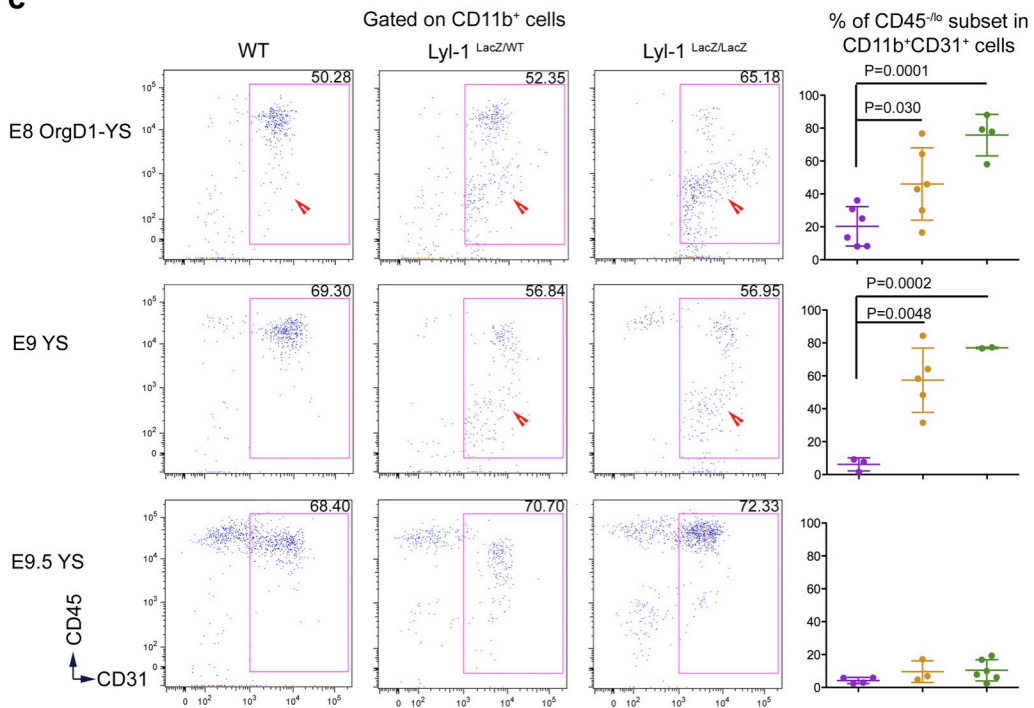
**a**



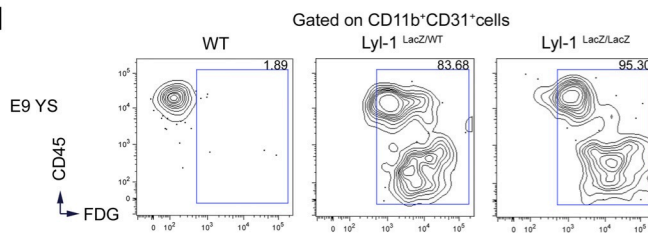
**b**



**c**



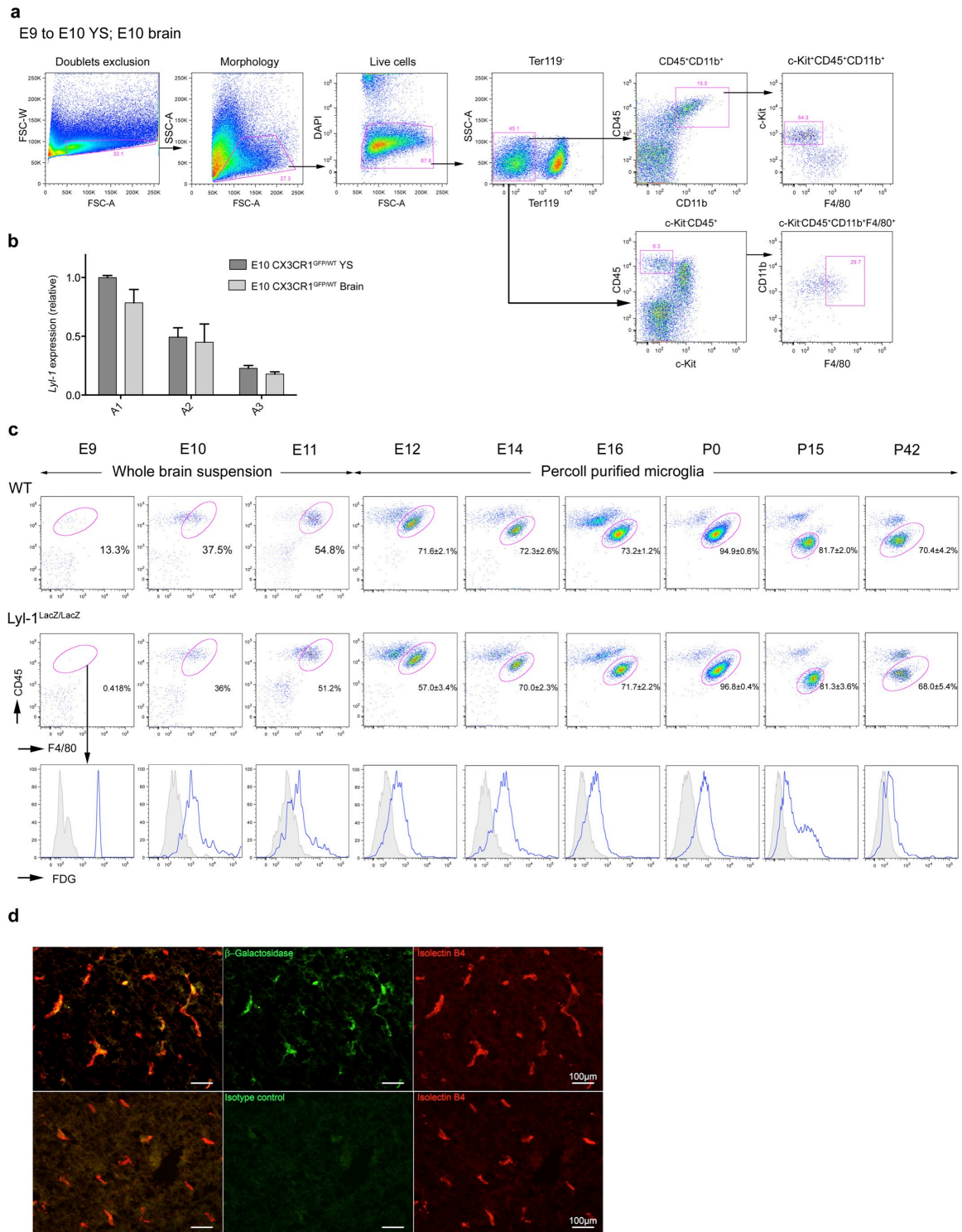
**d**



**Extended Figure 2, related to Figures 1 and 2:**

- a.** Gating strategy used to analyse FDG+/Lyl-1+ expression in MΦ progenitors from E9 and E9.5 YS from wild type, *lyl-1*<sup>WT/LacZ</sup> and *lyl-1*<sup>LacZ/LacZ</sup> embryos (Fig. 1e) and MΦ progenitors and mature MΦ in E10 YS and brain from WT and *lyl-1*<sup>LacZ/LacZ</sup> (Fig. 1g). Note that the gating strategy here excludes the C to A1 intermediate progenitor (CD11b<sup>+</sup>CD31<sup>+</sup>CD45<sup>neg/low</sup>).
- b.** qRT-PCR quantification of Lyl-1 expression in A1, A2 and A3 subsets isolated from WT YS and brain at E10, when all 3 subsets are present. Lyl-1 is expressed by the 3 subsets and its expression level decreases upon differentiation. Lyl-1 expression levels were normalized to the mean expression value obtained for A1 progenitors from *CX3CR1*<sup>WT/GFP</sup> E10-YS (3 independent experiments).
- c.** FDG/Lyl expression in wild type and *Lyl-1*<sup>LacZ/LacZ</sup> brain from E9 to adult stages. In *Lyl-1*<sup>LacZ/LacZ</sup> mutants, the entire microglia population is Lyl-1 positive, but Lyl-1 expression level decreases in the adult. Note that plain grey histogram indicates non-specific background β-Gal activity/FDG levels in wild type samples.
- d.** β-Galactosidase immuno-labeling of the brain of E14.5 *Lyl-1*<sup>WT/LacZ</sup> embryos. Top panels: Microglia, characterised by Isolectine B4 expression (Red), also display β-Gal/Lyl-1 expression (green). Lower panel shows the β-Gal isotype control.

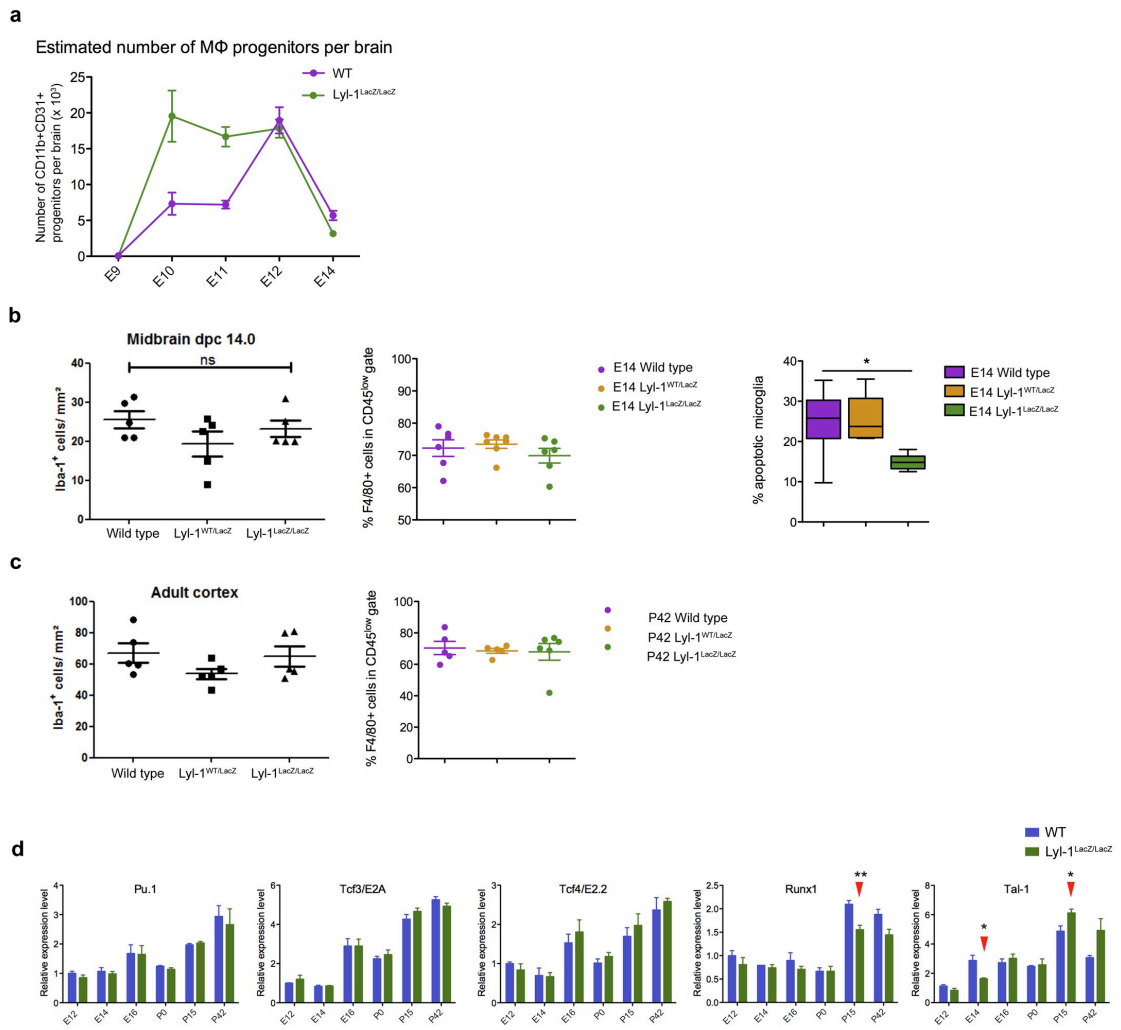
Extended Fig 2, related to Fig.1 and 2



**Extended Figure 3, related to Figure 2:**

- a.** Kinetic evolution of CD31+CD11b<sup>+</sup> MΦ/microglia progenitors estimated number in wild type and *lyl-1<sup>LacZ/LacZ</sup>* brain. Microglia was quantified on whole brain preparation (for WT and *lyl-1<sup>LacZ/LacZ</sup>* respectively n=: E9: 6, 4; E10: 9, 5; E11: 6, 7; E12: 6, 6; E14: 8, 6 independent preparations). While the number of progenitors is highly elevated initially in mutant brains, it resumes a normal evolution after E11.
- b.** Counting of iba-1-labelled microglia cell on midbrain sections (left) and cytometry analyses of CD11b<sup>+</sup>F4/80<sup>+</sup>CD45<sup>low</sup> microglia from percoll purified whole brain (middle). The two approaches correlate to show that there is no genotype-related difference in microglia amount at E14.5. Annexin V-7AAD quantification of apoptosis levels in CD11b<sup>+</sup>F4/80<sup>+</sup>CD45<sup>low</sup> microglia from E14 brains (Right) evidenced a significantly lower apoptosis level in *lyl-1<sup>LacZ/LacZ</sup>* compared to WT and *lyl-1<sup>WT/LacZ</sup>* brains that may accounts for the recovery of microglia population size after E12.5.
- c.** In adults, both iba<sup>+</sup> cell counting and cytometry analyses converged to show no genotype-associated difference in microglia pool size in WT and *lyl-1<sup>WT/LacZ</sup>* brains.
- d.** Quantitative RT-PCR analyses: CD11b<sup>+</sup>F4/80<sup>+</sup>CD45<sup>low</sup> microglia was isolated at sequential development stages. Bar graphs show the kinetic of expression of a selected set of genes that are not significantly modified in *Lyl-1* mutants at E12.5 and P0-P3, but may be so at post natal stages. Gene expression was normalized to the mean expression value in WT E12.5 microglia (n=3). Error bars indicate s.e.m.

Extended figure 3, related to figure 2



***Extended Figure 4, related to Figure 3:***

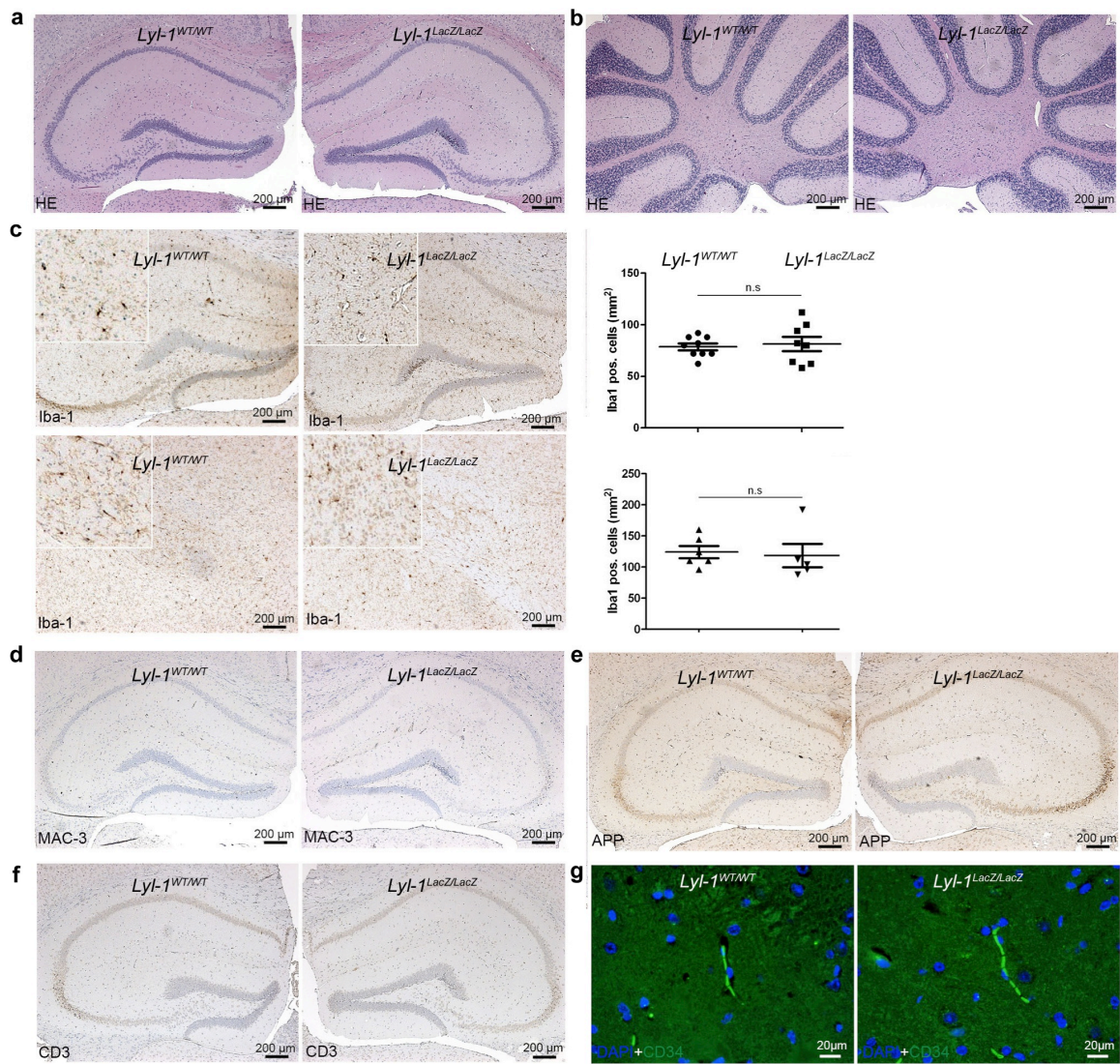
**a-g** Histological and immuno-staining of brain sections from adult wild type (left) and *Lyl-1<sup>LacZ/LacZ</sup>* (right) mice. Scale bars represent 200  $\mu$ m, except in **i** where they represent 20  $\mu$ m.

**a, b.** Structure of the hippocampus (a), and cerebellum (b) revealed by Haematoxylin-Eosine (HE) staining;

**c.** Iba-1 staining of microglia in the hippocampus (upper panel) and in amygdala (lower panel). Iba-1+ microglia quantification, expressed as mean  $\pm$  s.e.m, is shown in the right panel;

**d.** MAC-3 staining of hippocampal macrophages; **e.** Amyloid precursor protein (APP) staining for axonal damage; **f.** CD3 staining of T lymphocytes; **g.** CD34 labeling of endothelia (green) and DAPI for nuclei (blue) in the hippocampal area.

Extended figure 4, related to figure 3



## **REFERENCES**

- Alliot, F., Godin, I. and Pessac, B. (1999) 'Microglia derive from progenitors, originating from the yolk sac, and which proliferate in the brain', *Brain Res Dev Brain Res* 117(2): 145-52.
- Antony, J. M., Paquin, A., Nutt, S. L., Kaplan, D. R. and Miller, F. D. (2011) 'Endogenous microglia regulate development of embryonic cortical precursor cells', *J Neurosci Res* 89(3): 286-98.
- Askew, K., Li, K., Olmos-Alonso, A., Garcia-Moreno, F., Liang, Y., Richardson, P., Tipton, T., Chapman, M. A., Riecken, K., Beccari, S. et al. (2017) 'Coupled Proliferation and Apoptosis Maintain the Rapid Turnover of Microglia in the Adult Brain', *Cell Rep* 18(2): 391-405.
- Bertrand, J. Y., Giroux, S., Cumano, A. and Godin, I. (2005a) 'Hematopoietic stem cell development during mouse embryogenesis', *Methods Mol Med* 105: 273-88.
- Bertrand, J. Y., Jalil, A., Klaine, M., Jung, S., Cumano, A. and Godin, I. (2005b) 'Three pathways to mature macrophages in the early mouse yolk sac', *Blood* 106(9): 3004-11.
- Bruhl, A. B., Delsignore, A., Komossa, K. and Weidt, S. (2014) 'Neuroimaging in social anxiety disorder-a meta-analytic review resulting in a new neurofunctional model', *Neurosci Biobehav Rev* 47: 260-80.
- Capron, C., Lecluse, Y., Kaushik, A. L., Foudi, A., Lacout, C., Sekkai, D., Godin, I., Albagli, O., Poullion, I., Svinartchouk, F. et al. (2006) 'The SCL relative LYL-1 is required for fetal and adult hematopoietic stem cell function and B-cell differentiation', *Blood* 107(12): 4678-4686.
- Colangelo, V., Schurr, J., Ball, M. J., Pelaez, R. P., Bazan, N. G. and Lukiw, W. J. (2002) 'Gene expression profiling of 12633 genes in Alzheimer hippocampal CA1: transcription and neurotrophic factor down-regulation and up-regulation of apoptotic and pro-inflammatory signaling', *J Neurosci Res* 70(3): 462-73.
- Cumano, A., Dieterlen-Lievre, F. and Godin, I. (1996) 'Lymphoid potential, probed before circulation in mouse, is restricted to caudal intraembryonic splanchnopleura', *Cell* 86(6): 907-16.

- Cumano, A. and Godin, I. (2007) 'Ontogeny of the Hematopoietic System', *Annual Review of Immunology* 25: 745-785.
- Curtis, D. J., Salmon, J. M. and Pimanda, J. E. (2012) 'Concise Review: Blood Relatives: Formation and regulation of hematopoietic stem cells by the basic helix-loop-helix transcription factors stem cell leukemia and lymphoblastic leukemia-derived sequence 1', *Stem Cells* 30(6): 1053-8.
- Downs, K. M. and Davies, T. (1993) 'Staging of gastrulating mouse embryos by morphological landmarks in the dissecting microscope', *Development* 118: 1255-1266.
- Fiering, S. N., Roederer, M., Nolan, G. P., Micklem, D. R., Parks, D. R. and Herzenberg, L. A. (1991) 'Improved FACS-Gal: flow cytometric analysis and sorting of viable eukaryotic cells expressing reporter gene constructs', *Cytometry* 12(4): 291-301.
- Ginhoux, F., Greter, M., Leboeuf, M., Nandi, S., See, P., Gokhan, S., Mehler, M. F., Conway, S. J., Ng, L. G., Stanley, E. R. et al. (2010) 'Fate Mapping Analysis Reveals That Adult Microglia Derive from Primitive Macrophages', *Science* 330(6005): 841-845.
- Giroux, S., Kaushik, A.-L., Capron, C., Jalil, A., Kelaidi, C., Sablitzky, F., Dumenil, D., Albagli, O. and Godin, I. (2007) 'lxl-1 and tal-1/scl, two genes encoding closely related bHLH transcription factors, display highly overlapping expression patterns during cardiovascular and hematopoietic ontogeny', *Gene Expression Patterns* 7(3): 215.
- Gomez Perdiguero, E. and Geissmann, F. (2013) 'Myb-Independent Macrophages: A Family of Cells That Develops with Their Tissue of Residence and Is Involved in Its Homeostasis', *Cold Spring Harb Symp Quant Biol.*
- Gomez Perdiguero, E., Klapproth, K., Schulz, C., Busch, K., Azzoni, E., Crozet, L., Garner, H., Trouillet, C., de Bruijn, M. F., Geissmann, F. et al. (2015) 'Tissue-resident macrophages originate from yolk-sac-derived erythro-myeloid progenitors', *Nature* 518(7540): 547-51.
- Guo, W. and Wu, H. (2008) 'Detection of LacZ expression by FACS-Gal analysis'.

- Hoeffel, G., Chen, J., Lavin, Y., Low, D., Almeida, F. F., See, P., Beaudin, A. E., Lum, J., Low, I., Forsberg, E. C. et al. (2015) 'C-Myb+ Erythro-Myeloid Progenitor-Derived Fetal Monocytes Give Rise to Adult Tissue-Resident Macrophages', *Immunity* 42(4): 665-678.
- Jung, S., Aliberti, J., Graemmel, P., Sunshine, M. J., Kreutzberg, G. W., Sher, A. and Littman, D. R. (2000) 'Analysis of fractalkine receptor CX(3)CR1 function by targeted deletion and green fluorescent protein reporter gene insertion', *Mol Cell Biol* 20(11): 4106-14.
- Kierdorf, K., Erny, D., Goldmann, T., Sander, V., Schulz, C., Perdiguero, E. G., Wieghofer, P., Heinrich, A., Riemke, P., Holscher, C. et al. (2013) 'Microglia emerge from erythromyeloid precursors via Pu.1- and Irf8-dependent pathways', *Nat Neurosci* 16(3): 273-80.
- Matcovitch-Natan, O., Winter, D. R., Giladi, A., Vargas Aguilar, S., Spinrad, A., Sarrazin, S., Ben-Yehuda, H., David, E., Zelada Gonzalez, F., Perrin, P. et al. (2016) 'Microglia development follows a stepwise program to regulate brain homeostasis', *Science* 353(6301): aad8670.
- McCallum, A. P., Gallek, M. J., Ramey, W., Manziello, A., Witte, M. H., Bernas, M. J., Labiner, D. M. and Weinand, M. E. (2016) 'Cortical gene expression correlates of temporal lobe epileptogenicity', *Pathophysiology* 23(3): 181-90.
- McGrath, K. E., Frame, J. M. and Palis, J. (2015) 'Early hematopoiesis and macrophage development', *Semin Immunol* 27(6): 379-87.
- McGrath, K. E., Koniski, A. D., Malik, J. and Palis, J. (2003) 'Circulation is established in a stepwise pattern in the mammalian embryo', *Blood* 101(5): 1669-76.
- Mildner, A., Schmidt, H., Nitsche, M., Merkler, D., Hanisch, U. K., Mack, M., Heikenwalder, M., Bruck, W., Priller, J. and Prinz, M. (2007) 'Microglia in the adult brain arise from Ly-6ChiCCR2+ monocytes only under defined host conditions', *Nat Neurosci* 10(12): 1544-53.
- Palis, J., Robertson, S., Kennedy, M., Wall, C. and Keller, G. (1999) 'Development of erythroid and myeloid progenitors in the yolk sac and embryo proper of the mouse', *Development* 126(22): 5073-84.

- Paolicelli, R. C., Bolasco, G., Pagani, F., Maggi, L., Scianni, M., Panzanelli, P., Giustetto, M., Ferreira, T. A., Guiducci, E., Dumas, L. et al. (2011) 'Synaptic pruning by microglia is necessary for normal brain development', *Science* 333(6048): 1456-8.
- Pina, C. and Enver, T. (2007) 'Differential contributions of haematopoietic stem cells to foetal and adult haematopoiesis: insights from functional analysis of transcriptional regulators', *Oncogene* 26(47): 6750-65.
- Pirot, N., Deleuze, V., El-Hajj, R., Dohet, C., Sablitzky, F., Couttet, P., Mathieu, D. and Pinet, V. (2010) 'LYL1 activity is required for the maturation of newly formed blood vessels in adulthood', *Blood* 115(25): 5270-5279.
- Pirot, N., Delpech, H., Deleuze, V., Dohet, C., Courtade-Saidi, M., Basset-Leobon, C., Chalhoub, E., Mathieu, D. and Pinet, V. (2014) 'Lung endothelial barrier disruption in Lyl1-deficient mice', *Am J Physiol Lung Cell Mol Physiol* 306(8): L775-85.
- Prinz, M. and Priller, J. (2014) 'Microglia and brain macrophages in the molecular age: from origin to neuropsychiatric disease', *Nat Rev Neurosci* 15(5): 300-12.
- Schulz, C., Gomez Perdiguero, E., Chorro, L., Szabo-Rogers, H., Cagnard, N., Kierdorf, K., Prinz, M., Wu, B., Jacobsen, S. E., Pollard, J. W. et al. (2012) 'A lineage of myeloid cells independent of Myb and hematopoietic stem cells', *Science* 336(6077): 86-90.
- Sheng, J., Ruedl, C. and Karjalainen, K. (2015) 'Most Tissue-Resident Macrophages Except Microglia Are Derived from Fetal Hematopoietic Stem Cells', *Immunity* 43(2): 382-93.
- Soucie, E. L., Weng, Z., Geirsdottir, L., Molawi, K., Maurizio, J., Fenouil, R., Mossadegh-Keller, N., Gimenez, G., VanHille, L., Beniazza, M. et al. (2016) 'Lineage-specific enhancers activate self-renewal genes in macrophages and embryonic stem cells', *Science*.
- Souroullas, G. P. and Goodell, M. A. (2011) 'A new allele of Lyl1 confirms its important role in hematopoietic stem cell function', *Genesis* 49(6): 441-8.
- Souroullas, G. P., Salmon, J. M., Sablitzky, F., Curtis, D. J. and Goodell, M. A. (2009) 'Adult hematopoietic stem and progenitor cells require either Lyl1 or Scl for survival', *Cell Stem Cell* 4(2): 180-6.

- Thomas, D. M., Francescutti-Verbeem, D. M. and Kuhn, D. M. (2006) 'Gene expression profile of activated microglia under conditions associated with dopamine neuronal damage', *FASEB J* 20(3): 515-7.
- Tober, J., McGrath, K. E. and Palis, J. (2008) 'Primitive erythropoiesis and megakaryopoiesis in the yolk sac are independent of c-myb', *Blood* 111(5): 2636-2639.
- Ueno, M., Fujita, Y., Tanaka, T., Nakamura, Y., Kikuta, J., Ishii, M. and Yamashita, T. (2013) 'Layer V cortical neurons require microglial support for survival during postnatal development', *Nat Neurosci* 16(5): 543-551.
- Wehrspaun, C. C., Haerty, W. and Ponting, C. P. (2015) 'Microglia recapitulate a hematopoietic master regulator network in the aging human frontal cortex', *Neurobiology of Aging* 36(8): 2443.e9-2443.e20.
- Wilson, N. K., Foster, S. D., Wang, X., Knezevic, K., Schitte, J., Kaimakis, P., Chilarska, P. M., Kinston, S., Ouwehand, W. H., Dzierzak, E. et al. (2010) 'Combinatorial Transcriptional Control In Blood Stem/Progenitor Cells: Genome-wide Analysis of Ten Major Transcriptional Regulators', *Cell Stem Cell* 7(4): 532-544.
- Wolf, Y., Yona, S., Kim, K. W. and Jung, S. (2013) 'Microglia, seen from the CX3CR1 angle', *Front Cell Neurosci* 7: 26.
- Zaqout, S. and Kaindl, A. M. (2016) 'Golgi-Cox Staining Step by Step', *Frontiers in Neuroanatomy* 10: 38.
- Zhan, Y., Paolicelli, R. C., Sforzini, F., Weinhard, L., Bolasco, G., Pagani, F., Vyssotski, A. L., Bifone, A., Gozzi, A., Ragozzino, D. et al. (2014) 'Deficient neuron-microglia signaling results in impaired functional brain connectivity and social behavior', *Nat Neurosci* 17(3): 400-406.
- Zhang, Y., Chen, K., Sloan, S. A., Bennett, M. L., Scholze, A. R., O'Keefe, S., Phatnani, H. P., Guarnieri, P., Caneda, C., Ruderisch, N. et al. (2014) 'An RNA-sequencing transcriptome and splicing database of glia, neurons, and vascular cells of the cerebral cortex', *J Neurosci* 34(36): 11929-47.

Zohren, F., Souroullas, G. P., Luo, M., Gerdemann, U., Imperato, M. R., Wilson, N. K., Gottgens, B., Lukov, G. L. and Goodell, M. A. (2012) 'The transcription factor Lyl-1 regulates lymphoid specification and the maintenance of early T lineage progenitors', *Nat Immunol* 13(8): 761-769.

## 2.3. Result part 2: Additional data

### 2.3.1. Lyl-1 does not influence macrophage production from AGM-HSC

We also investigated whether *lyl-1* invalidation affects the MΦ population derived from the differentiation of intra-embryonic HSC. AGM (E10-E10.5) were dissected as described before (Bertrand et al., 2005a) and cultured on OP9 stroma to allow their differentiation. They were cultured in "Complete OptiMEM medium" supplemented with Flt-3 ligand (10 ng/ml), Stem Cell Factor (50 ng/ml) and EPO (50 ng/ml) and Il-7 (50 ng/ml, from Peprotech). After 4 days of culture, the number and type of progenitors produced was further characterized through clonogenic assays and cytometry analyses.

Contrary to what was observed for OrgD1-YS, in clonogenic assays, AGM-HSC from wild type and *lyl-1<sup>LacZ/LacZ</sup>* gave rise to similar numbers of MΦ progenitors (**Fig 16A**), as well as GM and EMp (data not shown). Moreover, cytometry analyses evidenced that the amounts of CD11b<sup>+</sup> and F4/80<sup>+</sup> MΦ produced during the 4 days in culture were similar in the three genotypes (**Fig 16B**). These cytometry analyses were performed at earlier (Day2) or later (D6 and D10) of culture, with identical results (data not shown). These data show that Lyl-1 does not regulate MΦ production from intra-embryonic HSC, as it does in the early YS.

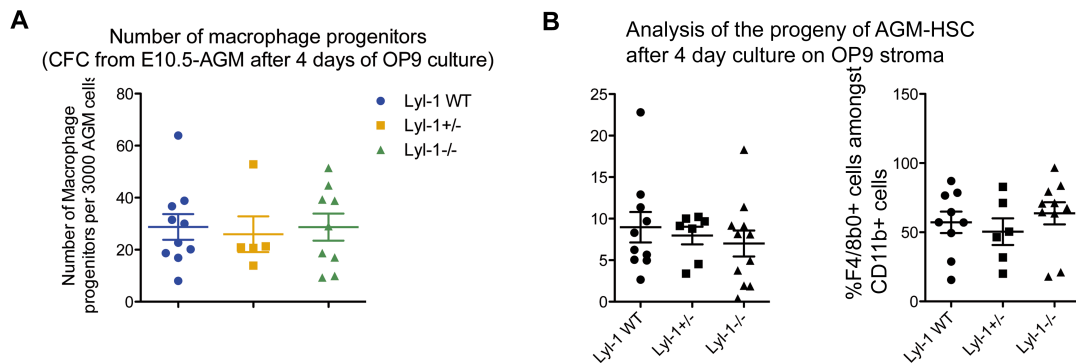


**Figure 16: Lyl-1 does not influence the production of MΦ from AGM-HSC.**

(A) Clonogenic potential of AGM-derived cells analyzed after a 4 days differentiation step on OP9 stroma. The number of EMp, GM and MΦ precursors is similar in the different genotypes. (B) Wild type and mutant AGM cells after a 4 days differentiation step on OP9 stroma allowed the cytometry analysis of Lyl-1 expression in HSC-derived myeloid cells. The amount of CD11b<sup>+</sup> cells and of F4/80 MΦ among CD11b<sup>+</sup> cells is similar in the 3 genotypes.

### 2.3.2. Identification of the differences in genes expression between YS-derived primitive and definitive macrophage by RNA sequencing

Because Lyl-1 expression discriminates the primitive and definitive MΦ lineages in the early YS, we can now assess the differences that exist between these two populations. Therefore, we now stated to implement RNA-Seq analyses of primitive and definitive YS population on wild type and *Lyl-1<sup>LacZ/LacZ</sup>* mutants. The aims of this study are to:

- 1- determine the specific features of primitive MΦ, compared to definitive MΦ from older embryos and
- 2- assess what is the effect of Lyl-1 inactivation on the poorly

known primitive population. The information gathered during this project might provide long sought after information on primitive population, and might shed a new light on the regulation of the properties of embryonic hematopoietic progenitors that may be impaired in specific pathological conditions arising from developmental defects.

For the experimental preparation, all the samples were primary cells sorted directly from either wild type or *Lyl-1<sup>LacZ/LacZ</sup>* mouse embryos, according to the common phenotype (c-Kit<sup>+</sup>CD45<sup>+</sup>CD11b<sup>+</sup>). Specifically, primitive MΦ progenitors were collected from wild type or *Lyl-1<sup>LacZ/LacZ</sup>* E9-YS (<18S); mixture of primitive and definitive MΦ progenitors were collected from wild type or *Lyl-1<sup>LacZ/LacZ</sup>* E10-YS; using FDG staining, the subsets of *Lyl-1*/FDG positive and negative MΦ progenitors were sorted from *Lyl-1<sup>LacZ/LacZ</sup>* E10-YS. I have already finished the sample preparation and sent the sample to analyze. The overall experimental strategy and aims of the RNA-Seq are showed in the **Table 3**.

**Table 3: Description of the experimental strategy and aims of the RNA-Seq**

Experimental strategy and aims of the study					
Development stage	E9 Yolk Sac		E10.5 Yolk Sac		
Types of MΦ progenitors in a wild type context	Primitive MΦ progenitors		Mixture of primitive and definitive MΦ progenitors that are phenotypically indistinguishable		
Sample	MΦ progenitors sorted from E9 YS		MΦ progenitors sorted from E10.5 YS		
Genotype	Wild type ①	<i>Lyl-1</i> <sup>-/-</sup> ②	Wild type ③	<i>Lyl-1</i> <sup>-/-</sup> ④	
Types of macrophages progenitors	Primitive/Normal	Primitive/Defective	Primitive/Normal AND Definitive/normal	Primitive/Defective AND Definitive/normal	
<b>Sample identification</b> <p>① E9-YS WT p-MΦ<sup>Prim</sup>            ② E9-YS <i>Lyl-1</i><sup>-/-</sup> p-MΦ<sup>Prim</sup>            ③ E10.5-YS WT p-MΦ<sup>Prim</sup> + p-MΦ<sup>Def</sup>            ④ E10.5-YS <i>Lyl-1</i><sup>-/-</sup> p-MΦ<sup>Prim</sup> + p-MΦ<sup>Def</sup>            ⑤ E10.5-YS <i>Lyl-1</i><sup>-/-</sup> <i>Lyl-1</i><sup>-/-</sup>/βGal- (p-MΦ<sup>Def</sup> ?)            ⑥ E10.5-YS <i>Lyl-1</i><sup>-/-</sup> <i>Lyl-1</i><sup>+/+</sup>/βGal+ (p-MΦ<sup>Prim</sup> ?)</p>	<b>Types of MΦ progenitors in a <i>Lyl-1</i><sup>-/-</sup> context</b> Lyl-1 positive and negative MΦ progenitors can be distinguished (β-Gal-Activity)				
	Sample	Sorted β-Gal/ <i>Lyl-1</i> Negative MΦ progenitors ⑤		Sorted β-Gal/ <i>Lyl-1</i> Positive MΦ progenitors ⑥	
	Genotype	<i>Lyl-1</i> <sup>-/-</sup>			
Types of macrophages progenitors	Definitive/Normal?		Primitive/Defective?		
<b>Aims of the study</b> <ul style="list-style-type: none"> <li><span style="color: pink;">—</span> What are the modifications resulting from <i>Lyl-1</i> invalidation ?</li> <li><span style="color: yellow;">—</span> Are <i>Lyl-1</i> features constant with YS development stage and sorting procedure ?</li> <li><span style="color: blue;">—</span> What are the differences between primitive and definitive MΦ progenitors ?</li> <li><span style="color: green;">—</span> Does <i>Lyl-1</i> expression discriminate the two populations ?</li> </ul>					

### 2.3.3. *Lyl-1* expressing primitive MΦ colonize the fetal liver

At early developmental stages, FL is considered as an intermediate hematopoietic site, where the size of hematopoietic cell pool largely amplifies to fulfill the requirement of embryonic development. Exogenous hematopoietic cells colonize the FL to initiate hematopoiesis at E9.5. In addition to supporting hematopoietic cells expansion, the FL is also the main hematopoietic site for the differentiation of myeloid cells. EMPs colonize the FL beginning at E9.5 (Kieusseian et al., 2012) and are highly enriched at E10.5-FL, where they expand and differentiate into multiple cell lineages. Moreover, considering the timing relative to progenitor numbers and lineage mapping correlations, it was suggested that the early MΦ population at E10-FL might be largely derived from the primitive progenitors. Hence, I detected the *Lyl-1* expression pattern within the MΦ progenitors pool at both E10-YS and E10-FL from wild type, *Lyl-1*<sup>WT/LacZ</sup> and *Lyl-1*<sup>LacZ/LacZ</sup> mice by using FACS-gal assay. I found that both E10-YS and E10-FL contain two distinct MΦ progenitors discriminated by their *Lyl-1* expression (**Fig 17**), confirming that primitive MΦ population also colonize the FL during early embryonic development.

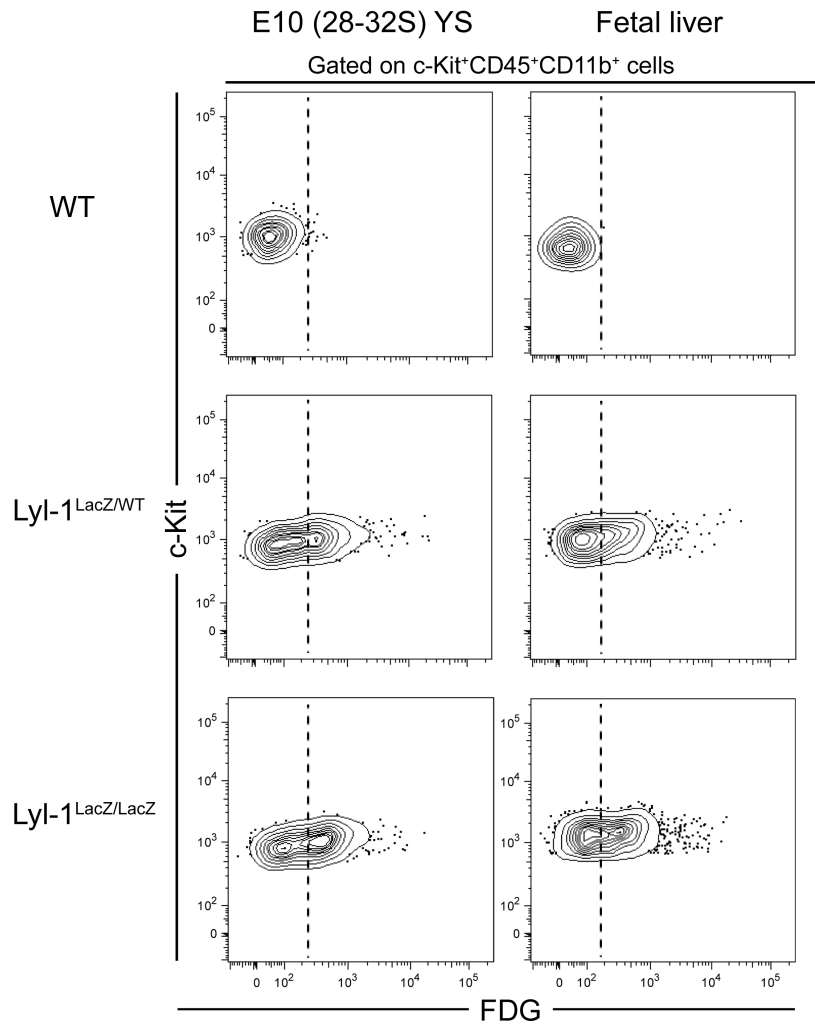


**Figure 17: Lyl-1<sup>+</sup> primitive MΦ progenitors are present in the fetal liver at E10.**

Representative profiles from 3 independent samples preparation, each cumulating 3-4 YS and FL from the same embryos. Both E10-YS and -FL harbor FDG<sup>+</sup>/Lyl-1<sup>+</sup> and FDG<sup>-</sup>/Lyl-1<sup>-</sup> MΦ progenitors.

### 2.3.4. Lyl-1 deficiency leads to a reduction of the microglia pool at E12

To assess the effect of Lyl-1 on microglia development, I quantified the percentages of F4/80+ microglia in wild type and *Lyl-1<sup>LacZ/LacZ</sup>* mice at E12 and E14 by using two different ways. Specifically, in the first method, the total brain cells were analyzed by FACS. Then the percentage of microglia within the whole brain was recorded and compared between wild type and *Lyl-1<sup>LacZ/LacZ</sup>* at different stages. In the second method, the total microglial population (progenitors and mature cells) was first purified by Percoll gradient centrifugation and then quantified by FACS analysis. I found a significant reduction of F4/80<sup>+</sup> microglia in the brain of *Lyl-1<sup>LacZ/LacZ</sup>* mutant mice at E12, whereas the percentage of microglia was not influenced at E14 in the method of Percoll purification (**Fig 18**), suggesting that Lyl-1 inactivation affects the microglia differentiation and maturation, resulting in the reduction of the mature microglia pool at E12. Contrary to what was observed in this second method, wild type and *Lyl-1<sup>LacZ/LacZ</sup>* mice displayed a significant decrease of the percentage of F4/80+ microglia at E14, but not at E12, compared to that of wild type in the first method (**Fig 18**). This interesting finding might be due to the less precise by using the whole brain tissue. Also it is possible that the proliferating defects of microglia caused by Lyl-1 inactivation occur at E12 and the effects on microglia pool display at E14.

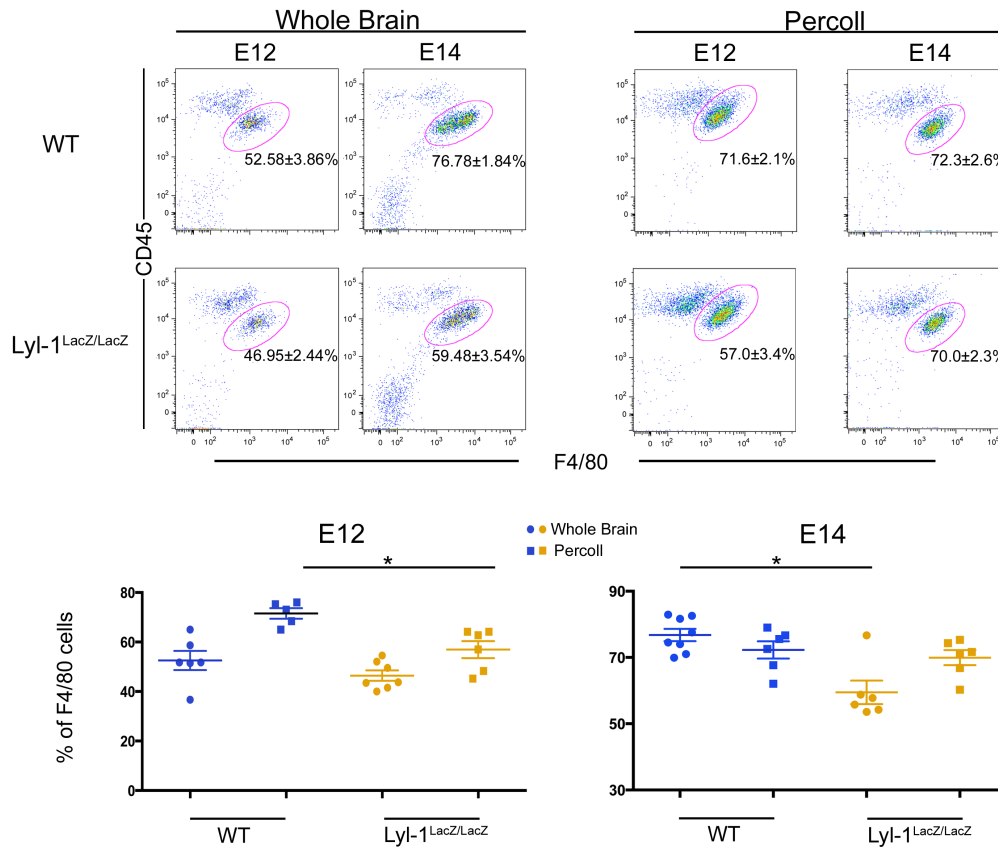


**Figure 18: *Lyl-1* deficiency leads to a reduction of the microglia pool at E12.5.**

Representative profiles from 3 independent samples preparation, each cumulating 2-3 brain repeats (mean  $\pm$  SD, below). Two developmental stages (E12 and E14) were analyzed. Left panel: the whole brain cells from wild type and *Lyl-1<sup>LacZ/LacZ</sup>* mutants were analyzed by FACS. Right Panel: microglial cells were purified from wild type and *Lyl-1<sup>LacZ/LacZ</sup>* mutants by Percoll gradient centrifugation and analyzed by FACS using the same gate strategy. Gated on CD11b+ cells. \*P  $\leq$  % 0.05 (Student's t test) significantly different from wild type in corresponding to % of F4/80 cells.

### 2.3.5. Lyl-1 inactivation results in a reduction of inflammatory-related genes expression

Inflammatory-related gene expression in microglia of wild type and *Lyl-1<sup>LacZ/LacZ</sup>* mutants was analyzed by qPT-PCR. Total RNA isolated from either at P0 or P15 brains was analyzed with primers corresponding to the IL-6, TNF- $\alpha$  and IL-1 $\beta$  genes. As shown in **Figure 19**, the transcripts of TNF- $\alpha$  and IL-1 $\beta$  in *Lyl-1* mutants microglia were seriously reduced compared with those of the wild type at P15. Decreases of expression in IL-6 were observed in *Lyl-1* mutants at both P0 and P15 (**Fig 19**), suggesting impaired functions in *Lyl-1* deficiency microglia.

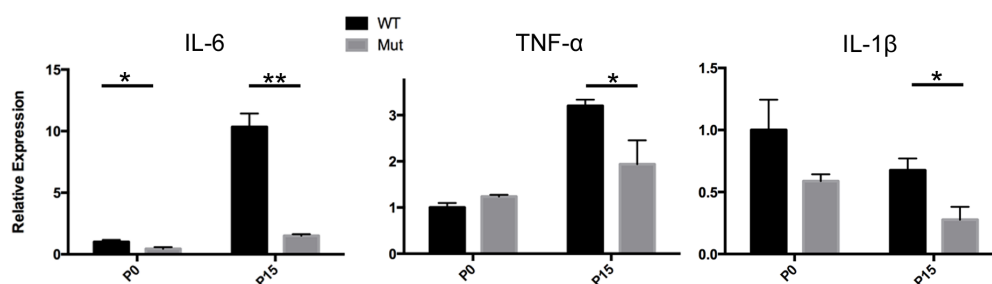


**Figure 19: Lyl-1 inactivation results in a reduction of inflammatory-related genes expression.**

Expression of inflammatory-related genes IL-6, TNF- $\alpha$  and IL-1 $\beta$  in wild type and *Lyl-1<sup>LacZ/LacZ</sup>* mutants at P0 and P15 was measured by qRT-PCR (mean  $\pm$  SD of three biological replicates). \*P  $\leq$  % 0.05, \*\*P  $\leq$  % 0.01 (Student's t test) significantly different from wild type in corresponding stages.

### **2.3.6. Bibliographic and database information evidencing a possible involvement of Lyl-1 in human microglia in health and diseases.**

We are eager to know whether the data we obtained in our murine model are relevant to human. We therefore started gathering information from bibliographic and database sources that evidencing a possible involvement of Lyl-1 in human microglia in health and diseases. This ongoing survey confirmed the expression of Lyl-1 in human microglia, but did not so far provide clear-cut evidences for Lyl-1 involvement in autism syndrome disorders, as well as in Alzheimer's disease.

It however repeatedly pointed to Lyl-1 implication in neuro-inflammatory processes, suggesting that Lyl-1 may have a neuro-protective function in a steady state situation. Our qRT-PCR results also involve Lyl-1 in the regulation of inflammatory process, but we find a reduced production of pro-inflammatory cytokines at P0 and P15. At these stages, Lyl-1 would therefore favour inflammation in a wild type context, a conclusion that does not fit easily with the information presented below. Further work is needed to understand Lyl-1 involvement in inflammatory processes and to explain this discrepancy.

#### ***2.3.6.1 Lyl-1 is expressed in murine and human microglia and no other brain cell types:***

➡ Lyl-1 is expressed in microglia, and to a lesser extent endothelial cells from the cerebral cortex, and no other brain cell types (see RNA-Seq transcriptome and splicing database of neurons, glia and vascular cells, and

[http://web.stanford.edu/gate2.inist.fr/group/barres\\_lab/brain\\_rnaseq.html](http://web.stanford.edu/gate2.inist.fr/group/barres_lab/brain_rnaseq.html)) (*Zhang et al., 2014*)

➡ Lyl-1 is expressed in P60 microglia and not in astrocytes, neurons and oligodendrocytes (See Sup Fig 7) (*Bennett et al., 2016*)

➡ Lyl-1 is identified in the "microglia module", compared to other brain cell types (*Zeisel et al., 2015*).

➡ Lyl-1 is expressed in the frontal cortex of healthy adult (transcriptome data sets; see Sup. Table 6 and Sup. Table 7) (*Wehrspaun et al., 2015*)

### **2.3.6.2 Lyl-1 modification in autism with FMR1-FM is not clearcut**

➡ Lyl-1 is significantly modified in autism with FMR1-FM (See Sup Table S3: SAM Rank 3267 out of 5139 differentially expressed genes (DEG), but it does not appear in Sup table sup 5 with RANK-Prod, 2281 DEG) (*Nishimura et al., 2007*).

➡ Lyl-1 was not modified in autism with 15q duplication (1281 DEG) (*Nishimura et al., 2007*).

### **2.3.6.3 Lyl-1 deregulation is observed in some Alzheimer disease (AD) models**

*a- In murine models:*

➡ Lyl-1 is reduced in the APP-PS1 mouse model of AD GSE74615: Cortical microglia in APP<sup>swe</sup>/PS1<sup>dE9</sup> model (WMG4x44kv2): Transcriptional analysis was performed on isolated astrocytes and microglia from the cortex of aged controls and APP<sup>swe</sup>/PS1<sup>dE9</sup> AD mice (See supTable s3) (*Kamphuis et al., 2016; Orre et al., 2014*)

➡ Lyl-1 is reduced in the 5xFAD mouse model of AD. This down-regulation is attenuated in Trem2 KO. GSE65067: WT and TREM2-deficient microglia model (MoGene)

A rare R47H mutation of TREM2 correlates with a substantial increase in the risk of developing Alzheimer disease (AD). TREM2 deficiency and haploinsufficiency augment  $\beta$ -amyloid (A $\beta$ ) accumulation due to a dysfunctional response of microglia, which fail to cluster around A $\beta$  plaques and become apoptotic (*Wang et al., 2015*).

➡ Other data to be analyzed: Lyl-1 is not significantly modified in three AD murine models:

- In the PS2APP model murine models of AD: GSE75431: Cortical CD11b cells in 7/13mo PS2APP model (*Srinivasan et al., 2016*)

- In GSE89482: Cortical Cx3cr1-GFP cells in 14-15mo PS2APP model (RNA-Seq).

- In GSE93179 and GSE93180: Hippocampal CD11b cells in Tau-P301L model (Mouse RNA-Seq)

*b- In human:*

➡ Lyl-1 is decreased 3.2 fold in the hippocampal cornu ammonis 1 of AD patients.

Samples: control and AD hippocampal cornu ammonis 1 (CA1) from domestic and international brain banks (pools from CA1 of six control or six AD subjects). Results in table 2: there is a 3.2 fold decrease in Lyl-1 expression in the hippocampal cornu ammonis 1 of AD patients, compared to control. (*Colangelo et al., 2002*).

➡ Other data to be analyzed:

- Lyl-1 is not significantly increased in AD patient fusiform gyrus: GSE95587: Alzheimer's Patient Fusiform Gyrus (whole tissue) (Human RNA-Seq)

- Lyl-1 is significantly increased in AD patient Temporal Cortex: GSE15222: Alzheimer's Patient Temporal Cortex (whole tissue) (illuminaHumanv1)

#### ***2.3.6.4 Lyl-1 appears involved in the regulation of neuro-inflammation***

*a- In murine models:*

➡ Lyl-1 is down regulated in the microglia of LPS-treated mice at P60.

In Tmem119 murine model, a down regulation of Lyl-1 is observed in the microglia of LPS-treated mice (WT) compared to untreated at P60. Data found in excel files.

[http://web.stanford.edu/group/barres\\_lab/brainseq2/brainseq2.html](http://web.stanford.edu/group/barres_lab/brainseq2/brainseq2.html) (*Bennett et al., 2016*)

NCBI bioproject: accession n° PRJNA307271

➡ Lyl-1 is down regulated 2.16 folds in the microglia from LPS-treated mice.

GSE75246; Data found in excel files. (*Srinivasan et al., 2016*)

➡ Lyl-1 belongs to the genes set most down-regulated in microglia activating conditions: To increase the understanding of microglial activation, microarray analysis was used to profile the transcriptome of BV-2 murine microglial cells

submitted to 3 activating conditions (LPS treatment, treatment with the HIV neurotoxic protein TAT, or with dopamine quinone). All these treatment have been linked to dopamine neuronal damage.

The focus was on genes differentially expressed in all three activating conditions, by comparison to the transcriptome of resting microglia.

The genes whose expression was most reduced by all activating conditions included Lyl-1, which is reduced 14-fold (See Supplemental Table 4) (*Thomas et al., 2006*).

➡ Lyl-1 might be associated with neuroprotection:

Methamphetamine (METH) is well known for its ability to cause damage to dopamine (DA) nerve endings of the striatum. DA released into the synapse by METH is very likely the source of downstream reactants that provoke microglial activation and the ensuing damage to DA nerve endings. In the comparison of murine microglia BV-2 cells treated or not with DA-quinone (DAQ) which acts downstream of meth to damage DA neurons, the authors they find Lyl-1 amongst the genes decreased at least 2.8 folds (See Table 2). They consider that the decreased genes are associated with neuroprotection. (*Kuhn et al., 2008*)

#### ***2.3.6.5 Lyl-1 is significantly lower in TLE patients with high seizure frequency***

➡ To find whether there is genetic basis to temporal lobe epilepsy (TLE), whole genome analyses was performed to identify differential gene expression in the temporal lobes of TLE patients with high vs. low baseline seizure frequency. Samples: 24 patients in high or low seizure frequency groups (median seizures/month) who underwent anterior temporal lobectomy with amygdalo-hippocampectomy for intractable TLE.

The authors find that high seizure frequency is associated the low expression of 7 genes, including Lyl-1 (See Table 3) (*McCallum et al., 2016*)

## **References:**

- Bennett, M.L., Bennett, F.C., Liddel, S.A., Ajami, B., Zamanian, J.L., Fernhoff, N.B., Mulinyawe, S.B., Bohlen, C.J., Adil, A., Tucker, A., *et al.* (2016). New tools for studying microglia in the mouse and human CNS. *Proceedings of the National Academy of Sciences* *113*, E1738-E1746.
- Colangelo, V., Schurr, J., Ball, M.J., Pelaez, R.P., Bazan, N.G., and Lukiw, W.J. (2002). Gene expression profiling of 12633 genes in Alzheimer hippocampal CA1: transcription and neurotrophic factor down-regulation and up-regulation of apoptotic and pro-inflammatory signaling. *J Neurosci Res* *70*, 462-473.
- Kamphuis, W., Kooijman, L., Schetters, S., Orre, M., and Hol, E.M. (2016). Transcriptional profiling of CD11c-positive microglia accumulating around amyloid plaques in a mouse model for Alzheimer's disease. *Biochim Biophys Acta* *1862*, 1847-1860.
- Kuhn, D.M., Francescutti-Verbeem, D.M., and Thomas, D.M. (2008). Dopamine Disposition in the Presynaptic Process Regulates the Severity of Methamphetamine-Induced Neurotoxicity. *Annals of the New York Academy of Sciences* *1139*, 118-126.
- McCallum, A.P., Gallek, M.J., Ramey, W., Manziello, A., Witte, M.H., Bernas, M.J., Labiner, D.M., and Weinand, M.E. (2016). Cortical gene expression correlates of temporal lobe epileptogenicity. *Pathophysiology* *23*, 181-190.
- Nishimura, Y., Martin, C.L., Vazquez-Lopez, A., Spence, S.J., Alvarez-Retuerto, A.I., Sigman, M., Steindler, C., Pellegrini, S., Schanen, N.C., Warren, S.T., *et al.* (2007). Genome-wide expression profiling of lymphoblastoid cell lines distinguishes different forms of autism and reveals shared pathways. *Human Molecular Genetics* *16*, 1682-1698.
- Orre, M., Kamphuis, W., Osborn, L.M., Jansen, A.H., Kooijman, L., Bossers, K., and Hol, E.M. (2014). Isolation of glia from Alzheimer's mice reveals inflammation and dysfunction. *Neurobiol Aging* *35*, 2746-2760.
- Srinivasan, K., Friedman, B.A., Larson, J.L., Lauffer, B.E., Goldstein, L.D., Appling, L.L., Borneo, J., Poon, C., Ho, T., Cai, F., *et al.* (2016). Untangling the brain's neuroinflammatory and neurodegenerative transcriptional responses. *7*, 11295.

- Thomas, D.M., Francescutti-Verbeem, D.M., and Kuhn, D.M. (2006). Gene expression profile of activated microglia under conditions associated with dopamine neuronal damage. *FASEB J* 20, 515-517.
- Wang, Y., Cella, M., Mallinson, K., Ulrich, J.D., Young, K.L., Robinette, M.L., Gilfillan, S., Krishnan, G.M., Sudhakar, S., Zinselmeyer, B.H., *et al.* (2015). TREM2 Lipid Sensing Sustains the Microglial Response in an Alzheimer's Disease Model. *Cell* 160, 1061-1071.
- Wehrspaun, C.C., Haerty, W., and Ponting, C.P. (2015). Microglia recapitulate a hematopoietic master regulator network in the aging human frontal cortex. *Neurobiology of Aging* 36, 2443.e2449-2443.e2420.
- Zeisel, A., Munoz-Manchado, A.B., Codeluppi, S., Lonnerberg, P., La Manno, G., Jureus, A., Marques, S., Munguba, H., He, L., Betsholtz, C., *et al.* (2015). Brain structure. Cell types in the mouse cortex and hippocampus revealed by single-cell RNA-seq. *Science* 347, 1138-1142.
- Zhang, Y., Chen, K., Sloan, S.A., Bennett, M.L., Scholze, A.R., O'Keefe, S., Phatnani, H.P., Guarnieri, P., Caneda, C., Ruderisch, N., *et al.* (2014). An RNA-sequencing transcriptome and splicing database of glia, neurons, and vascular cells of the cerebral cortex. *J Neurosci* 34, 11929-11947.

# **3 GENERAL DISCUSSION AND PERSPECTIVES**

### **3.1 Lyl-1 expression discriminates the YS-derived primitive and definitive macrophages.**

It is essential to define the expression pattern of transcription factor in hematopoietic cells during specific steps of development, differentiation and maintenance since the various features of hematopoietic cells are tightly controlled by the balance between the different hematopoietic transcription factor (Novershtern et al., 2011). In a previous study, we observed that *Lyl-1* transcripts were present in the YS blood islands (Giroux et al., 2007). Likewise, *LacZ* expression driven by *Lyl-1* promoter was observed in the YS blood islands of transgenic mice (Chan et al., 2007). Using FACS-Gal staining and *in vitro* assays to detect the possible presence of a minor Lyl-1 expressing subset in the YS, we first confirm that Lyl-1 is expressed by a small subset of CD11b<sup>+</sup>CD31<sup>+</sup> MΦ precursors, as well as a fraction of F4/80<sup>+</sup> mature MΦ. Consistent with this expression, the disruption of *Lyl-1* HLH domain leads to an increased production of MΦ progenitors, while the amount of YS-derived GM and EMp precursors remains unmodified. We further show that *Lyl-1* disruption does not modify the production of MΦ from AGM-HSC, obtained after an *in vitro* differentiation step to allow their differentiation. Thus, these data together suggests that Lyl-1 function during MΦ development appears specific to a subset of early YS progenitors.

During mouse embryogenesis, the first YS-derived MΦ population, called primitive, derives from monopotent MΦ progenitors generated as early as E7.5. GM precursors and EMp that will give rise to the second wave of YS-derived MΦ emerge a few hours later, from the 2-5S stage (Bertrand et al., 2005b; Palis et al., 1999). MΦ precursors from the first and second YS waves share the same phenotype and can only be discriminated by their kinetics of appearance (Bertrand et al., 2005b). By focusing on the YS that is before 5S stage, we gathered several evidences pointing to Lyl-1 expression and function as a distinctive feature of MΦ precursors from the first

(primitive) YS wave. The characterization of FDG<sup>+</sup> cells sorted from E8 YS and FACS-Gal analyses correlate to show that Lyl-1 expression is restricted to the primitive MΦ precursor pool and that all primitive MΦ precursors present at this early stage express Lyl-1. Moreover, the primitive MΦ precursor pool was expanded upon *Lyl-1* bHLH deletion in both heterozygous and homozygous mutants. *In vitro* clonogenic assays of FDG<sup>+</sup>/Lyl-1<sup>+</sup> versus FDG<sup>-</sup>/Lyl-1<sup>-</sup> myeloid progenitors sorted from Lyl-1<sup>WT/LacZ</sup> E10-YS, as well as comparison of *c-Myb* expression levels between these two subsets by qRT-PCR, further confirm our hypothesis. Altogether, these data establish that during YS ontogeny, Lyl-1 expression and function are specific to the primitive MΦ population. Using *Lyl-1* as a marker to discriminate early YS-derived primitive and definitive MΦ population, we can further characterize their specific features, which remain largely unknown. For example, our ongoing RNA sequencing experiments will provide the gene specificities of primitive and definitive MΦ progenitors and the modifications induced by Lyl-1 invalidation. The selected candidate genes from RNA sequencing will be further validated to gather more information about how Lyl-1 controls the expansion of primitive MΦ pool.

On the other hand, the lack of Lyl-1 function in MΦ progenitors derived from both late YS and AGM-HSC in the early embryo does not exclude that Lyl-1 might independently play a role during myeloid differentiation in the adult. Indeed, a function of Lyl-1 as a repressor of myeloid differentiation was previously inferred from the differentiation block along the MΦ lineage, which occurs when *Lyl-1* is over-expressed in the human monoblastic leukemia cell line U937 (Meng et al., 2005).

### 3.2 YS-derived primitive macrophages (*Lyl-1* positive) give rise to the embryonic microglia.

In a previous study, we hypothesized that the microglial population of the developing brain might originate from progenitors generated in the early YS, since cells capable to give rise to growing colonies when cultured on astroglial monolayers could be obtained from the YS at E8 (0-4S stage), but not from the P-Sp/AGM (Alliot et al., 1999). The contribution of YS-derived primitive M $\Phi$  to the microglial population was recently established through fate mapping experiments using an inducible fluorescent reporter under the control of an endogenous promoter of *Runx1*, a transcription factor expressed by early YS cells (Ginhoux et al., 2010). Interestingly, the authors also showed that P-Sp/AGM-derived cells do not contribute to the microglial population. The data presented here complement these studies by uncovering *Lyl-1* expression in microglial progenitors, as well as the maintenance of *Lyl-1* expression in mature F4/80<sup>+</sup> microglial cells throughout embryonic development and adulthood. However, in our latest FACS-gal assay experiments, we noticed that in the *Lyl-1*<sup>LacZ/LacZ</sup> brain, the FDG levels was barely detected at P42, while at P15 it showed a bimodal expression, suggesting the presence of two populations discriminated by their *Lyl-1* expression at the protein level (§2.2, Extended Fig 2c). On the other hand, our qRT-PCR analyses indicated that the transcript levels of *Lyl-1* were high at both stages (§2.2, Fig 2f). These data together make us wondering whether there is other source of M $\Phi$  replacing the microglial pool during the first two postnatal weeks. Previous evidences showed that once the microglial pool is established during embryonic development, the cells themselves are maintained throughout adult life by virtue of longevity and limited self-renewal without input from definitive hematopoiesis (Ajami et al., 2007; Ginhoux et al., 2010; Gomez Perdiguero et al., 2015; Mildner et al., 2007). However, the promoter-controlled CreER-*loxP* tracking system or chimeric animals obtained by parabiosis used in these fate mapping studies

does not provide sufficient temporal resolution to conclude the origin of microglia in adulthood unambiguously. For example, the fluorescence labeled myeloid progenies were only detected in the aging adult mice. Hence, there is a big gap between postnatal developmental period and adulthood to be detected. Moreover, M $\Phi$  progenitors from both primitive and EMp-derived transient definitive waves were labeled upon tamoxifen induction at E8.5 and these protocols only led to 30-40 % microglia labeling, although the levels were likely to be underestimated, suggesting the possibility of bi-source of microglia in adulthood. In fact, microglial numbers in mouse brain change dramatically during postnatal development, with an initial increase during the first 14 postnatal days, then declining in the third postnatal week, and finally reduced by 50% by 6 weeks of age (Nikodemova et al., 2015). Additionally, by using temporal-spatial resolution fate mapping approach, Xu et al recently showed that in zebrafish, that the adult brain continues to be colonized by new M $\Phi$  progenitors that arise from the ventral wall of dorsal aorta, a tissue also producing definitive hematopoiesis in mouse, resulting in the replacement of embryonic-derived microglia with adult-derived microglia (Xu et al., 2015). Thus, considering the highly conserved hematopoietic program between mammalian and zebrafish and evidences observed from our results, it is quite necessary to re-investigate the origin of microglia in adult mice, especially focusing on the postnatal developmental period.

Furthermore, except for microglia, little is known about the contribution of YS-derived primitive M $\Phi$  to embryonic development. Indeed, in our previous confocal analyses, we observed the presence of Lyl-1 positive M $\Phi$  in the embryo body at E10.5 (Giroux et al., 2007). Moreover, we show here that Lyl-1 positive M $\Phi$  progenitors colonize to the FL as early as E10. Therefore, it is possible that primitive M $\Phi$  progenitors also participate to other resident M $\Phi$  populations in the embryo. Unfortunately, the *Lyl-1<sup>LacZ</sup>* reporter mice do not allow neither confocal imaging of YS-derived primitive M $\Phi$ , nor lineage tracing of primitive M $\Phi$  progenies. Therefore,

the following central key objective is to generate novel *Lyl-1* indicator (e.g. conditional and inducible targeting *Lyl-1<sup>Tomato</sup>*) mouse strains that will be instrumental to trace the migration and colonization of primitive MΦ population during embryonic development, as well as adulthood, which will gain more insight into the specific feature of the primitive hematopoiesis. Once the mouse strains are obtained, a fate-mapping study of the murine primitive MΦ taking advantage of constitutive and conditional *Lyl-1* promoter-driven Cre recombines expression will be performed to detect their contribution to the major tissue-resident MΦ compartments during embryonic development and the maintenance during adulthood.

### **3.3 *Lyl-1* regulates the development and functions of microglia and is involved in neuro-developmental diseases.**

As for microglial development, we identify here two key stages, when the effects of *Lyl-1* invalidation occur, resulting in the reduction of microglial pools at E12.5 and P0-P3. These two stages correspond to the end of "early" and "pre-microglia" stages, as described in the stepwise microglia development program recently defined (Matcovitch-Natan et al., 2016). Interestingly, after these stages, the microglia population in *Lyl-1* mutants "rescues" its deficient size through a highly reduced apoptosis levels at E14 and, around birth, through a significantly decreased compared to wild type microglia, of the expression level of *Mafb*, which controls microglia self-renewal in the adult (Matcovitch-Natan et al., 2016; Soucie et al., 2016). These observations suggest that the reduction of microglia compartment seemed to be recovered spontaneously without external input. Correspondingly, Bruttger et al recently found that the microglial compartment was reconstituted within 1 week of depletion by efficient self-renewal (Bruttger et al., 2015). To evaluate the consequences of *Lyl-1* inactivation during later stages of microglia and neural

development, our collaborators investigated the consequences on brain development of microglial defect in *Lyl-1* mutant mice, with a focus on behavioral changes. They evidenced that *Lyl-1* deficient mice display typical phenotypes for social anxiety disorders. However, what extent and how these striking behavioral changes correlate to specific changes in *Lyl-1* deficient microglia need to be examined in details. Indeed, microglial cells actively contribute to the normal embryonic development of the CNS, thus, any modification of their phenotype, activity and density during development may have long term consequences on the structure and function of CNS networks that might result in disorders arising from impaired neurodevelopment. Antony et al recently evidenced that alterations in microglial number as a consequence of genetic or pathological events could perturb neural development by directly affecting embryonic neural precursors, possibly causing late-onset neurodevelopmental disorders (Antony et al., 2011). Therefore, it will be of great importance to precise how and which stage that *Lyl-1* inactivation leads to impaired microglia development, and ultimately to neuro-developmental diseases. This aim can be achieved through generating a conditional (*Lyl-1*<sup>fl/fl</sup>) mouse strains, in which conditional inactivation of the *Lyl-1* gene will be performed at E12 or P0-3, and the phenotypes of *Lyl-1* conditional knockout mice will be characterized in adulthood. In the case of conditional deletion at E12, studies associated with neural development and function will be performed since the decreased microglial numbers affect the neural development (Antony et al., 2011). Moreover, the behavior studies will be also performed in adult animals to assess the long-term consequences caused by embryonic defects. As for conditional deletion at P0-P3, synaptic pruning and behavior studies in adult animals will be analyzed.

In conclusion, we identify for the first time a transcription factor that seems to specifically discriminate YS-derived primitive and definitive M $\Phi$  population. From the data gathered here, it appears that *Lyl-1* restricts the production of primitive M $\Phi$ . Moreover, the discovery that *Lyl-1* expression discriminates the whole primitive M $\Phi$

lineage (progenitors and mature cells) from its definitive counterpart might contribute to uncover the specificity of the regulatory network that influences primitive M $\Phi$  differentiation. This is especially relevant with reference to microglia, as further characterization of Lyl-1 positive brain cells may have potential therapeutic outcome for neurodegenerative diseases.

# **4 RÉSUMÉ DE LA THÈSE EN FRANÇAIS**

### ***Fonction du facteur de transcription Lyl-1 dans le développement du lignage macrophagique.***

Au cours de l'embryogenèse, il existe un programme conservé d'hématopoïèse dite "CSH-indépendante", car elle précède le développement des cellules souches hématopoïétiques (CSH). Cette production de cellules hématopoïétiques indépendante des CSH, se déroule dans le Sac Vitellin (SV) et est subdivisée en deux vagues. La première vague, dite primitive, produit des progéniteurs monopotents, à l'origine respectivement de cellules érythroïdes, de mégacaryocytes et de macrophages (MΦ), tous qualifiés de primitifs. Les progéniteurs primitifs apparaissent dans le SV à partir du jour embryonnaire (E) E7-7.5, bien avant la formation des CSH, qui apparaissent dans la région aortique à partir de E9.5. Lors de la deuxième vague, le SV produit des progéniteurs multipotents, érythro-myéloïdes (EMp). Les EMp émergent à E8.25-E8.5 et augmentent en nombre dans le SV à E9. Parce que les progéniteurs de ces deux vagues sont mélangés dans la circulation systémique, leur contribution relative à l'hématopoïèse embryonnaire reste mal connue. Lyl-1 est un facteur de transcription de type bHLH est étroitement apparenté à Scl/Tal-1, qui est nécessaire à la spécification de des progéniteurs du SV, ainsi qu'à celle de CSH de la région aortique. En outre, en utilisant la souche Lyl-1<sup>lacZ/LacZ</sup>, chez laquelle le domaine HLH est invalidé et remplacé par le gène rapporteur LacZ, nous avons précédemment montré que le profil d'expression de Lyl-1 pendant l'ontogenèse recouvrait largement celui de Scl/Tal-1, indiquant que Lyl-1 pourrait jouer un rôle durant le développement de l'hématopoïèse embryonnaire.

### ***L'expression de Lyl-1 caractérise les progéniteurs de macrophages primitifs de la première vague du Sac Vitellin.***

Pour étudier cette hypothèse, nous avons d'abord évalué si Lyl-1 jouait un rôle dans le développement des cellules hématopoïétiques du SV. Nous avons soumis des SV de E8 provenant d'embryon Lyl-1<sup>LacZ/LacZ</sup>, Lyl-1<sup>WT/LacZ</sup> et sauvages à des tests

clonogéniques après les avoir maintenus en culture organotypique pendant 1 jour (OrgD1). Dans ce système de culture, le SV est disséqué avant que la circulation du SV ne se connecte à celle de l'embryon proprement dit, ce qui évite une contamination par les premières CSH, permettant ainsi l'analyse spécifique des progéniteurs du SV. De plus, l'étape de culture permet le développement des progéniteurs des deux vagues du SV, ce qui rend ce système de culture adapté pour l'étude initiale de l'effet de l'inactivation d'un gène. Nous avons observé que l'inactivation de *Lyl-1* augmentait significativement la production de progéniteurs MΦ, alors que la production des autres types de progéniteurs, y compris les EMp et les progéniteurs granulo-monocytaires (GM), n'était pas modifiée.

Puis, nous avons testé si l'inactivation de *Lyl-1* affectait de manière similaire la population MΦ dérivée de la différenciation des CSH. À E10-10.5, la région aortique contient des CSH et des progéniteurs du SV qui ont colonisé le compartiment intra-embryonnaire via le flux sanguin, y compris des progéniteurs engagés MΦ, GM et EMp, ainsi que des MΦ matures. Pour évaluer spécifiquement le potentiel de différenciation des CSH vers la lignée MΦ, les cellules de la région aortique d'embryons sauvages, *Lyl-1*<sup>WT/LacZ</sup> et *Lyl-1*<sup>LacZ/LacZ</sup> ont été cultivées sur la lignée stromale OP9 pour engager leur différenciation. Après 4 jours de culture, le nombre et le type de progéniteurs produits ont été caractérisés par des tests clonogéniques. Contrairement à ce qui a été observé pour les SV (E8-OrgD1), la production des progéniteurs MΦ, GM et EMp était similaire pour les trois génotypes. De plus, l'analyse en cytométrie de flux a montré la quantité de MΦ (CD11b+F4/80+) produite était similaire dans les trois génotypes à différents temps de culture. Ces données suggèrent que *Lyl-1* ne régule pas la production de MΦ à partir de CSH intra-embryonnaires, comme c'est le cas au niveau du SV.

Au cours du développement, les MΦ se développent à partir de progéniteurs c-Kit+CD31+CD45- (fraction C) qui acquièrent l'expression de CD11b et CD45 (fraction A1). Puis la différenciation de MΦ est caractérisée d'abord par la baisse

d'expression de c-Kit (fraction A2), puis par celle de CD31, couplée à l'augmentation de l'expression de CX3CR1 et de F4/80 (fraction A3). En raison des effets sur la production de MΦ que nous avons trouvés chez des souris  $Lyl-1^{LacZ/LacZ}$ , j'ai analysé en cytométrie le phénotype et la distribution relative de ces sous-populations dans les SV E8-OrgD1 et E9. J'ai également utilisé le test Facs-Gal, comme rapporteur de l'expression de  $Lyl-1$ : ce test permet la caractérisation en cytométrie des cellules qui possèdent une activité  $\beta$ -Galactosidase ( $\beta$ -Gal), en utilisant son substrat fluorescent, le FDG. J'ai montré que les SV mutants (E8-OrgD1 et E9) comportaient une sous-population CD45-/low dans la population CD11b+CD31+ (progéniteurs A1-A2). Cette sous-population disparaît des SV sauvages à E9 et après E9.5 dans les génotypes mutants. Il est important de noter que cette sous-population transitoire, intermédiaire entre les populations C et A1 s'est avéré être 100%  $Lyl-1$  positive.

J'ai ensuite évalué l'expression de  $Lyl-1$  dans les progéniteurs MΦ à E9, quelques heures avant l'émergence des EMp, en utilisant le test Facs-Gal. J'ai trouvé que l'ensemble des progéniteurs MΦ (CD31+CD45+CD11b) exprimait  $Lyl-1$  à ce stade. Fait intéressant, quelques heures plus tard (E9.5), des progéniteurs MΦ  $Lyl-1$  négatifs apparaissaient dans le SV, suggérant que deux populations distinctes de MΦ peuvent être discriminées par l'expression de  $Lyl-1$ .

Il est bien établi que le SV génère deux vagues de MΦ: la première appelée primitive, provient de progéniteurs MΦ monopotents qui apparaissent à E7.5-E8, en l'absence de progéniteurs en amont, tels que les EMp et les GM. La deuxième vague de MΦ est le produit des EMp qui donnent naissance à des MΦ définitifs. Les MΦ de la première et deuxième vague ne peuvent pas être distingués par leur phénotype. De plus, ils se mélangent rapidement dans le SV, et peu après dans le flux sanguin systémique. Par conséquent, les caractéristiques spécifiques des MΦ primitifs n'ont pas encore été caractérisées en détail. Comme mentionné précédemment, l'inactivation de  $Lyl-1$  affecte uniquement la production des MΦ dans le SV (E8 OrgD1 et E9), et non dans la population dérivée des CSH intra-embryonnaires. De plus, le SV génère deux

vagues de MΦ, de sorte que à E9.5, le SV abrite à la fois les progéniteurs MΦ primitifs de la première vague et les progéniteurs MΦ de la deuxième vague, qui proviennent de la différenciation myéloïde des EMP via un progéniteur GM. Dans la mesure où l'ensemble des progéniteurs MΦ (C-A1-A2) du SV ( $Lyl-1^{WT/LacZ}$ ) exprimait *Lyl-1*, alors que seul une fraction des progéniteurs MΦ l'exprimait à E9.5, nous avons envisagé que les progéniteurs MΦ *Lyl-1* positifs pourraient représenter la population primitive, présente aux stades les plus précoces. Malheureusement, les progéniteurs MΦ des deux vagues de SV ne peuvent pas être discriminés par leur phénotype, de sorte que la seule façon d'évaluer si l'inactivation de *Lyl-1* cible spécifiquement les progéniteurs MΦ primitifs était d'utiliser leur différente cinétique d'apparition, malgré le nombre réduit de progéniteurs présents.

Les premiers progéniteurs EMP et GM apparaissent dans le SV au stade 3-5 Somites (S). Nous avons donc analysé l'activité β-Gal dans les SV  $Lyl-1^{WT/LacZ}$  de E8, au stade 0-5S. A ce stade où le SV contient uniquement des progéniteurs MΦ primitifs, tous les progéniteurs MΦ CD11b+CD31+ exprimaient *Lyl-1*. De plus, en triant les fractions *Lyl-1*/FDG positives et négatives à partir de SV  $Lyl-1^{WT/LacZ}$  à E8 et testant ces deux fractions en tests clonogéniques, nous avons trouvé que la plupart des progéniteurs hématopoïétiques provenaient de la fraction *Lyl-1*/FDG négative. En revanche, la quasi totalité des progéniteurs MΦ étaient systématiquement présents dans la fraction *Lyl-1*/FDG positive. Les tests clonogéniques ont également montré que moins d'un progéniteur GM et EMP par SV étaient détectés au stade 0-5S, tant chez les SV sauvages que mutants, confirmant que le test a été effectué à un moment où il est possible de discriminer les progéniteurs MΦ primitifs de ceux qui dérivent des EMP de la seconde vague du SV. Nous avons également observé systématiquement une augmentation de 2-3 fois du pourcentage (et du nombre absolu par SV) des colonies de MΦ primitifs obtenues à partir de SV  $Lyl-1^{WT/LacZ}$  et  $Lyl-1^{LacZ/LacZ}$ , par rapport au type sauvage.

Pour obtenir des preuves plus solides, j'ai testé le potentiel hématopoïétique des progéniteurs Lyl-1 positifs par rapport à celui des progéniteurs Lyl-1 négatifs à un stade ultérieur. Plus précisément, les progéniteurs c-Kit+CD45+CD11b+ provenant de SV Lyl-1<sup>WT/LacZ</sup> de E10 ont été fractionnés en populations FDG+/Lyl-1+ et FDG-/Lyl-1- et soumis à un test clonogénique. Leur progénie a été comparée à celle provenant de SV sauvages et Lyl-1<sup>WT/LacZ</sup> de E9, un stade où seuls les progéniteurs MΦ primitifs sont présents. J'ai trouvé que les SV de E9 non triés sur le FDG produisaient presque exclusivement des colonies MΦ, alors qu'à E10, le SV générait aussi des colonies GM et granulocytiques. De plus, la majorité des progéniteurs triés FDG+/Lyl-1+ ne donnaient naissance qu'à des colonies MΦ, alors que les progéniteurs FDG-/Lyl-1- produisaient également des colonies GM ou granulocytiques, ce qui caractérise leur type définitif.

Les résultats des trois approches entreprises convergent pour montrer que l'expression de Lyl-1 discrimine les progéniteurs MΦ primitifs et définitifs du SV. De plus, nous trouvons que la fonction Lyl-1 pendant le développement normal semble être de réguler négativement la génération et l'expansion de la lignée des MΦ primitifs, comme le montre la production accrue de la sous-population intermédiaire C à A1, ainsi que celle des progéniteurs MΦ dans les SV Lyl-1<sup>LacZ/LacZ</sup>.

Pour développer davantage les résultats des analyses *in vitro* et celles de cytométrie de flux mentionnées ci-dessus, nous avons débuté les prélèvements destinés à des analyses de RNA-Seq pour (1) déterminer les caractéristiques spécifiques des progéniteurs MΦ primitifs, par comparaison avec les progéniteurs MΦ définitifs des embryons plus âgés; (2) évaluer quel est l'effet de l'inactivation de Lyl-1 sur la population MΦ primitive. Les informations recueillies à partir de ce test RNA-Seq pourraient fournir des informations longtemps recherchées sur la population primitive, et pourraient apporter un éclairage nouveau sur la régulation des propriétés des progéniteurs hématopoïétiques embryonnaires.

***Les progéniteurs MΦ primitifs exprimant Lyl-1 donnent naissance à la microglie embryonnaire.***

Les MΦ issus des progéniteurs primitifs exprimant Lyl-1 pourraient contribuer à diverses populations de MΦ de l'embryon en développement. J'ai donc analysé la contribution des progéniteurs MΦ Lyl-1 positifs au compartiment des MΦ matures, en mettant l'accent sur le SV et le foie fœtal (FF) de E10.5, ainsi que sur le cerveau en développement.

La contribution relative des progéniteurs des deux vagues du SV aux premières étapes du développement du FF est encore mal caractérisée. En utilisant le test Facs-Gal, j'ai montré que le FF à E10.5 contenait deux types de progéniteurs MΦ discriminés par l'expression Lyl-1, confirmant que les populations primitive et définitive colonisent également le FF au début du développement embryonnaire.

Il a été récemment établi grâce à des expériences de "fate mapping" que la microglie (MΦ du système nerveux central) provenait exclusivement de progéniteurs MΦ produits par le SV. Cependant, comme indiqué ci-dessus, les lignées de MΦ primitifs et les MΦ dérivés des EMp coexistent dans le SV de sorte que leurs contributions respectives à la microglie est naturellement l'objet de questionnements : puisque les progéniteurs MΦ primitifs et ceux issus des EMp partagent le même phénotype et sont tous deux présents dans le SV aux stades où les expériences de "fate mapping" ont été réalisées, la contribution respective des progéniteurs MΦ primitifs et de ceux dérivant des EMp au développement de la microglie reste incertaine. En utilisant le test Facs-Gal, j'ai trouvé que, alors que le SV de E10.5 comprenait les deux populations de progéniteurs MΦ FDG/Lyl-1 positive et négative, le cerveau des mêmes embryons abritait des progéniteurs MΦ FDG+/Lyl-1+. De même, les MΦ matures (F4/80+) du SV de E10.5 contiennent les deux populations (FDG+/Lyl-1+ et FDG-/Lyl-1-), tandis que dans le cerveau à E10.5, les MΦ matures sont exclusivement FDG+/Lyl-1+. Ces données suggèrent fortement que la source initiale

des progéniteurs MΦ responsables du développement de la microglie est la population primitive exprimant Lyl-1.

L'hématopoïèse primitive est conservée dans des embryons dépourvus de l'expression de c-Myb et la vague primitive est considérée comme indépendante de c-Myb pour son développement. De plus, il a été démontré que l'expression de c-Myb n'est pas nécessaire au développement de la microglie. Ainsi, pour renforcer notre conclusion sur l'origine primitive de la microglie, j'ai effectué des analyses en qRT-PCR pour détecter s'il y avait une différence dans l'expression du transcrite c-Myb entre la population de progéniteurs Lyl-1 positifs et négatifs (E10.5). Les résultats ont montré que les progéniteurs myéloïdes FDG-/Lyl-1- du SV présentent un taux de c-Myb similaire à celui des progéniteurs définitifs du foie fœtal, qui dépendent de c-Myb pour leur développement. En revanche, les progéniteurs MΦ FDG+/Lyl-1+ du SV et du cerveau présentent des taux de c-Myb extrêmement bas, similaires à celui des progéniteurs MΦ primitifs du SV de E9, renforçant ainsi leur statut primitif et la relation de lignage entre les progéniteurs MΦ FDG+/Lyl-1+ et la microglie.

***L'inactivation de Lyl-1 altère la maturation des MΦ aux stades embryonnaires précoces.***

Pour obtenir de plus amples informations sur la fonction Lyl-1 pendant le développement des MΦ, j'ai utilisé des souris Cx3cr1<sup>WT/GFP</sup>, chez lesquelles l'expression la GFP corrèle avec celle du récepteur de la fractalkine CX3CR1, qui est le marqueur microglial de référence. J'ai d'abord utilisé ces souris pour trier les fractions A1, A2 et A3 à partir de SV et de cerveaux de E10.5 et j'ai analysé les niveaux de transcrits de Lyl-1 pendant la différenciation MΦ. J'ai trouvé que les niveaux d'ARNm de Lyl-1 étaient similaires dans le SV et le cerveau pour chacune des fractions. L'expression de Lyl-1 est maintenue tout au long de la différenciation avec une diminution des progéniteurs A1 aux MΦ matures A3, ce qui implique une exigence différente envers Lyl-1 pendant la maturation.

J'ai également construit une souche de souris double mutante  $Cx3cr1^{GFP}:Lyl-1^{LacZ}$  pour analyser finement l'influence de l'inactivation de *Lyl-1* au cours de la différenciation MΦ. J'avais initialement observé que la taille de l'ensemble de la population MΦ était similaire dans les trois génotypes. Mais, en utilisant les nouveaux génotypes développés ( $Cx3cr1^{GFP/WT}:Lyl-1^{WT/WT}$ ,  $Cx3cr1^{GFP/WT}:Lyl-1^{LacZ/WT}$  et  $Cx3cr1^{GFP/WT}:Lyl-1^{LacZ/LacZ}$ ), j'ai d'abord observé une distribution inverse des fractions A1, A2 et A3 dans le SV et le cerveau des embryons normaux, le SV contenant principalement des progéniteurs A1 et A2, alors que le cerveau contient principalement des MΦ matures. Ceci suggère que le cerveau précoce est un environnement favorable à une maturation rapide des MΦ. De plus, ces analyses ont révélé que, comparativement aux souris  $Cx3cr1^{GFP/WT}:Lyl-1^{WT/WT}$ , le SV et le cerveau des souris mutantes  $Cx3cr1^{GFP/WT}:Lyl-1^{LacZ/LacZ}$  contenaient un excès de progéniteurs A1 et un déficit marqué en MΦ matures. Ainsi, ces données suggèrent que l'inactivation de *Lyl-1* perturbe la maturation des MΦ et de la microglie.

#### ***Lyl-1 contrôle le pool de microglies embryonnaires à deux stades de développement.***

Des données antérieures ont montrées que le compartiment de la microglie était établi autour de E11.5 et maintenu par prolifération locale sans apport ultérieurs de monocytes circulants, du moins en conditions normales. Donc, pour détecter si l'expression de *Lyl-1* était maintenue pendant le développement de la microglie, j'ai mesuré les niveaux d'ARNm de *Lyl-1* dans la microglie triée à partir des souris sauvages et mutantes ( $Lyl-1^{LacZ/LacZ}$ ) à différents stades de développement embryonnaire (E12, 14, 16), postnataux (P) (P0, P15) et chez l'adulte (P42). J'ai également mesuré l'activité bGal à ces stades par le test Facs-Gal. Dans la microglie sauvage, le niveau d'expression de *Lyl-1* (transcrits) augmente en fin de développement embryonnaire et est fortement enrichi aux stades P15 et P42. L'expression de *Lyl-1* (activité bGal) est également maintenue dans la microglie tout au long du développement embryonnaire chez les souris mutantes  $Lyl-1^{LacZ/LacZ}$ .

Cependant, cette activité bGal diminue significativement à P15 et est à peine détectée à P42 dans la microglie mutante.

Pour évaluer l'effet de Lyl-1 sur le développement de la microglie, j'ai ensuite étudié sa cinétique de croissance chez les souris sauvages, Lyl-1<sup>WT/LacZ</sup> et Lyl-1<sup>LacZ/LacZ</sup> de E9.5 à E14.5. Pour cela, le nombre de cellules microgliales par cerveau a été estimé en rapportant au nombre total de cellules cérébrales le pourcentage de cellules microgliales déterminé par l'analyse en cytométrie. J'ai observé une cinétique de croissance microgliale similaire pour les souris sauvages et Lyl-1<sup>WT/LacZ</sup>. En revanche, dans le cerveau des souris Lyl-1<sup>LacZ/LacZ</sup>, on observe initialement (E10.5-11.5) un excès de progéniteurs microgliaux (CD31+CD45+CD11b+), mais ces progéniteurs diminuent rapidement pour atteindre de même niveau que chez les embryons sauvages à E14.5. En termes de microglie mature, j'ai trouvé une réduction significative de la microglie F4/80+ dans le cerveau des souris Lyl-1<sup>LacZ/LacZ</sup> à E12, alors que la quantité de microglie n'était pas été modifiée avant ce stade, suggérant que l'inactivation de Lyl-1 affecte la prolifération de la microglie, mais pas la colonisation du cerveau. Bien que la microglie soient encore réduite chez les mutants à E14, le pool de population semble se rétablir de lui-même. En utilisant une méthode similaire, j'ai trouvé que la taille du contingent microglial était de nouveau réduite chez les mutants à P0-3. Ce deuxième épisode déficitaire est transitoire, comme celui qui a lieu à E12, puisque la taille du contingent microglial à P42 est de nouveau normale.

Pour mieux comprendre le mécanisme de régulation de Lyl-1 dans le développement de la microglie, j'ai ensuite évalué la survie et l'expansion de la microglie dans les cerveaux sauvages et mutants à ces deux stades. L'analyse de l'incorporation de l'analogue de la thymidine BrdU dans la microglie à E12 a montré une incorporation plus importante dans la microglie sauvage que dans celle des mutants, indiquant une réduction du taux de prolifération de la microglie mutante. En outre, l'analyse de la liaison d'AnnexinV à la microglie a montré une fréquence similaire d'apoptose dans la

microglie sauvage et mutante à E12 et P0-3. Fait intéressant, la fréquence des cellules apoptotiques était beaucoup plus faible à E14 chez les mutants  $Lyl-1^{LacZ/LacZ}$ . Cette donnée pourrait être mise en relation avec la récupération progressive du contingent microglial chez les mutants après E12.

Des données combinant des stratégies de déplétion génétique et d'analyse transcriptomique ont montrées que la microgliogenèse était étroitement régulée au cours du développement. La différenciation et la prolifération de la microglie dépendent de l'expression du récepteur CSF-1R, qui joue ses rôles à travers deux ligands, CSF-1 et IL-34. Le développement de la microglie dépend également des facteurs Pu.1 et Irf8, etc. Pour mieux définir la fonction  $Lyl-1$  durant le développement de la microglie, j'ai effectué des analyses en qRT-PCR sur la microglie aux stades embryonnaires (E12, E14, E16), postnataux (P0-3, P15) et chez l'adulte (P42). J'ai quantifié les transcrits de gènes connus pour être impliqués dans le développement et la différenciation des M $\Phi$  et de la microglie (Cx3cr1, Irf8, Csf1-r, Mafk, Runx1, Pu.1), ainsi que les régulateurs du développement hématopoïétique (Scl/Tal-1, Lmo2) et facteurs associés (Tcf3/E2A, Tcf4/E2.2). L'analyse des gènes régulés différemment dans la microglie déficientes en  $Lyl-1$  et sauvage a montré la diminution chez le mutant  $Lyl-1^{LacZ/LacZ}$  de plusieurs gènes importants dans le développement de la microglie à des stades spécifiques, : Cx3cr1 à E12, lmo2, Csf1-r et Irf8 à la fois à E12 et à P0. J'ai aussi trouvé que le niveau d'expression de Mafk, qui contrôle l'auto-renouvellement de la microglie chez l'adulte, était significativement diminué dans la microglie mutante autour de la naissance. Une explication possible est que le microenvironnement conduit à l'activation de l'auto-renouvellement de la microglie à travers la régulation négative de Mafk pour compenser les défauts de la microglie à ce stade. De façon intéressante, les diminutions d'expression géniques observées dans ces analyses en qRT-PCR se produisent aux stades identifiés comme impactés par la délétion de  $Lyl-1$  dans notre analyse cinétique.

## ***La microglie déficiente des mutants *Lyl-1* induit des troubles d'anxiété sociale chez l'adulte***

La microglie joue un rôle clé dans le développement du cerveau, dans le maintien de l'homéostasie et des fonctions cérébrales. Au cours du développement, elle a une fonction de surveillance, piège les cellules mortes et les agents pathogènes et façonne le réseau synaptique par un processus d'élagage. Aussi, une altération des fonctions microgliales est considérée comme impliquée dans de nombreuses maladies du neuro-développement telles que l'autisme, la schizophrénie ou les troubles obsessionnels compulsifs. Par exemple, l'inactivation du récepteur de chimiokine *Cx3cr1* chez la souris conduit à une réduction transitoire de la microglie dans la période postnatale précoce et à une perturbation de l'élagage synaptique médiée par la microglie, entraînant une détérioration de la connectivité cérébrale fonctionnelle et une altération du comportement social. Considérant que la microglie joue des rôles clés dans la neurogenèse, nous avons voulu savoir si l'inactivation de *Lyl-1* dans la microglie pouvait altérer les processus neuro-développementaux.

La microglie produit et sécrète des cytokines, interleukines, des facteurs de croissance, etc., qui sont impliqués dans la communication cellulaire, régulent l'inflammation et les réponses immunitaires, la croissance cellulaire, la survie et la différenciation. J'ai analysé les niveaux de transcription de trois gènes importants dans ces processus (*IL-1 $\beta$* , *IL-6* et *TNF- $\alpha$* ) dans la microglie de souris sauvage et *Lyl-1<sup>LacZ/LacZ</sup>* à P0 et P15. Les résultats de qRT-PCR ont montré que les niveaux d'expression génique de ces trois gènes étaient beaucoup plus faibles chez les mutants à P15, suggérant que les fonctions liées à l'inflammation sont altérées chez le mutant.

Nous avons également établi une collaboration avec le groupe de Marco Prinz à l'Université de Fribourg en Allemagne pour mieux comprendre les conséquences de l'inactivation de *Lyl-1* chez la souris adulte. Mon rôle dans cette collaboration était de préparer les échantillons de tissus pour les analyses effectuées dans ce groupe. Les

résultats de comptage du nombre de cellules de microgliales iba+ sur des tranches de cerveau ont corrélé avec notre quantification par cytométrie de flux pour montrer un nombre réduit de cellules microgliales chez le nouveau-né, mais pas chez les mutants à E14.5 et chez l'adulte. De plus, nos collaborateurs ont démontré que la microglie néonatale était dysmorphique. Leur découverte majeure provient d'analyses comportementales de mutants adultes qui ont mis en évidence une altération du comportement social. L'implication Lyl-1 dans le développement de désordre du spectre de l'autisme a été confirmée par des expériences d'imagerie de résonance magnétique fonctionnelle, montrant que les souris  $Lyl-1^{LacZ/LacZ}$  présentent une hyperactivité dans des zones du cerveau impliquées dans l'anxiété sociale.

### ***Implication possible des défauts de Lyl-1 dans d'autres maladies neurologiques***

Nous avons recueilli des informations bibliographiques et des bases de données pour évaluer si LYL-1 régulait également la microglie humaine dans des conditions normales et pathologiques. Les informations obtenues ont confirmé l'expression de LYL-1 dans la microglie humaine, mais n'ont pas jusqu'à présent fourni d'indications claires sur son implication dans les troubles du syndrome autistique, ainsi que dans la maladie d'Alzheimer. Elles convergent cependant pour impliquer LYL-1 dans le contrôle des processus neuro-inflammatoires.

## **5 REFERENCES**

- Adolfsson, J., Mansson, R., Buza-Vidas, N., Hultquist, A., Liuba, K., Jensen, C.T., Bryder, D., Yang, L., Borge, O.J., Thoren, L.A., *et al.* (2005). Identification of Flt3+ lympho-myeloid stem cells lacking erythro-megakaryocytic potential a revised road map for adult blood lineage commitment. *Cell* *121*, 295-306.
- Aguzzi, A., Barres, B.A., and Bennett, M.L. (2013). Microglia: scapegoat, saboteur, or something else? *Science* *339*, 156-161.
- Ajami, B., Bennett, J.L., Krieger, C., Tetzlaff, W., and Rossi, F.M. (2007). Local self-renewal can sustain CNS microglia maintenance and function throughout adult life. *Nat Neurosci* *10*, 1538-1543.
- Akashi, K., Traver, D., and Miyamoto, T. (2000). A clonogenic common myeloid progenitor that gives rise to all myeloid lineages. *Nature* *404*, 193-197.
- Akashi, K., Traver, D., and Zon, L.I. (2005). The complex cartography of stem cell commitment. *Cell* *121*, 160-162.
- Alliot, F., Godin, I., Pessac, B., (1999). Microglia derive from progenitors, originating from the yolk sac, and which proliferate in the brain. *Brain Research Development: Brain Research* *117*, 145-152.
- Antony, J. M., Paquin, A., Nutt, S. L., Kaplan, D. R., and Miller, F. D. (2011). Endogenous microglia regulate development of embryonic cortical precursor cells. *J Neurosci Res* *89*, 286-298.
- Arno, B., Grassivaro, F., Rossi, C., Bergamaschi, A., Castiglioni, V., Furlan, R., Greter, M., Favaro, R., Comi, G., Becher, B., *et al.* (2014). Neural progenitor cells orchestrate microglia migration and positioning into the developing cortex. *Nat Commun* *5*, 5611.
- Askew, K., Li, K., Olmos-Alonso, A., Garcia-Moreno, F., Liang, Y., Richardson, P., Tipton, T., Chapman, M.A., Riecken, K., Beccari, S., *et al.* (2017). Coupled Proliferation and Apoptosis Maintain the Rapid Turnover of Microglia in the Adult Brain. *Cell Rep* *18*, 391-405.
- Bain, C.C., Hawley, C.A., Garner, H., Scott, C.L., Schridde, A., Steers, N.J., Mack, M., Joshi, A., Guilliams, M., Mowat, A.M., *et al.* (2016). Long-lived self-renewing bone marrow-derived macrophages displace embryo-derived cells to inhabit adult serous cavities. *Nat Commun* *7*, ncomms11852.
- Baron, M.H., Isern, J., and Fraser, S.T. (2012). The embryonic origins of erythropoiesis in mammals. *Blood* *119*, 4828-4837.
- Baron, M.H., Vacaru, A., and Nieves, J. (2013). Erythroid development in the mammalian embryo. *Blood Cells Mol Dis* *51*, 213-219.
- Beaupain, D., Martin, C. and Dieterlen-Lièvre, F. (1979). Are developmental hemoglobin changes related to the origin of stem cells and site of erythropoiesis? *Blood* *53*, 212-225.
- Bennett, M.L., Bennett, F.C., Liddelow, S.A., Ajami, B., Zamanian, J.L., Fernhoff, N.B., Mulinyawe, S.B., Bohlen, C.J., Adil, A., Tucker, A., *et al.* (2016). New tools for studying microglia in the mouse and human CNS. *Proc Natl Acad Sci U S A* *113*, E1738-1746.

- Bertrand, J.Y., Chi, N.C., Santoso, B., Teng, S., Stainier, D.Y., and Traver, D. (2010). Haematopoietic stem cells derive directly from aortic endothelium during development. *Nature* *464*, 108-111.
- Bertrand, J.Y., Giroux, S., Golub, R., Klaine, M., Jalil, A., Boucontet, L., Godin, I., and Cumano, A. (2005a). Characterization of purified intraembryonic hematopoietic stem cells as a tool to define their site of origin. *Proc Natl Acad Sci U S A* *102*, 134-139.
- Bertrand, J.Y., Jalil, A., Klaine, M., Jung, S., Cumano, A., and Godin, I. (2005b). Three pathways to mature macrophages in the early mouse yolk sac. *Blood* *106*, 3004-3011.
- Bertrand, J.Y., and Traver, D. (2009) Hematopoietic cell development in the zebrafish embryo. *Curr Opin Hematol* *16*, 243-248.
- Boiers, C., Carrelha, J., Lutteropp, M., Luc, S., Green, J.C., Azzoni, E., Woll, P.S., Mead, A.J., Hultquist, A., Swiers, G., *et al.* (2013). Lymphomyeloid contribution of an immune-restricted progenitor emerging prior to definitive hematopoietic stem cells. *Cell Stem Cell* *13*, 535-548.
- Boisset, J.C., van Cappellen, W., Andrieu-Soler, C., Galjart, N., Dzierzak, E., and Robin, C. (2010). In vivo imaging of haematopoietic cells emerging from the mouse aortic endothelium. *Nature* *464*, 116-120.
- Boyer, S.W., Beaudin, A.E., and Forsberg, E.C. (2012). Mapping differentiation pathways from hematopoietic stem cells using Flk2/Flt3 lineage tracing. *Cell Cycle* *11*, 3180-3188.
- Boyer, S.W., Schroeder, A.V., Smith-Berdan, S., and Forsberg, E.C. (2011). All hematopoietic cells develop from hematopoietic stem cells through Flk2/Flt3-positive progenitor cells. *Cell Stem Cell* *9*, 64-73.
- Bruttger, J., Karram, K., Wortge, S., Regen, T., Marini, F., Hoppmann, N., Klein, M., Blank, T., Yona, S., Wolf, Y., *et al.* (2015). Genetic Cell Ablation Reveals Clusters of Local Self-Renewing Microglia in the Mammalian Central Nervous System. *Immunity* *43*, 92-106.
- Buttgereit, A., Lelios, I., Yu, X., Vrohings, M., Krakoski, N.R., Gautier, E.L., Nishinakamura, R., Becher, B., and Greter, M. (2016). Sall1 is a transcriptional regulator defining microglia identity and function. *Nat Immunol* *17*, 1397-1406.
- Capron, C., Lacout, C., Lecluse, Y., Wagner-Ballon, O., Kaushik, A.L., Cramer-Borde, E., Sablitzky, F., Dumenil, D., and Vainchenker, W. (2011). LYL-1 deficiency induces a stress erythropoiesis. *Exp Hematol* *39*, 629-642.
- Capron, C., Lecluse, Y., Kaushik, A.L., Foudi, A., Lacout, C., Sekkai, D., Godin, I., Albagli, O., Poullion, I., Svinartchouk, F., *et al.* (2006). The SCL relative LYL-1 is required for fetal and adult hematopoietic stem cell function and B-cell differentiation. *Blood* *107*, 4678-4686.
- Casano, A. M., Albert, M., and Peri, F. (2016). Developmental apoptosis mediates entry and positioning of microglia in the zebrafish brain. *Cell Rep* *16*, 897-906.
- Chan, W.Y., Follows, G.A., Lacaud, G., Pimanda, J.E., Landry, J.R., Kinston, S., Knezevic, K., Piltz, S., Donaldson, I.J., Gambardella, L., *et al.* (2007). The paralogous

hematopoietic regulators *Lyl1* and *Scl* are coregulated by *Ets* and *GATA* factors, but *Lyl1* cannot rescue the early *Scl*/phenotype. *Blood* 109, 1908-1916.

Chen, M.J., Li, Y., De Obaldia, M.E., Yang, Q., Yzaguirre, A.D., Yamada-Inagawa, T., Vink, C.S., Bhandoola, A., Dzierzak, E., and Speck, N.A. (2011). Erythroid/myeloid progenitors and hematopoietic stem cells originate from distinct populations of endothelial cells. *Cell Stem Cell* 9, 541-552.

Chitu, V., and Stanley, E.R. (2006). Colony-stimulating factor-1 in immunity and inflammation. *Curr Opin Immunol* 18, 39-48.

Christensen, J.L., and Weissman, I.L. (2001). *Flk-2* is a marker in hematopoietic stem cell differentiation: a simple method to isolate long-term stem cells. *Proc Natl Acad Sci U S A* 98, 14541-14546.

Clements, W.K., and Traver, D. (2013). Signalling pathways that control vertebrate haematopoietic stem cell specification. *Nat Rev Immunol* 13, 336-348.

Colonna, M., and Butovsky, O. (2017). Microglia Function in the Central Nervous System During Health and Neurodegeneration. *Annu Rev Immunol* 35, 441-468.

Cordeiro Gomes, A., Hara, T., Lim, V.Y., Herndler-Brandstetter, D., Nevius, E., Sugiyama, T., Tani-Ichi, S., Schlenner, S., Richie, E., Rodewald, H.R., *et al.* (2016). Hematopoietic Stem Cell Niches Produce Lineage-Instructive Signals to Control Multipotent Progenitor Differentiation. *Immunity* 45, 1219-1231.

Costa, G., Kouskoff, V., and Lacaud, G. (2012). Origin of blood cells and HSC production in the embryo. *Trends Immunol* 33, 215-223.

Coull, J.A., Beggs, S., Boudreau, D., Boivin, D., Tsuda, M., Inoue, K., Gravel, C., Salter, M.W., and De Koninck, Y. (2005). BDNF from microglia causes the shift in neuronal anion gradient underlying neuropathic pain. *Nature* 438, 1017-1021.

Cumano, A., Dieterlen-Lièvre, F., and Godin, I. (1996). Lymphoid potential, probed before circulation in mouse, is restricted to caudal intraembryonic splanchnopleura. *Cell* 86, 907-916.

Cumano, A., Ferraz, J.C., Klaine, M., Di Santo, J.P., and Godin, I. (2001). Intraembryonic, but not yolk sac hematopoietic precursors, isolated before circulation, provide long-term multilineage reconstitution. *Immunity* 15, 477-485.

Cumano, A., and Godin, I. (2007). Ontogeny of the hematopoietic system. *Annu Rev Immunol* 25, 745-785.

Curtis, D.J., Salmon, J.M., and Pimanda, J.E. (2012). Concise review: Blood relatives: formation and regulation of hematopoietic stem cells by the basic helix-loop-helix transcription factors stem cell leukemia and lymphoblastic leukemia-derived sequence 1. *Stem Cells* 30, 1053-1058.

Davies, L.C., Jenkins, S.J., Allen, J.E., and Taylor, P.R. (2013). Tissue-resident macrophages. *Nat Immunol* 14, 986-995.

de Bruijn, M.F., Speck, N.A., Peeters, M.C., and Dzierzak, E. (2000). Definitive hematopoietic stem cells first develop within the major arterial regions of the mouse embryo. *EMBO J* 19, 2465-2474.

Delassus, S., and Cumano, A. (1996). Circulation of hematopoietic progenitors in the mouse embryo. *Immunity* 4, 97-106.

Derecki, N.C., Cronk, J.C., Lu, Z., Xu, E., Abbott, S.B., Guyenet, P.G., and Kipnis, J. (2012). Wild-type microglia arrest pathology in a mouse model of Rett syndrome. *Nature* 484, 105-109.

Dieterlen-Lièvre, F. (1975). On the origin of haemopoietic stem cells in the avian embryo: an experimental approach. *J Embryol Exp Morphol* 33, 607-619.

Doerks, T., Copley, R.R., Schultz, J., Ponting, C.P., and Bork, P. (2002). Systematic identification of novel protein domain families associated with nuclear functions. *Genome Res* 12, 47-56.

Dykstra, B., Kent, D., Bowie, M., McCaffrey, L., Hamilton, M., Lyons, K., Lee, S.J., Brinkman, R., and Eaves, C. (2007). Long-term propagation of distinct hematopoietic differentiation programs in vivo. *Cell Stem Cell* 1, 218-229.

Ema, H., Sudo, K., Seita, J., Matsubara, A., Morita, Y., Osawa, M., Takatsu, K., Takaki, S., and Nakauchi, H. (2005). Quantification of self-renewal capacity in single hematopoietic stem cells from normal and Lnk-deficient mice. *Dev Cell* 8, 907-914.

Ensan, S., Li, A., Besla, R., Degousee, N., Cosme, J., Roufaiel, M., Shikatani, E.A., El-Maklizi, M., Williams, J.W., Robins, L., *et al.* (2016). Self-renewing resident arterial macrophages arise from embryonic CX3CR1(+) precursors and circulating monocytes immediately after birth. *Nat Immunol* 17, 159-168.

Epelman, S., Lavine, K.J., Beaudin, A.E., Sojka, D.K., Carrero, J.A., Calderon, B., Brija, T., Gautier, E.L., Ivanov, S., Satpathy, A.T., *et al.* (2014). Embryonic and adult-derived resident cardiac macrophages are maintained through distinct mechanisms at steady state and during inflammation. *Immunity* 40, 91-104.

Ferkowicz, M.J. (2003). CD41 expression defines the onset of primitive and definitive hematopoiesis in the murine embryo. *Development* 130, 4393-4403.

Frade, J.M., and Barde, Y.A. (1998). Microglia-derived nerve growth factor causes cell death in the developing retina. *Neuron* 20, 35-41.

Frame, J.M., Fegan, K.H., Conway, S.J., McGrath, K.E., and Palis, J. (2016). Definitive Hematopoiesis in the Yolk Sac Emerges from Wnt-Responsive Hemogenic Endothelium Independently of Circulation and Arterial Identity. *Stem Cells* 34, 431-444.

Frame, J.M., McGrath, K.E., and Palis, J. (2013). Erythro-myeloid progenitors: "definitive" hematopoiesis in the conceptus prior to the emergence of hematopoietic stem cells. *Blood Cells Mol Dis* 51, 220-225.

Gautier, E.L., Shay, T., Miller, J., Greter, M., Jakubzick, C., Ivanov, S., Helft, J., Chow, A., Elpek, K.G., Gordonov, S., *et al.* (2012). Gene-expression profiles and transcriptional regulatory pathways that underlie the identity and diversity of mouse tissue macrophages. *Nat Immunol* 13, 1118-1128.

Geissmann, F., Manz, M.G., Jung, S., Sieweke, M.H., Merad, M., and Ley, K. (2010). Development of monocytes, macrophages, and dendritic cells. *Science* 327, 656-661.

Gekas, C., Dieterlen-Lievre, F., Orkin, S.H., and Mikkola, H.K. (2005). The placenta is a niche for hematopoietic stem cells. *Dev Cell* 8, 365-375.

Gibbings, S.L., Thomas, S.M., Atif, S.M., McCubbrey, A.L., Desch, A.N., Danhorn, T., Leach, S.M., Bratton, D.L., Henson, P.M., Janssen, W.J., *et al.* (2017). Three

Unique Interstitial Macrophages in the Murine Lung at Steady State. *Am J Respir Cell Mol Biol* 57, 66-76.

Ginhoux, F., Greter, M., Leboeuf, M., Nandi, S., See, P., Gokhan, S., Mehler, M.F., Conway, S.J., Ng, L.G., Stanley, E.R., *et al.* (2010). Fate mapping analysis reveals that adult microglia derive from primitive macrophages. *Science* 330, 841-845.

Ginhoux, F., and Williams, M. (2016). Tissue-Resident Macrophage Ontogeny and Homeostasis. *Immunity* 44, 439-449.

Giroux, S., Kaushik, A.L., Capron, C., Jalil, A., Kelaidi, C., Sablitzky, F., Dumenil, D., Albagli, O., and Godin, I. (2007). *lxl-1* and *tal-1/scl*, two genes encoding closely related bHLH transcription factors, display highly overlapping expression patterns during cardiovascular and hematopoietic ontogeny. *Gene Expr Patterns* 7, 215-226.

Godin, I., and Cumano, A. (2002). The hare and the tortoise: an embryonic haematopoietic race. *Nat Rev Immunol* 2, 593-604.

Godin, I., Dieterlen-Lièvre, F., and Cumano, A. (1995). Emergence of multipotent hemopoietic cells in the yolk sac and paraaortic splanchnopleura in mouse embryos, beginning at 8.5 days postcoitus. *Proc Natl Acad Sci USA* 92, 773-777.

Godin, I., Garcia-Porrero, J.A., Dieterlen-Lièvre, F., and Cumano, A. (1999). Stem cell emergence and hemopoietic activity are incompatible in mouse intraembryonic sites. *J Exp Med* 190, 43-52.

Goldmann, T., Wieghofer, P., Jordao, M.J., Prutek, F., Hagemeyer, N., Frenzel, K., Amann, L., Staszewski, O., Kierdorf, K., Krueger, M., *et al.* (2016). Origin, fate and dynamics of macrophages at central nervous system interfaces. *Nat Immunol* 17, 797-805.

Gomez Perdiguero, E., and Geissmann, F. (2013). Myb-independent macrophages: a family of cells that develops with their tissue of residence and is involved in its homeostasis. *Cold Spring Harb Symp Quant Biol* 78, 91-100.

Gomez Perdiguero, E., Klapproth, K., Schulz, C., Busch, K., Azzoni, E., Crozet, L., Garner, H., Trouillet, C., de Bruijn, M.F., Geissmann, F., *et al.* (2015). Tissue-resident macrophages originate from yolk-sac-derived erythro-myeloid progenitors. *Nature* 518, 547-551.

Gosselin, D., Link, V.M., Romanoski, C.E., Fonseca, G.J., Eichenfield, D.Z., Spann, N.J., Stender, J.D., Chun, H.B., Garner, H., Geissmann, F., *et al.* (2014). Environment drives selection and function of enhancers controlling tissue-specific macrophage identities. *Cell* 159, 1327-1340.

Greer, J.M., and Capecchi, M.R. (2002). *Hoxb8* is required for normal grooming behavior in mice. *Neuron* 33, 23-34.

Haar, J.L., and Ackerman, G.A. (1971) Ultrastructural changes in mouse yolk sac associated with the initiation of vitelline circulation. *Anat Rec* 170, 437-455.

Hashimoto, D., Chow, A., Noizat, C., Teo, P., Beasley, M.B., Leboeuf, M., Becker, C.D., See, P., Price, J., Lucas, D., *et al.* (2013). Tissue-resident macrophages self-maintain locally throughout adult life with minimal contribution from circulating monocytes. *Immunity* 38, 792-804.

Herbomel, P., Thisse, B., and Thisse, C. (1999). Ontogeny and behaviour of early macrophages in the zebrafish embryo. *Development* 126, 3735-3745.

- Herbomel, P., Thisse, B., and Thisse, C. (2001). Zebrafish early macrophages colonize cephalic mesenchyme and developing brain, retina, and epidermis through a M-CSF receptor-dependent invasive process. *Dev Biol* 238, 274-288.
- Hirschi, K.K. (2012). Hemogenic endothelium during development and beyond. *Blood* 119, 4823-4827.
- Hock, H. (2010). Some hematopoietic stem cells are more equal than others. *J Exp Med* 207, 1127-1130.
- Hock, H., and Orkin, S.H. (2005). Stem cells: the road not taken. *Nature* 435, 573-575.
- Hoeffel, G., Chen, J., Lavin, Y., Low, D., Almeida, F.F., See, P., Beaudin, A.E., Lum, J., Low, I., Forsberg, E.C., *et al.* (2015). C-Myb(+) erythro-myeloid progenitor-derived fetal monocytes give rise to adult tissue-resident macrophages. *Immunity* 42, 665-678.
- Hoeffel, G., and Ginhoux, F. (2015). Ontogeny of Tissue-Resident Macrophages. *Front Immunol* 6, 486.
- Hoeffel, G., Wang, Y., Greter, M., See, P., Teo, P., Malleret, B., Leboeuf, M., Low, D., Oller, G., Almeida, F., *et al.* (2012). Adult Langerhans cells derive predominantly from embryonic fetal liver monocytes with a minor contribution of yolk sac-derived macrophages. *J Exp Med* 209, 1167-1181.
- Hofer, T., Busch, K., Klapproth, K., and Rodewald, H.R. (2016). Fate Mapping and Quantitation of Hematopoiesis In Vivo. *Annu Rev Immunol* 34, 449-478.
- Hristova, M., Cuthill, D., Zbarsky, V., Acosta-Saltos, A., Wallace, A., Blight, K., Buckley, S.M., Peebles, D., Heuer, H., Waddington, S.N., *et al.* (2010). Activation and deactivation of periventricular white matter phagocytes during postnatal mouse development. *Glia* 58, 11-28.
- Imperato, M.R., Cauchy, P., Obier, N., and Bonifer, C. (2015). The RUNX1-PU.1 axis in the control of hematopoiesis. *Int J Hematol* 101, 319-329.
- Inman, K.E., and Downs, K.M. (2007). The murine allantois: emerging paradigms in development of the mammalian umbilical cord and its relation to the fetus. *Genesis* 45, 237-258.
- Ivanova, N.B., Dimos, J.T., Schaniel, C., Hackney, J.A., Moore, K.A., and Lemischka, I.R. (2002). A stem cell molecular signature. *Science* 298, 601-604.
- Ivanovs, A., Rybtsov, S., Anderson, R.A., Turner, M.L., and Medvinsky, A. (2014). Identification of the niche and phenotype of the first human hematopoietic stem cells. *Stem Cell Reports* 2, 449-456.
- Jaffredo, T., Gautier, R., Eichmann, A., and Dieterlen-Lièvre, F. (1998). Intraaortic hemopoietic cells are derived from endothelial cells during ontogeny. *Development* 125, 4575-4583.
- Jones, M., Chase, J., Brinkmeier, M., Xu, J., Weinberg, D.N., Schira, J., Friedman, A., Malek, S., Grembecka, J., Cierpicki, T., *et al.* (2015). Ash1l controls quiescence and self-renewal potential in hematopoietic stem cells. *J Clin Invest* 125, 2007-2020.
- Jones, S. (2004). An overview of the basic helix-loop-helix proteins. *Genome Biol* 5, 226.

- Jung, S., Aliberti, J., Graemmel, P., Sunshine, M., Kreutzberg, G., Sher, A., and Littman, D (2000). Analysis of fractalkine receptor CX(3)CR1 function by targeted deletion and green fluorescent protein reporter gene insertion. *Mol Cell Biol* *20*, 4106-4114.
- Kiel, M.J., Yilmaz, O.H., Iwashita, T., Yilmaz, O.H., Terhorst, C., and Morrison, S.J. (2005). SLAM family receptors distinguish hematopoietic stem and progenitor cells and reveal endothelial niches for stem cells. *Cell* *121*, 1109-1121.
- Kierdorf, K., Erny, D., Goldmann, T., Sander, V., Schulz, C., Perdiguero, E.G., Wieghofer, P., Heinrich, A., Riemke, P., Holscher, C., *et al.* (2013). Microglia emerge from erythromyeloid precursors via Pu.1- and Irf8-dependent pathways. *Nat Neurosci* *16*, 273-280.
- Kieusseian, A., Brunet de la Grange, P., Burlen-Defranoux, O., Godin, I., and Cumano, A. (2012). Immature hematopoietic stem cells undergo maturation in the fetal liver. *Development* *139*, 3521-3530.
- Kingsley, P.D., Malik, J., Fantauzzo, K.A., and Palis, J. (2004). Yolk sac-derived primitive erythroblasts enucleate during mammalian embryogenesis. *Blood* *104*, 19-25.
- Kissa, K., and Herbomel, P. (2010). Blood stem cells emerge from aortic endothelium by a novel type of cell transition. *Nature* *464*, 112-115.
- Kondo, M., Weissman, I.L., and Akashi, K. (1997). Identification of clonogenic common lymphoid progenitors in mouse bone marrow. *Cell* *91*, 661-672.
- Kumaravelu, P., Hook, L., Morrison, A.M., Ure, J., Zhao, S., Zuyev, S., Ansell, J., and Medvinsky, A. (2002). Quantitative developmental anatomy of definitive haematopoietic stem cells/long-term repopulating units (HSC/RUs): role of the aorta-gonad-mesonephros (AGM) region and the yolk sac in colonisation of the mouse embryonic liver. *Development* *129*, 4891-4899.
- Kurotaki, D., Sasaki, H., and Tamura, T. (2017). Transcriptional control of monocyte and macrophage development. *Int Immunol* *29*, 97-107.
- Lancrin, C., Sroczynska, P., Stephenson, C., Allen, T., Kouskoff, V., and Lacaud, G. (2009). The haemangioblast generates haematopoietic cells through a haemogenic endothelium stage. *Nature* *457*, 892-895.
- Larsson, J., and Karlsson, S. (2005). The role of Smad signaling in hematopoiesis. *Oncogene* *24*, 5676-5692.
- Lassila, O., Martin, C., Toivanen, P., and Dieterlen-Lièvre, F. (1982). Erythropoiesis and lymphopoiesis in the chick yolk-sac-embryo chimeras: contribution of yolk sac and intraembryonic stem cells. *Blood* *59*, 377-381.
- Lavin, Y., Winter, D., Blecher-Gonen, R., David, E., Keren-Shaul, H., Merad, M., Jung, S., and Amit, I. (2014). Tissue-resident macrophage enhancer landscapes are shaped by the local microenvironment. *Cell* *159*, 1312-1326.
- Lichanska, A.M., Browne, C.M., Henkel, G.W., Murphy, K.M., Ostrowski, M.C., Mc Kercher, S.R., *et al.* (1999). Differentiation of the mononuclear phagocyte system during mouse embryogenesis: the role of transcription factor PU.1. *Blood* *94*, 127-138.

- Lim, S.H., Park, E., You, B., Jung, Y., Park, A.R., Park, S.G., and Lee, J.R. (2013). Neuronal synapse formation induced by microglia and interleukin 10. *PLoS One* *8*, e81218.
- Lukov, G.L., Rossi, L., Souroullas, G.P., Mao, R., and Goodell, M.A. (2011). The expansion of T-cells and hematopoietic progenitors as a result of overexpression of the lymphoblastic leukemia gene, *Lyl1* can support leukemia formation. *Leuk Res* *35*, 405-412.
- Lux, C., Yoshimoto, M., McGrath, K., Conway, S., Palis, J., and Yoder, C. (2008). All primitive and definitive hematopoietic progenitor cells emerging before E10 in the mouse embryo are products of the yolk sac. *Blood* *111*, 3435-3438.
- Marin-Teva, J.L., Dusart, I., Colin, C., Gervais, A., van Rooijen, N., and Mallat, M. (2004). Microglia promote the death of developing Purkinje cells. *Neuron* *41*, 535-547.
- Martinez-Agosto, J.A., Mikkola, H.K., Hartenstein, V., and Banerjee, U. (2007). The hematopoietic stem cell and its niche: a comparative view. *Genes Dev* *21*, 3044-3060.
- Mass, E., Ballesteros, I., Farlik, M., Halbritter, F., Gunther, P., Crozet, L., Jacome-Galarza, C.E., Handler, K., Klughammer, J., Kobayashi, Y., *et al.* (2016). Specification of tissue-resident macrophages during organogenesis. *Science* *353*.
- Matcovitch-Natan, O., Winter, D.R., Giladi, A., Vargas Aguilar, S., Spinrad, A., Sarrazin, S., Ben-Yehuda, H., David, E., Zelada Gonzalez, F., Perrin, P., *et al.* (2016). Microglia development follows a stepwise program to regulate brain homeostasis. *Science* *353*, aad8670.
- McCormack, M.P., Shields, B.J., Jackson, J.T., Nasa, C., Shi, W., Slater, N.J., Tremblay, C.S., Rabbitts, T.H., and Curtis, D.J. (2013). Requirement for *Lyl1* in a model of *Lmo2*-driven early T-cell precursor ALL. *Blood* *122*, 2093-2103.
- McGrath, K.E., Frame, J.M., Fegan, K.H., Bowen, J.R., Conway, S.J., Catherman, S.C., Kingsley, P.D., Koniski, A.D., and Palis, J. (2015a). Distinct Sources of Hematopoietic Progenitors Emerge before HSCs and Provide Functional Blood Cells in the Mammalian Embryo. *Cell Rep* *11*, 1892-1904.
- McGrath, K.E., Frame, J.M., Fromm, G.J., Koniski, A.D., Kingsley, P.D., Little, J., Bulger, M., and Palis, J. (2011). A transient definitive erythroid lineage with unique regulation of the  $\beta$ -globin locus in the mammalian embryo. *Blood* *117*, 4600-4608.
- McGrath, K.E., Frame, J.M., and Palis, J. (2015b). Early hematopoiesis and macrophage development. *Semin Immunol* *27*, 379-387.
- McGrath, K.E., Koniski, A.D., Malik, J., and Palis, J. (2003). Circulation is established in a stepwise pattern in the mammalian embryo. *Blood* *101*, 1669-1676.
- Medvinsky, A., Gan, O.I., Semenova, M.L., and Samoylina, N.L. (1996). Development of day-8 colony-forming unit-spleen hematopoietic progenitors during early murine embryogenesis: spatial and temporal mapping. *Blood* *87*, 557-566.
- Medvinsky, A., Rybtsov, S., and Taoudi, S. (2011). Embryonic origin of the adult hematopoietic system: advances and questions. *Development* *138*, 1017-1031.
- Mellentin, J.D., Smith, S.D., and Cleary, M.L. (1989). *Lyl-1*, a novel gene altered by chromosomal translocation in T cell leukemia, codes for a protein with a helix-loop-helix DNA binding motif. *Cell* *58*, 77-83.

- Meng, Y.S., Khoury, H., Dick, J.E., and Minden, M.D. (2005). Oncogenic potential of the transcription factor LYL1 in acute myeloblastic leukemia. *Leukemia* *19*, 1941-1947.
- Metzger, D., Clifford, J., Chiba, H., and Chambon, P. (1995). Conditional sitespecific recombination in mammalian cells using a ligand-dependent chimeric Cre recombinase. *Proc Natl Acad Sci USA* *92*, 6991-6995.
- Metzger, D., and Feil, R. (1999). Engineering the mouse genome by site-specific recombination. *Curr Opin Biotechnol* *10*, 470-476.
- Mikkola, H.K., and Orkin, S.H. (2006). The journey of developing hematopoietic stem cells. *Development* *133*, 3733-3744.
- Mildner, A., Schmidt, H., Nitsche, M., Merkler, D., Hanisch, U.K., Mack, M., Heikenwalder, M., Bruck, W., Priller, J., and Prinz, M. (2007). Microglia in the adult brain arise from Ly-6C<sup>hi</sup>CCR2<sup>+</sup> monocytes only under defined host conditions. *Nat Neurosci* *10*, 1544-1553.
- Miyamoto, A., Cui, X., Naumovski, L., and Cleary, M.L. (1996). Helix-loop-helix proteins LYL1 and E2a form heterodimeric complexes with distinctive DNAbinding properties in hematolymphoid cells. *Mol Cell Biol* *16*, 2394-2401.
- Morita, Y., Ema, H., and Nakauchi, H. (2010). Heterogeneity and hierarchy within the most primitive hematopoietic stem cell compartment. *J Exp Med* *207*, 1173-1182.
- Morrison, S.J., Hemmati, H.D., Wandycz, A.M., and Weissman, I.L. (1995). The purification and characterization of fetal liver hematopoietic stem cells. *Proc Natl Acad Sci USA* *92*, 10302-10306.
- Mosser, C.A., Baptista, S., Arnoux, I., and Audinat, E. (2017). Microglia in CNS development: Shaping the brain for the future. *Prog Neurobiol* *149-150*, 1-20.
- Muller, A.M., Medvinsky, A., Strouboulis, J., Grosveld, F., and Dzierzak, E. (1994). Development of hematopoietic stem cell activity in the mouse embryo. *Immunity* *1*, 291-301.
- Nakorn, T.N., Miyamoto, T., and Weissman, I.L. (2003). Characterization of mouse clonogenic megakaryocyte progenitors. *Proc Natl Acad Sci U S A* *100*, 205-210.
- Nayak, D., Roth, T.L., and McGavern, D.B. (2014). Microglia development and function. *Annu Rev Immunol* *32*, 367-402.
- Nikodemova, M., Kimyon, R.S., De, I., Small, A.L., Collier, L.S., and Watters, J.J. (2015). Microglial numbers attain adult levels after undergoing a rapid decrease in cell number in the third postnatal week. *J Neuroimmunol* *278*, 280-288.
- Novershtern, N., Subramanian, A., Lawton, L.N., Mak, R.H., Haining, W.N., McConkey, M.E., Habib, N., Yosef, N., Chang, C.Y., Shay, T., *et al.* (2011). Densely interconnected transcriptional circuits control cell states in human hematopoiesis. *Cell* *144*, 296-309.
- Oguro, H., Ding, L., and Morrison, S.J. (2013). SLAM family markers resolve functionally distinct subpopulations of hematopoietic stem cells and multipotent progenitors. *Cell Stem Cell* *13*, 102-116.
- Okabe, Y., and Medzhitov, R. (2016). Tissue biology perspective on macrophages. *Nat Immunol* *17*, 9-17.

- Olson, M.C., and Scott, E.W. (1995). PU. 1 is not essential for early myeloid gene expression but is required for terminal myeloid differentiation. *Immunity* 3, 703-714.
- Osawa, M., Hanada, K., Hamada, H., and Nakauchi, H. (1996). Long-term lymphohematopoietic reconstitution by a single CD34-low/negative hematopoietic stem cell. *Science* 273, 242-245.
- Orkin, S.H. (2000). Diversification of haematopoietic stem cells to specific lineages. *Nat Rev Genet* 1, 57-64.
- Orkin, S.H., and Zon, L.I. (2008). Hematopoiesis: an evolving paradigm for stem cell biology. *Cell* 132, 631-644.
- Ottersbach, K., and Dzierzak, E. (2005). The murine placenta contains hematopoietic stem cells within the vascular labyrinth region. *Dev Cell* 8, 377-387.
- Palis, J. (2014). Primitive and definitive erythropoiesis in mammals. *Front Physiol* 5, 3.
- Palis, J. (2016). Hematopoietic stem cell-independent hematopoiesis: emergence of erythroid, megakaryocyte, and myeloid potential in the mammalian embryo. *FEBS Lett* 590, 3965-3974.
- Palis, J., Chan, R.J., Koniski, A., Patel, R., Starr, M., and Yoder, M.C. (2001). Spatial and temporal emergence of high proliferative potential hematopoietic precursors during murine embryogenesis. *Proc Natl Acad Sci U S A* 98, 4528-4533.
- Palis, J., Robertson, S., Kennedy, M., Wall, C., and Keller, G. (1999). Development of erythroid and myeloid progenitors in the yolk sac and embryo proper of the mouse. *Development* 126, 5073-5084.
- Paolicelli, R.C., Bolasco, G., Pagani, F., Maggi, L., Scianni, M., Panzanelli, P., Giustetto, M., Ferreira, T.A., Guiducci, E., Dumas, L., *et al.* (2011). Synaptic pruning by microglia is necessary for normal brain development. *Science* 333, 1456-1458.
- Parkhurst, C.N., Yang, G., Ninan, I., Savas, J.N., Yates, J.R., 3rd, Lafaille, J.J., Hempstead, B.L., Littman, D.R., and Gan, W.B. (2013). Microglia promote learning-dependent synapse formation through brain-derived neurotrophic factor. *Cell* 155, 1596-1609.
- Perdiguerro, E.G., and Geissmann, F. (2016). The development and maintenance of resident macrophages. *Nat Immunol* 17, 2-8.
- Pietras, E.M., Reynaud, D., Kang, Y.A., Carlin, D., Calero-Nieto, F.J., Leavitt, A.D., Stuart, J.M., Gottgens, B., and Passegue, E. (2015). Functionally Distinct Subsets of Lineage-Biased Multipotent Progenitors Control Blood Production in Normal and Regenerative Conditions. *Cell Stem Cell* 17, 35-46.
- Pina, C., and Enver, T. (2007). Differential contributions of haematopoietic stem cells to foetal and adult hematopoiesis: insights from functional analysis of transcriptional regulators. *Oncogene* 26, 6750-6765.
- Prinz, M., Erny, D., and Hagemeyer, N. (2017). Ontogeny and homeostasis of CNS myeloid cells. *Nat Immunol* 18, 385-392.
- Prinz, M., and Priller, J. (2014). Microglia and brain macrophages in the molecular age: from origin to neuropsychiatric disease. *Nat Rev Neurosci* 15, 300-312.

- Prinz, M., Priller, J., Sisodia, S.S., and Ransohoff, R.M. (2011). Heterogeneity of CNS myeloid cells and their roles in neurodegeneration. *Nat Neurosci* *14*, 1227-1235.
- Ramos, C.A., Bowman, T.A., Boles, N.C., Merchant, A.A., Zheng, Y., Parra, I., Fuqua, S.A., Shaw, C.A., and Goodell, M.A. (2006). Evidence for diversity in transcriptional profiles of single hematopoietic stem cells. *PLoS Genet* *2*, e159.
- Ransohoff, R.M., and Cardona, A.E. (2010). The myeloid cells of the central nervous system parenchyma. *Nature* *468*, 253-262.
- Reagan, M.R., and Rosen, C.J. (2016). Navigating the bone marrow niche: translational insights and cancer-driven dysfunction. *Nat Rev Rheumatol* *12*, 154-168.
- Rogers, J.T., Morganti, J.M., Bachstetter, A.D., Hudson, C.E., Peters, M.M., Grimmig, B.A., Weeber, E.J., Bickford, P.C., and Gemma, C. (2011). CX3CR1 deficiency leads to impairment of hippocampal cognitive function and synaptic plasticity. *J Neurosci* *31*, 16241-16250.
- Rossi, F., Casano, A.M., Henke, K., Richter, K., and Peri, F. (2015). The SLC7A7 Transporter Identifies Microglial Precursors prior to Entry into the Brain. *Cell Rep* *11*, 1008-1017.
- Rowe, R.G., Mandelbaum, J., Zon, L.I., and Daley, G.Q. (2016). Engineering Hematopoietic Stem Cells: Lessons from Development. *Cell Stem Cell* *18*, 707-720.
- San-Marina, S., Han, Y., Liu, J., and Minden, M.D. (2012). Suspected leukemia oncoproteins CREB1 and LYL1 regulate Op18/STMN1 expression. *Biochim Biophys Acta* *1819*, 1164-1172.
- Sánchez, M., Holmes, A., Miles, C., and Dzierzak, E. (1996). Characterization of the first definitive hematopoietic stem cells in the AGM and liver of the mouse embryo. *Immunity* *5*, 513-525.
- San-Marina, S., Han, Y., Suarez Saiz, F., Trus, M.R., and Minden, M.D. (2008). Lyl1 interacts with CREB1 and alters expression of CREB1 target genes. *Biochim Biophys Acta* *1783*, 503-517.
- Schulz, C., Gomez Perdiguero, E., Chorro, L., Szabo-Rogers, H., Cagnard, N., Kierdorf, K., Prinz, M., Wu, B., Jacobsen, S.E., Pollard, J.W., *et al.* (2012). A lineage of myeloid cells independent of Myb and hematopoietic stem cells. *Science* *336*, 86-90.
- Sheng, J., Ruedl, C., and Karjalainen, K. (2015). Most Tissue-Resident Macrophages Except Microglia Are Derived from Fetal Hematopoietic Stem Cells. *Immunity* *43*, 382-393.
- Shivdasani, R., Mayer, E., and Orkin, S. (1995). Absence of blood formation in mice lacking the T-cell leukaemia oncoprotein tal-1/SCL. *Nature* *373*, 432-434.
- Sieburg, H.B., Cho, R.H., Dykstra, B., Uchida, N., Eaves, C.J., and Muller-Sieburg, C.E. (2006). The hematopoietic stem compartment consists of a limited number of discrete stem cell subsets. *Blood* *107*, 2311-2316.
- Smith, L.G., Weissman, I.L., and Heimfeld, S. (1991). Clonal analysis of hematopoietic stem-cell differentiation in vivo. *Proc Natl Acad Sci USA* *88*, 2788-2792.

- Soucie, E.L., Weng, Z., Geirsdottir, L., Molawi, K., Maurizio, J., Fenouil, R., Mossadegh-Keller, N., Gimenez, G., VanHille, L., Beniazza, M., *et al.* (2016). Lineage-specific enhancers activate self-renewal genes in macrophages and embryonic stem cells. *Science* *351*, aad5510.
- Souroullas, G.P., and Goodell, M.A. (2011). A new allele of *Lyl1* confirms its important role in hematopoietic stem cell function. *Genesis* *49*, 441-448.
- Souroullas, G.P., Salmon, J.M., Sablitzky, F., Curtis, D.J., and Goodell, M.A. (2009). Adult hematopoietic stem and progenitor cells require either *Lyl1* or *Scl* for survival. *Cell Stem Cell* *4*, 180-186.
- Speck, N.A. (2001). Core binding factor and its role in normal hematopoietic development. *Curr Opin Hematol* *8*, 192-196.
- Stevens, B., Allen, N.J., Vazquez, L.E., Howell, G.R., Christopherson, K.S., Nouri, N., Micheva, K.D., Mehalow, A.K., Huberman, A.D., Stafford, B., *et al.* (2007). The classical complement cascade mediates CNS synapse elimination. *Cell* *131*, 1164-1178.
- Swinnen, N., Smolders, S., Avila, A., Notelaers, K., Paesen, R., Ameloot, M., Brone, B., Legendre, P., and Rigo, J.M. (2013). Complex invasion pattern of the cerebral cortex by microglial cells during development of the mouse embryo. *Glia* *61*, 150-163.
- Takahashi, K., Rochford, C.D., and Neumann, H. (2005). Clearance of apoptotic neurons without inflammation by microglial triggering receptor expressed on myeloid cells-2. *J Exp Med* *201*, 647-657.
- Tavian, M., Robin, C., Coulombel, L., and Peault, B. (2001). The human embryo, but not its yolk sac, generates lympho-myeloid stem cells: mapping multipotent hematopoietic cell fate in intraembryonic mesoderm. *Immunity* *15*, 487-495.
- Theise, N.D., Krause, D.S., and Sharkis, S. (2003). Comment on "Little evidence for developmental plasticity of adult hematopoietic stem cells". *Science* *299*, 1317.
- Tober, J., Koniski, A., McGrath, K.E., Vemishetti, R., Emerson, R., de Mesy-Bentley, K.K., Waugh, R., and Palis, J. (2007). The megakaryocyte lineage originates from hemangioblast precursors and is an integral component both of primitive and of definitive hematopoiesis. *Blood* *109*, 1433-1441.
- Tober, J., McGrath, K.E., and Palis, J. (2008). Primitive erythropoiesis and megakaryopoiesis in the yolk sac are independent of *c-myb*. *Blood* *111*, 2636-2639.
- Tong, L., Prieto, G.A., Kramar, E.A., Smith, E.D., Cribbs, D.H., Lynch, G., and Cotman, C.W. (2012). Brain-derived neurotrophic factor-dependent synaptic plasticity is suppressed by interleukin-1beta via p38 mitogen-activated protein kinase. *J Neurosci* *32*, 17714-17724.
- Ueno, M., Fujita, Y., Tanaka, T., Nakamura, Y., Kikuta, J., Ishii, M., and Yamashita, T. (2013). Layer V cortical neurons require microglial support for survival during postnatal development. *Nat Neurosci* *16*, 543-551.
- van de Laar, L., Saelens, W., De Prijck, S., Martens, L., Scott, C.L., Van Isterdael, G., Hoffmann, E., Beyaert, R., Saeys, Y., Lambrecht, B.N., *et al.* (2016). Yolk Sac Macrophages, Fetal Liver, and Adult Monocytes Can Colonize an Empty Niche and Develop into Functional Tissue-Resident Macrophages. *Immunity* *44*, 755-768.

- van Eekelen, J.A.M., Bradley, C.K., Göthert, J.R., Robb, L., Elefanty, A.G., Begley, C.G., and Harvey, A.R. (2003). Expression pattern of the stem cell leukaemia gene in the CNS of the embryonic and adult mouse. *Neuroscience* *122*, 421-436.
- van Galen, P., Kreso, A., Mbong, N., Kent, D.G., Fitzmaurice, T., Chambers, J.E., Xie, S., Laurenti, E., Hermans, K., Eppert, K., *et al.* (2014). The unfolded protein response governs integrity of the haematopoietic stem-cell pool during stress. *Nature* *510*, 268-272.
- Veiga-Fernandes, H., and Pachnis, V. (2017). Neuroimmune regulation during intestinal development and homeostasis. *Nat Immunol* *18*, 116-122.
- Wadman, I., Li, J., Bash, R.O., Forster, A., Osada, H., Rabbitts, T.H., and Baer, R. (1994). Specific in vivo association between the bHLH and LIM proteins implicated in human T cell leukemia. *EMBO J* *13*, 4831-4839.
- Wake, H., Moorhouse, A.J., Miyamoto, A., and Nabekura, J. (2013). Microglia: actively surveying and shaping neuronal circuit structure and function. *Trends Neurosci* *36*, 209-217.
- Wakselman, S., Bechade, C., Roumier, A., Bernard, D., Triller, A., and Bessis, A. (2008). Developmental neuronal death in hippocampus requires the microglial CD11b integrin and DAP12 immunoreceptor. *J Neurosci* *28*, 8138-8143.
- Wang, J., Wegener, J. E., Huang, T. W., Sripathy, S., De Jesus-Cortes, H., Xu, P., *et al.* (2015). Wild-type microglia do not reverse pathology in mouse models of Rett syndrome. *Nature* *521*, E1-E4.
- Wang, L.D., and Wagers, A.J. (2011). Dynamic niches in the origination and differentiation of haematopoietic stem cells. *Nat Rev Mol Cell Biol* *12*, 643-655.
- Wang, L.H., and Baker, N.E. (2015). E Proteins and ID Proteins: Helix-Loop-Helix Partners in Development and Disease. *Dev Cell* *35*, 269-280.
- Wang, Y., Szretter, K.J., Vermi, W., Gilfillan, S., Rossini, C., Cella, M., Barrow, A.D., Diamond, M.S., and Colonna, M. (2012). IL-34 is a tissue-restricted ligand of CSF1R required for the development of Langerhans cells and microglia. *Nat Immunol* *13*, 753-760.
- Weingarden, H., and Renshaw, K.D. (2015). Shame in the obsessive compulsive related disorders: A conceptual review. *J Affect Disord* *171*, 74-84.
- Weissman, I.L. (2000). Stem cells: units of development, units of regeneration, and units in evolution. *Cell* *100*, 157-168.
- Wilson, N.K., Foster, S.D., Wang, X., Knezevic, K., Schutte, J., Kaimakis, P., Chilarska, P.M., Kinston, S., Ouwehand, W.H., Dzierzak, E., *et al.* (2010). Combinatorial transcriptional control in blood stem/progenitor cells: genome-wide analysis of ten major transcriptional regulators. *Cell Stem Cell* *7*, 532-544.
- Wilson, N.K., Miranda-Saavedra, D., Kinston, S., Bonadies, N., Foster, S.D., Calero-Nieto, F., Dawson, M.A., Donaldson, I.J., Dumon, S., Frampton, J., *et al.* (2009). The transcriptional program controlled by the stem cell leukemia gene *Scl/Tal1* during early embryonic hematopoietic development. *Blood* *113*, 5456-5465.
- Wolf, Y., Yona, S., Kim, K.W., and Jung, S. (2013). Microglia, seen from the CX3CR1 angle. *Front Cell Neurosci* *7*, 26.

- Wu, Y., Dissing-Olesen, L., MacVicar, B.A., and Stevens, B. (2015). Microglia: Dynamic Mediators of Synapse Development and Plasticity. *Trends Immunol* *36*, 605-613.
- Wynn, T.A., Chawla, A., and Pollard, J.W. (2013). Macrophage biology in development, homeostasis and disease. *Nature* *496*, 445-455.
- Wynn, T.A., and Vannella, K.M. (2016). Macrophages in Tissue Repair, Regeneration, and Fibrosis. *Immunity* *44*, 450-462.
- Xu, J., Wang, T., Wu, Y., Jin, W., and Wen, Z. (2016). Microglia colonization of developing zebrafish midbrain is promoted by apoptotic neuron and lysophosphatidylcholine. *Dev Cell* *38*, 214-222.
- Xu, J., Zhu, L., He, S., Wu, Y., Jin, W., Yu, T., Qu, J.Y., *et al.* (2015). Temporal-spatial resolution fate mapping reveals distinct origins for embryonic and adult microglia in zebrafish. *Dev Cell* *34*, 632-641.
- Yang, L., Bryder, D., Adolfsson, J., Nygren, J., Mansson, R., Sigvardsson, M., and Jacobsen, S.E. (2005). Identification of Lin(-)Sca1(+)kit(+)CD34(+)Flt3- short-term hematopoietic stem cells capable of rapidly reconstituting and rescuing myeloablated transplant recipients. *Blood* *105*, 2717-2723.
- Yoder, M.C. (2014). Inducing definitive hematopoiesis in a dish. *Nat Biotechnol* *32*, 539-541.
- Yoshimoto, M., Montecino-Rodriguez, E., Ferkowicz, M.J., Porayette, P., Shelley, W.C., Conway, S.J., Dorshkind, K., and Yoder, M.C. (2011). Embryonic day 9 yolk sac and intra-embryonic hemogenic endothelium independently generate a B-1 and marginal zone progenitor lacking B-2 potential. *Proc Natl Acad Sci USA* *108*, 1468-1473.
- Yoshimoto, M., Porayette, P., Glosson, N.L., Conway, S.J., Carlesso, N., Cardoso, A.A., Kaplan, M.H., and Yoder, M.C. (2012). Autonomous murine T-cell progenitor production in the extra-embryonic yolk sac before HSC emergence. *Blood* *119*, 5706-5714.
- Zambrowicz, B.P., Imamoto, A., Fiering, S., Herzenberg, L.A., Kerr, W.G., and Soriano, P. (1997). Disruption of overlapping transcripts in the ROSA beta geo 26 gene trap strain leads to widespread expression of beta-galactosidase in mouse embryos and hematopoietic cells. *Proc Natl Acad Sci USA* *94*, 3789-3794.
- Zhan, Y., Paolicelli, R.C., Sforzini, F., Weinhard, L., Bolasco, G., Pagani, F., Vyssotski, A.L., Bifone, A., Gozzi, A., Ragozzino, D., *et al.* (2014). Deficient neuron-microglia signaling results in impaired functional brain connectivity and social behavior. *Nat Neurosci* *17*, 400-406.
- Zhang, D.E., Hetherington, C.J., Meyers, S., Rhoades, K.L., Larson, C.J., Chen, H.M., Hiebert, S.W., and Tenen, D.G. (1996). CCAAT enhancer-binding protein (C/EBP) and AML1 (CBF alpha2) synergistically activate the macrophage colony-stimulating factor receptor promoter. *Mol Cell Biol* *16*, 1231-1240.
- Zeisel, A., Muñoz-Manchado, A. B., Codeluppi, S., Lönnerberg, P., La Manno, G., Juréus, A., *et al.* (2015). Cell types in the mouse cortex and hippocampus revealed by single-cell RNA-seq. *Science* *347*, 1138-1142.

Zhong, Y., Jiang, L., Hiai, H., Toyokuni, S., and Yamada, Y. (2007). Overexpression of a transcription factor LYL1 induces T- and B-cell lymphoma in mice. *Oncogene* 26, 6937-6947.

Zohren, F., Souroullas, G.P., Luo, M., Gerdemann, U., Imperato, M.R., Wilson, N.K., Gottgens, B., Lukov, G.L., and Goodell, M.A. (2012). The transcription factor Lyl-1 regulates lymphoid specification and the maintenance of early T lineage progenitors. *Nat Immunol* 13, 761-769.

Zusso, M., Methot, L., Lo, R., Greenhalgh, A.D., David, S., and Stifani, S. (2012). Regulation of postnatal forebrain amoeboid microglial cell proliferation and development by the transcription factor Runx1. *J Neurosci* 32, 11285-11298.

**Titre : Fonctions du facteur de transcription *Lyl-1* dans le développement du lignage macrophagique**

**Mots clés :** *Lyl-1*, Embryon, Macrophage, Microglie, Neuro-développement, Autisme.

**Résumé:** Les macrophages (MΦ) du système nerveux central forment la microglie, qui contrôle son homéostasie. Plusieurs modèles de "fate mapping" ont montré que la microglie provenait du Sac vitellin (SV). Celui-ci produit les MΦ en deux vagues indépendantes. Dans la première, des progéniteurs restreints génèrent des MΦ primitifs, alors que dans la seconde, des progéniteurs érythro-myéloïdes produisent des MΦ définitifs. Les progéniteurs primitifs et définitifs ont les mêmes phénotype et voie de différenciation. Leurs spécificités et leurs contributions aux étapes ultérieures du développement sont donc encore incompréhensibles. Nous montrons que l'expression du facteur de transcription *Lyl-1* discrimine les populations de MΦ primitifs et définitifs.

Les MΦ primitifs *Lyl-1*<sup>+</sup> fournissent la microglie de l'embryon. De plus, l'inactivation de *Lyl-1* disruption conduit à une production accrue de MΦ primitive dans le SV précoce, puis à une réduction du contingent microglial à deux stades spécifiques du développement. *Lyl-1* est spécifiquement exprimé par la microglie et aucun autre type cellulaire nerveux. Son inactivation conduit à des modifications comportementales typiques de l'anxiété sociale. Nous identifions donc *Lyl-1* comme un marqueur des MΦ primitifs du SV qui donnent naissance à la microglie de l'embryon. Nous montrons également que *Lyl-1* contrôle l'expansion et la différenciation de la microglie, et est ainsi impliqué dans la régulation des processus du neuro-développement.

**Title : Functions of the transcription factor *Lyl-1* in the development of the macrophage lineage**

**Keywords :** *Lyl-1*, Embryo, Macrophage, Microglia, Neuro-development, Autism.

**Abstract:** Microglia are tissue macrophages (MΦ) of the central nervous system that control tissue homeostasis. Different fate mapping models have shown that microglia originates from the yolk sac (YS). Macrophages production in the YS occurs in two independent waves. In the first, primitive MΦ originate from restricted progenitors, while in the second, definitive MΦ are produced by erythro-myeloid progenitors. Because primitive and definitive MΦ progenitors share the same phenotype and differentiation pathway, their specific features and contribution to further developmental steps are still poorly understood. We here show that the expression of the transcription factor *Lyl-1* discriminates primitive

and definitive MΦ populations. YS-derived *Lyl-1*<sup>+</sup> primitive MΦ contribute to embryonic microglia. Moreover, *Lyl-1* disruption results in an increased production of primitive MΦ progenitors in the early YS. It also leads to the reduction of the microglia pool at two specific development stages. *Lyl-1* is specifically expressed in microglia, but not other brain cells and its inactivation leads to behavioral changes typical for social anxiety disorders. Thus, we identify *Lyl-1* as a marker for YS primitive MΦ that will give rise to the entire microglia. We show that *Lyl-1* controls microglia expansion and differentiation and is involved in the regulation of neurodevelopmental processes.

